The Bhuj Earthquake of 2001

Prepared by:
D. Abrams, M. Aschheim, P. Bodin, S. Deaton,
S. Dotson, D. Frost, S.K. Ghosh, S. Horton, A. Johnston,
J. Nichols, T. Rossetto, M. Tuttle, M. Withers

December 2001

Copyright 2001
Board of Trustees at the University of Illinois
All Rights Reserved

TABLE OF CONTENTS

	Preface	D. Abrams
1.	Prior Seismic Activity	P. Bodin
2.	Mainshock Rupture	P. Bodin
3.	Aftershock Measurements	S. Horton, P. Bodin, M. Withers
4.	Liquefaction Features	M. Tuttle
5.	Geotechnical Observations	S. Deaton and D. Frost
6.	Indian Standards for Building Construction	J. Nichols
7.	Building Damage	D. Abrams
8.	Performance of Engineered Buildings	S.K. Ghosh
9.	Performance of Lifelines and Industrial Facilities	M. Aschheim
10.	Seismic Vulnerability Predictions for Reinforced Concrete Structures	T. Rossetto
11.	Socio-Economic Aspects	S. Dotson
12.	Correlations with Mid-America	A. Johnston

PREFACE

The decision to send a team of earthquake engineering researchers and seismologists half way around the world to investigate a tragic earthquake was indeed a difficult one to make considering the circumstances. Logistical problems, from obtaining visas to transporting large equipment packages to mobilization in the field, were enough by themselves to find every reason for not having a reconnaissance effort. Moreover, risks posed by health and safety of investigators in the disaster region, along with the myriad of political issues and high costs associated with an international study of this degree, required much contemplation before a decision was made to deploy a team of investigators. However, an affirmative decision was made because of the benefits that the investigation would have with regard to the Center's emphasis on earthquake loss reduction in the Central United States. Whereas no two earthquakes and their resulting consequences are identical, similarities between the New Madrid and Bhuj earthquakes, as noted is this report, were sufficient to justify sending a team.

The Republic Day Earthquake

The earthquake occurred at 8:47 am (Indian time) on Friday, January 26, 2001, an Indian national holiday known as Republic Day. The epicenter was approximately 50 kilometers northeast of the town of Bhuj in the northwestern part of the Indian state of Gujarat near the Rann of Kachchh (also spelled "Kutch"). The moment magnitude of the earthquake was recorded at 7.7 making it the largest earthquake in this region since the Alah Bund earthquake of 1819.

The official death toll was reported at 35,000 with over 300,000 injuries. Unofficial reports gave estimates exceeding 100,000 fatalities making this the highest death toll since the 1976 Tangshan earthquake. A periodical (*Indian Today*, February 12, 2001) reported approximate numbers of casualties at 12,000 in Bhuj, 10,000 in Anjar, 10,000 in Bachau, 12,000 in Jamnagar and 1,000 in the city of Ahmedabad, 255 km from epicenter. The primary cause of death was the collapse of building structures, many of which were older unreinforced stone masonry dwellings, or conversely, modern high-rise reinforced concrete frame buildings.

Direct economic losses were estimated in the range of $5 billion, an order of magnitude less than that anticipated for a repeat of one of the New Madrid earthquakes. The limited loss was because the epicentral region was sparsely populated with few industrial facilities. Damage to local salt-processing plants was substantial, and losses to the port of Kandla were significant at approximately $33 million. Building damage in Surat resulted in interruptions to the diamond industry at $4.5 million per day. Real estate prices in Ahmedabad declined from 25% to 50% soon after the earthquake because of fears with respect to seismic safety of high-rise residential construction with soft ground-level stories.

Though much closer to a plate boundary than the New Madrid seismic zone, the Bhuj earthquake occurred in a stable continental region classifying it as an intraplate event much like those observed in the central United States. The epicentral area was between a series of recognized faults: the Kutch Mainland Fault, the Katrot-Bhuj Fault, and the North Kathicwar Fault. The Rann is a desert-like plain susceptible to flooding in the summer but very dry during January; however, signs of ground water percolation were evident. Fountains of water as tall as two meters were observed following the earthquake across wide areas. Signs of sand blows and lateral spreading in soils were predominant in the epicentral region. These highly pronounced liquefaction features of the Bhuj earthquake were reminiscent of those reported in 1811 and 1812 as a result of the New Madrid earthquakes.

Much of the building construction that collapsed within 50 kilometers of the epicenter was non-engineered, unreinforced masonry. Either stone rubble or cut stone was predominant for low-rise residential construction in villages or towns. Whereas much of the ancient unreinforced masonry construction in the city of Ahmedabad survived the earthquake, many recently constructed frame buildings (five to ten stories) suffered collapse despite peak ground accelerations as small as 0.1g. This was attributable to a rapid growth in construction over the last decade and local codes restricting building size. A significantly large number of engineered, reinforced-concrete frame structures with masonry infills collapsed as a result of soft ground-level stories with severe lateral stiffness and strength discontinuities at the base story. Masonry infill panels were typically not placed at these base stories to provide an open space for parking and to permit larger building footprints relative to the lot size per a local municipal ordinance. Though Indian standards for earthquake resistant construction are on a par with modern building codes in other parts of the world, often construction quality was impaired because of the lack of third-party design reviews and/or inspection.

In addition to correlations in seismicity and ground failures, pre-event attitudes of the Gujarati people with regard to an impeding earthquake hazard were similar to that of the populace of the central United States. Much like the limited concern of Midwesterners to a repeat of the New Madrid earthquakes, the Gujaratis had mostly forgotten about the 1819 Alah Bund earthquake that caused extensive damage in the town of Bhuj and the surrounding area. Industries in the area were typically not insured against earthquake loss, and less than 12% of the population had earthquake insurance. Damage to insured property was on the order of $100 million, or 2% of the total direct loss. Immediately following the earthquake, many people were insuring against future earthquake losses as well as mitigating effects of future hazards through seismic rehabilitation of their buildings.

The MAE Center Investigation

The synergy of the MAE Center's engineering and seismological teams provided a unique opportunity to study relations between damage distributions and ground motion characteristics. Anomalies in damage-distance relations, such as towns with little damage close to the epicenter or towns with much damage far from the epicenter, were identified through cross-disciplinary discoveries of the epicentral location and apparent pockets of damage. Findings such as these are important for assessing the degree of uncertainty related to synthesizing damage across regions in other parts of the world, including Mid-America.

The MAE Center reconnaissance team convened in Mumbai (formerly Bombay) on Friday, February 9, 2001. Two teams, a group of engineers led by Dan Abrams and a group of seismologists led by Arch Johnston, met with local hosts, Ramesh Raiker of Strutwel Designers in Mumbai and Kirit Budhbhatti, a professor at the Institute of Science and Technology for Advanced Studies and Research (ISTAR) in Vidyanagar, Gujarat to share information, develop final strategies and review reporting assignments. Soon afterwards, the engineering team flew to Ahmedabad to explore damage in this major urban area with a population of over 4.8 million, and to coordinate reconnaissance efforts with other teams including the Earthquake Engineering Research Institute's team that was just returning from Bhuj to Ahmedabad. Each evening the MAE engineering team consisting of Dan Abrams, Mark Aschheim, David Frost, S.K. Ghosh, Apurva Parikh, Ramesh Raikar, Tiziana Rossetto, and James Wilcoski shared information with other teams staying at the Fortune Landmark Hotel, including a highly informative video presentation of an aerial survey of the damaged area conducted by the EERI team. The MAE engineering team left Ahmedabad on the morning of February 13 and traveled via land transport toward Bhuj stopping at several sites along the way to observe relative degrees of damage. The

engineering team set up camp at the Garha Safari Lodge near the Rudramata dam, 15 kilometers north of Bhuj, for a four-day period to meet with the seismological team and visit damage sites in the surrounding area. They returned from Bhuj to Mumbai on Friday, February 16 to disembark India.

The MAE seismological team, led by Arch Johnston and consisting of Steve Horton, Paul Bodin and Gary Patterson, flew to Bhuj early on the morning of February 10 to set up a central command post at the Budhabhatti garage in central Bhuj, from which they deployed an array of instrumentation stations for measuring ground motions due to aftershocks. Nearly two-thousand pounds of ground-motion instrumentation were shipped from CERI in Memphis to Mumbai and then transported via truck to Bhuj. Seven stations were established in the epicentral region between the village of Lodai and the town of Bhachau. Steve Horton and Paul Bodin remained in Bhuj for an additional week following February 16 to maintain their instrumentation stations before being relieved by CERI researchers Jim Bollwerk and Paul Rydelek. Approximately 90 aftershocks were recorded per day over a 17 day period, including a magnitude 5.1 shock on February 15 and a magnitude 5.3 shock on February 20. On February 28, the aftershock array was removed from the field, and repackaged for shipment back to Memphis. Martitia Tuttle joined the CERI team to investigate liquefaction features with local assistance provided by C.P. and Kusala Rajendran and Mahesh Thakkar.

Contents of Report

This report consists of twelve chapters each independently authored by a member of the MAE Center investigative team. Each chapter was intended to be a stand-alone summary on a particular aspect of the Bhuj earthquake. Little or no editing was done other than to assign figure and page numbers. Opinions and findings expressed in each chapter are those of the respective author(s) and not necessarily those of the Mid-America Earthquake Center, the Center for Research and Information, or the National Science Foundation. The first three chapters address seismological features of the earthquake explaining prior seismic activity, main-shock rupture and aftershock measurements. Liquefaction features and other geotechnical observations are discussed in Chapters 4 and 5. A summary of current Indian standards for seismically resistant building construction is given in Chapter 6 followed by summaries of building damage and performance of engineered buildings in Chapters 7 and 8. Performance of lifelines and industrial facilities is reported on in Chapter 9, followed by a discussion of seismic vulnerability predictions for reinforced concrete structures in Chapter 10. Socio-economic aspects of the tragedy are presented in Chapter 11. The report concludes with a discussion of correlations with Mid-American seismology in Chapter 12.

Acknowledgments

Much of the reconnaissance investigation described in this report was funded by the Mid-America Earthquake Center, which is supported primarily by the Earthquake Engineering Research Centers Program of the National Science Foundation under Award Number EEC-9701785.

Contributions from authors of each of the twelve chapters in this report are gratefully acknowledged. The support and teamwork of the University of Memphis Center for Earthquake Research and Information, under the direction of Arch Johnston, was essential to make this study a reality. Much appreciation is extended to Mr. Ramesh Raikar of Strutwel Consultants in Mumbai, friend and colleague of team member S.K. Ghosh of Northbrook, Illinois, and Kirit Budhbhatti of ISTAR for their generous assistance with the MAE investigation. A special note of

thanks is given to Mr. Apurva Parikh, a structural engineer with Multi-Media Engineers in Ahmedabad and alumnus of the University of Illinois, for his never-ending generosity in assisting the MAE Center engineering team in and around Ahmedabad. Appreciation is also extended to Professor Sudhir Sapre of the School of Architecture, Building Science and Construction Technology of the Center for Environmental Planning and Technology (CEPT) in Ahmedabad for escorting the MAE team to damage sites for a day in Ahmedabad, as well as Mr. Nayan Parikh, an extremely knowledgeable Gujarati bridge engineer, for advising the engineering team on bridge damage before their deployment to the field. Gratitude is also extended to FEDEX for shipping seismic instrumentation to India from Memphis and its return. Sue Dotson and Sandy Shannon are thanked for formatting and producing this report.

It is impossible to express sufficient appreciation to the general populace of Gujarat for their kind graciousness and remarkable sense of resilience in this time of their tragedy. Through their cooperation, valuable information and insights were accessible that would otherwise be lost. But more importantly, their spirit and friendliness instilled within our team members the enthusiasm and strength to conduct a highly energetic and rewarding investigation.

Daniel P. Abrams
Lead Investigator

Chapter 1: Prior Seismic Activity

by

Paul Bodin[1]
Assistant Research Professor
Center for Earthquake Research and Information
The University of Memphis

1. Summary

The most interesting seismological aspects of the Bhuj earthquake are: (1) its apparent depth, (2) its apparent lack of surface rupture, (3) its potential to understand the scaling of continental intraplate earthquakes, (4) its relationship to the regional tectonics, and (5) its comparison to New Madrid. The most important engineering seismology aspects may be the nature of ground motion produced by the combination of: (1) the source characteristics, (2) crustal propagation characteristics, and (3) site response characteristics. In studying all of these aspects, it is usual to do so with reference to the seismic history of a region.

The seismic history of the Kachchh Peninsula, site of the 26 January, 2001, Bhuj Earthquake, is poorly known. Our ignorance is a consequence of two related phenomena: a low rate of seismicity (relative to plate boundary regions), and inattention by seismologists (who have tended to study the more active areas). Following convention, we divide the topic into three periods: Paleoseismic (generally based on geological examination of faults or earthquake effects), Historical (based on historical accounts of damage and ground motion intensity) and Instrumental (in which seismographs recorded ground motions of earthquakes). The paleoseismic record is so sparse that we will simply mention what is known in passing in the section about historical seismicity.

Figure 1-1: Fort Sindri, on the footwall of the 1819 Great Rann of Kachchh earthquake rupture, before (top) and after (bottom) the earthquake

2. Historical Seismicity

The seismic history of Kachchh is dominated by the Great Rann of Kachchh (Kutch, Cutch, Kuchchh and Kachh, are all variants to be found in the literature) earthquake on 16 June, 1819. This earthquake was the subject of a classic study by R.D. Oldham, and forms one of the great touchpoints of modern earthquake investigations. As well as being contemporaneous with the 1811-12 New Madrid earthquakes, the 1819 Great Rann of Kachchh earthquake plays a role in Kachchh

[1] PB, CERI, 3890 Central Avenue, St. 1, Memphis, TN 38152-3050 USA,
email: bodin@ceri.memphis.edu

seismic hazard that is the correlative of the great New Madrid earthquakes. Interestingly, seismic hazard in Gujarat was dominated by thinking of a return time for the Great Rann of Kachchh earthquake. This 'second coming' the Bhuj earthquake was not, but it has rather opened the doors for a deeper understanding of regional seismic hazard.

The source fault of the 1819 earthquake is known about largely because of its enormous surface effects. The Fort at Sindri (Figure 1-1), presumably built on a local hill, was observed to have foundered, and sank relative to sea level such that only the remains of the tower protruded above the sea surface during monsoon inundation. Nearby a large natural structure was formed (or perhaps increased in height—there is debate on this point), the Allah Bundh (or Dam of God, to distinguish it from man-made stream diversions).

Work on the Great Rann of Kachchh earthquake of 1819 intensified during the past decade. A series of papers have reconsidered historical geodetic surveys and macroseismic effects (damage and felt reports), and analyzed geomorphological and geological observations of the Allah Bundh. A very brief summary of these studies is that the 1819 earthquake was probably of moment magnitude, Mw, between 7.6 and 7.8, that while shallow enough to deform the surface along the Allah Bundh, there may have been no actual ground rupture. The Allah Bundh is apparently a fault-generated fold above a "blind thrust". Moreover, there is paleoseismic evidence in the form of soft-surface deformation for a previous large event, possibly coinciding with a historical account of a large earthquake in the region during the 11th century.

The 1819 earthquake was followed by extensive aftershocks. The region reverberated with moderately large earthquakes in 1844 and 1845 (Rajendran and Rajendran, 2000) and again in 1857 (Bilham and Gaur, 2000). Given the scant historical accounts of these earthquakes, we can at present only speculate about whether they were aftershocks of the Great Rann earthquake. Of course it is now abundantly clear that there are other seismic source zones within Kachchh than the Allah Bundh.

3. Instrumental Seismicity

We entered the era of observational seismology about the same time we entered the 20th century, so we have about one hundred years of seismological observations of earthquakes large enough to be recorded by global seismic stations. For about the past 40 years, a standardized global network capable of recording any earthquake of magnitude about M=5 (and possibly down to M~4.5) in Gujarat has been in operation. Drawing on compilations of Quittmeyer and Jacob (1979), and on the global seismicity catalogs of the NEIC, we can make a map of the instrumental seismicity prior to the Bhuj earthquake (Figure 1-1). The global data do not well constrain the depth of events, except that it would appear they are crustal earthquakes (not extremely deep), and epicentral uncertainties on the order of 10s of kilometers are to be expected.

There is only one instrumental earthquake in Kachchh that stands out—the Mw=6.1 "Anjar" earthquake of 1956. This earthquake was large enough (it was responsible for at least 113 fatalities) to invite modeling of its waveforms. Chung and Gao (1992) did so, and constrained the Anjar earthquake's location and focal mechanism to be as shown in Figure 1-2 (reverse slip on an East-striking fault, similar to the Bhuj earthquake), and estimated its focal depth to have been 10 km.

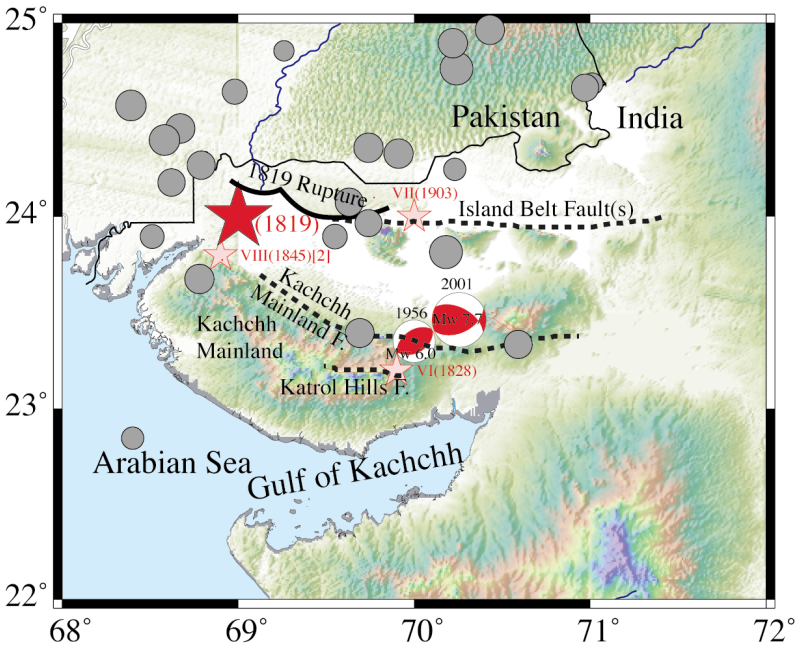

Figure 1-2: Historic and instrumental seismicity of Kachchh prior to the 2001 Bhuj earthquake. Stars are the locations of historical earthquakes from Gowd et al. (1995), along with the year of their occurrence and the peak intensity. Gray circles are instrumental epicenters in the period 1914-2000. Sources are: Quittmeyer and Jacob (1979) through 1975, and from the NEIC catalog. Epicenters scaled by magnitude (smallest M~4, largest M~5). Smaller focal mechanism is for the 1956 Anjar earthquake (from Chung and Gao, 1995), Larger is the Harvard CMT for the 2001 Bhuj earthquake

Another prior earthquake worthy of special mention was an event that preceded the Bhuj earthquake by about one month. On 24 December, 2000, an earthquake was felt widely northwest of the Bhuj aftershock zone. The PDE lists this event as M=4.6. Given the rarity of earthquakes in the region, it is tempting to regard this Christmas time earthquake as a "foreshock" to the Bhuj earthquake. It seems, however, that it was on a different fault. Interestingly, it is possible that a number of small earthquakes recorded on the LBR1 station of the MAEC/ISTAR temporary aftershock (including a series of events with extremely similar waveforms) were small aftershocks of this event (Figure 1-3).

The rate and spatial distribution of earthquakes smaller than about M4-4.5 is totally conjectural. This contrasts with the central US, where a 25-year observation period of small earthquakes on local networks permits us to focus on some clearly microseismically active structures.

One study, published in an Indian journal, suggests that the most seismically active belt in Kachchh is associated with an approximately 100-km long segment of the Katrol Hills Fault (Sohoni et al, 1999). It is not made clear what observations support this conclusion.

From the instrumental seismicity, we conclude that the region is subject to a rather low rate of M>4.5 earthquakes (without doing the computation, it is likely that the volume-averaged seismic moment release rate is similar to or less than the New Madrid Seismic Zone). Aside from the above mentioned study pointing at the Katrol Hills fault, the prior seismicity do not clearly

delineate any of the surface faults as being source zones. Only the Anjar earthquake might qualify as a prior indicator that a major blind thrust fault threatened Kachchh, and more work is required to clarify the spatial association of these two earthquakes.

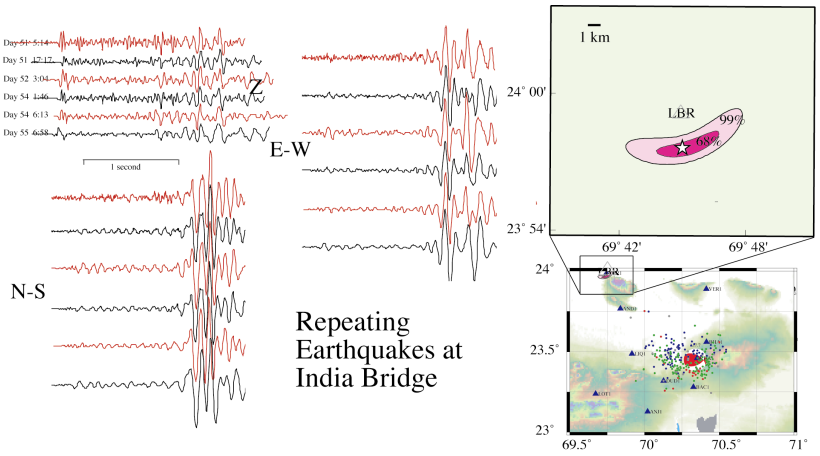

Figure 1-3: Earthquakes near India Bridge (location shown in inset maps—from the work of J. Gomberg, USGS, personal communication). These may be aftershocks of the 24 December, 2000 earthquake, alternatively they may be evidence of background seismicity

4. A Question of Depth…

In the aftermath of the Bhuj earthquake, one of the questions that haunts seismologists is whether the prior seismicity (often called background seismicity, to distinguish it from very large earthquakes and their aftershocks) was as deep as the Bhuj earthquake and its aftershocks.

Such deep mainshock rupture as indicated by the profound depth distribution of aftershocks (see Chapter 2.3)—and even the nucleation of aftershocks apparently throughout the crust—is surprising. It calls into questions commonly held beliefs about to what depth tectonic stress can be stored in the crust and the mechanics of earthquake rupture itself. Common understanding is that only the upper crust (say 10-20 km) of typical continental crust is usually seismogenic). At greater depths (generally corresponding to about 300° C, depending on the composition of the crustal rocks, e.g. Scholz, 1992) the rocks are thought to deform in a more ductile fashion, and fault mechanics tends to discourage the abrupt stick-slip behavior that gives rise to earthquakes. What little we have been able to piece together about the composition and thermal regime of the Kachchhi crust does not help to resolve this problem. Kachchh crust is likely to have rather elevated heat flow (e.g. Roy and Rao, 2000), and the composition of the deep crust is entirely a matter of conjecture.

If prior seismicity was distributed deeply, that would suggest the existence of thermo-mechanical properties that just happen to create a seismogenic lower crust in Kachchh. This would be

interesting and important—a rather rare find.[2] On the other hand, if background seismicity is distributed in depth like most other parts of the world—with a seismogenic upper crust and a ductile lower crust, then the Bhuj earthquake would present the possibility to gain deep insight with profound seismic hazard implications for the central US. That would mean the operation of deformation mechanisms that permit deep rupture during large earthquakes, yet not nucleation of small earthquakes in "usual" times, but only during the period of rapid strain rates that must inevitably follow a large rupture. It would imply that the active seismicity we see in the central US, which extends to about 15 km deep, might be only the "tip of the iceberg" and only represents the top half of what could rupture in large earthquakes, like 1811-12. Much more potential seismic moment release could be packed into shorter active faults than would ever be possible on faults in the mobile crustal rocks that form the majority of the world's observations and inform the theories of earthquake rupture mechanics. A test of this possibility would be if the aftershocks of the Bhuj earthquake get shallower with time.

5. References

Bilham, R. (1998) Slip parameters for the Rann of Kachchh, India, 16 June 1819, earthquake, quantified from contemporary accounts. In: Stewart, I.S. & Vita-Vinzi, C. (eds) Coastal Tectonics. Geological Society, London, Special Publications, **146**, 295-319.

Bilham, R. and V.K. Gaur (2000) Geodetic contributions to the study of seismotectonics in India. Current Science, **79,** 1259-1269.

Chung, W-Y, and H. Gao (1995) Source parameters of the Anjar earthquake of July 21, 1956, India, and its seismotectonic implications for the Kutch rift basin. Tectonophysics, **242**, 281-292.

Gowd, T.N., S.V. Srirama Rao, and K.B. Chary (1996) Stress field and seismicity in the Indian shield: effects of the collision between India and Eurasia. Pure and Applied Geophysics. **146**: 1-27.

Mandal, P., B.K. Rastogi, and H.K. Gupta (2000) Recent Indian Earthquakes. Current Science, **79**, 1334-1347.

Oldham, R. D. (1926) The Cutch (Kachh) earthquake of the 16th June, 1819 with a revision of the great earthquake of the 12th June, 1897, India Geological Survey Memoir, **28**, 71-147.

Quittmeyer, R.C., and K.H. Jacob (1979) Historical and modern seismicity of Pakistan, Afghanistan, northwestern India, and southeastern Iran. Bulletin of the Seismological Society of America, **69**, 773-923.

Rajendran, C.P., and K. Rajendran (2001) Characteristics of deformation and past seismicity associated with the 1819 Kutch earthquake, northwestern India, Bulletin of the Seismological Society of America, in press.

[2] Some support for this possibility may come from another prior Indian earthquake—but one far from Kachchh; the 1992 Jabalpur earthquake (Mandal et al, 2000). The Jabalpur earthquake was extremely deep (>35 km), and was a reverse rupture within a similar old rift zone. Another deep intraplate earthquake was the Saguenay, Canada, earthquake of 1988. Both of these earthquakes were extremely deep, yet both much smaller than the Bhuj.earthquake.

Roy, S. and R.U.M Rao (2000) Heat flow in the Indian Shield. Journal of Geophysical Research 105, 25,587-25,604.

Scholz, C.H. (1992) The Mechanics of Earthquakes and Faulting. Cambridge University Press, Cambridge. 439 pp.

Sohoni, P.S., J.N. Malik, S.S. Merh, and R.V. Karanth (1999) Active tectonics astride Katrol Hill zone, Kachchh, western India, Journal of the Geological Society of India, **53**, 579-586.

Chapter 2: Mainshock Rupture

by

Paul Bodin[1]
Assistant Research Professor
Center for Earthquake Research and Information
The University of Memphis

1. Summary

A frustrating enigma of the Bhuj earthquake is that the properties we most seek to understand—its rupture location, source processes, and nearfield ground motions—are subject to very little direct observational constraint. Instead of ground motions being recorded by strong motion accelerographs, we have only the ambiguous testimony of the damage and geological effects to infer what ground motions were. Instead of a surface rupture making manifest which fault (and how much of it) ruptured, we have widespread secondary effects of lateral spreads. Instead of clear images of surface deformation from Interferometric Radar images, or satellite geodetic surface displacement vectors, we are left clutching at straws. The Bhuj earthquake was the 21st century, first really important earthquake, and yet in many ways many of our modern tools to understand the details of such events were frustrated for various reasons. That gloomy statement made, we can say some preliminary things about the rupture now, and future studies of existing observations should permit us to constrain the source processes in ways we cannot at present. But this will take time. Future developments hinge on analyzing regional seismograms (recorded at Indian network stations) of the mainshock and the larger aftershocks.

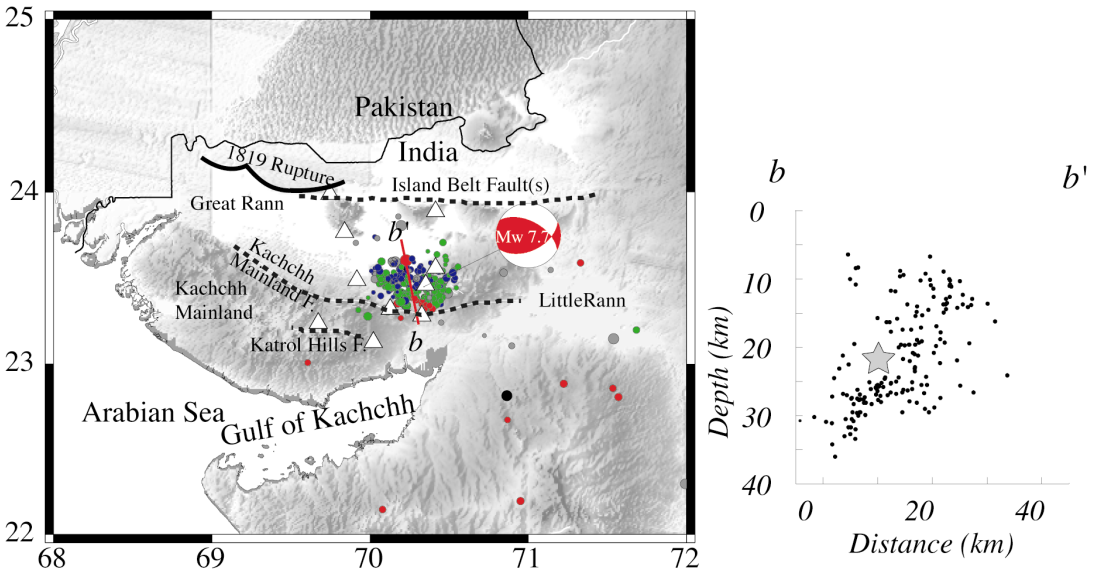

Figure 2-1: Aftershock distribution in map and cross-section (inset). Locations shown on inset are JHD relocations of the best-recorded aftershocks in the set. Surface mapped faults are shown schematically

[1] PB, CERI, 2890 Central Avenue, St. 1, Memphis, TN 38152-3050 USA,
email: bodin@ceri.memphis.edu

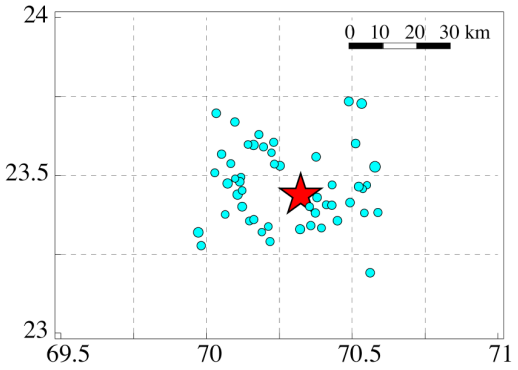

Figure 2-2: Relocated epicenters of the largest aftershocks (circles) and the mainshock (star). The relocations are by Engdahl and Bergman (personal communication) and are joint "relative" relocations, using MAEC/ISTAR portable aftershock data for the overlapping events as constraints

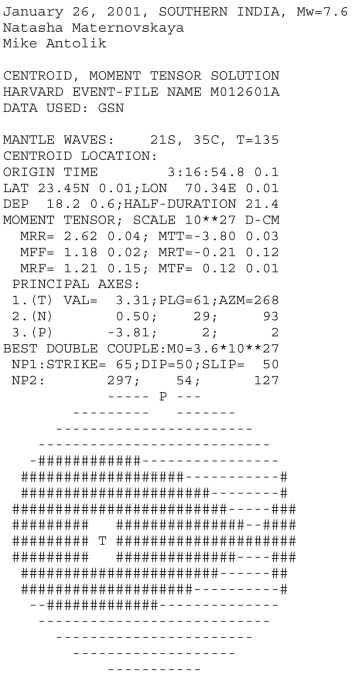

Figure 2-3: Harvard centroid moment tensor solution for the Bhuj earthquake. The solution uses long-period mantle waves of GSN stations to estimate the overall size and orientation of the Bhuj earthquake rupture

What we would really like to know about the mainshock is where the rupture took place, how much it slipped, how much strain it took to drive it. The observations we have available so far are intensity data, teleseismic observations, and aftershock occurrence—all observations nearly half a century old. Fortunately recently developed analytical methods and cheap fast computers permit us to present some preliminary estimates of the processes we want to model.

2. Aftershock Observations

In the absence of surface rupture and geodetic deformation, aftershock data provide evidence to suggest source location and orientation. Stations from the MAEC/ISTAR temporary seismic network were well-distributed with respect to the aftershocks, and provide a reasonable picture of the aftershock distribution. Figure 2-1 reveals the distribution of aftershocks recorded by our temporary network. Only about 300 aftershocks of the estimated total of ~2200 that were recorded on enough stations to locate are shown in the figure. The aftershocks highlight an area that does not coincide with a mapped fault. Although the epicenter lies close to the surface trace of the Kachchh Mainland fault, the aftershocks dip strongly southward (along section b-b' in Figure 2-1); a surface projection of the aftershock cloud would daylight somewhere south of the Island Belt fault zone. The aftershocks are distributed through a volume, but the densest part of the cloud lies between 10 km deep and 35 km deep, suggesting that perhaps fault slip was largest in this depth range. The mainshock hypocenter, derived from teleseismic seismograms, is in the center of the aftershock swarm at a depth of about 20 km.

Figure 2-2 illustrates that there are strong concentrations of aftershocks along two trends—one east of the epicenter, and one several 10s of km to the west. The epicenter is relocated to lie in a quiescent zone for the larger aftershocks

that are shown on the figure. One possible interpretation of these observations is that from its initiation, the rupture proceeded both up-dip, and down-dip, as well as to the east and to the west. The eastward propagation stopped relatively quickly, while the westward propagation continued a bit farther before it was stopped. The down-dip propagation may have converged a bit—making a bit of a "point" at the bottom of the rupture. The up-dip propagation climbed to at least 10-5 km. The resulting rupture plane would have a sort of triangular aspect, some 50-60 km across the top and tapering down to 10 km or so at the deep point.

3. Teleseismic Observations

The Bhuj earthquake was well-recorded by the seismograph stations of the Global Seismographic Network. The waveforms so recorded were analyzed very quickly, and a moment tensor calculated by Harvard for the Centroid Moment Tensor (CMT) catalog (Figure 2-3). The resulting CMT indicated a deep crustal rupture, on one of two possible roughly E-W striking fault planes, dipping about 50° - 55°. The seismic moment was estimated to be about 3.6 X 10^{27} Dyne-cm.

Once a fault plane has been chosen, models of slip on the fault can be generated. All such models use the fit of synthetic seismograms to observed teleseismic phases in order to find the best-fitting model (e.g. Figure 2-4). For the Bhuj earthquake, the earliest model we are aware of, and illustrated in Figures 2-4 through 2-6, was offered by researchers at the University of Tokyo (Yagi and Kikuchi, 2001). Figure 2-5 illustrates the overall slip model they compute for the southward-dipping nodal plane, and Figure 2-6 shows a snapshot of how the slip was modeled to have proceeded in time. We show these images as examples of teleseismic waveform-constrained models of the mainshock source processes, not because we believe them to be the

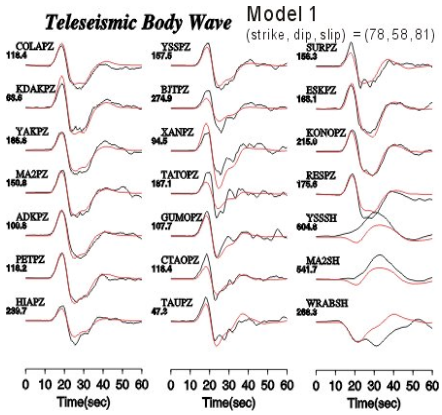

Figure 2-4: Illustration of fits to teleseismic body waveforms (from Yagi and Kikuchi, 2001)

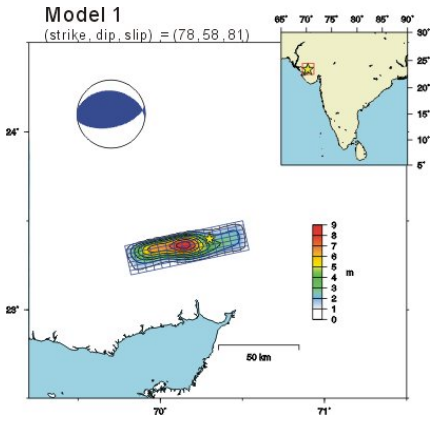

Figure 2-5: Slip distribution on south dipping plane (from Yagi and Kikuchi, 2001)

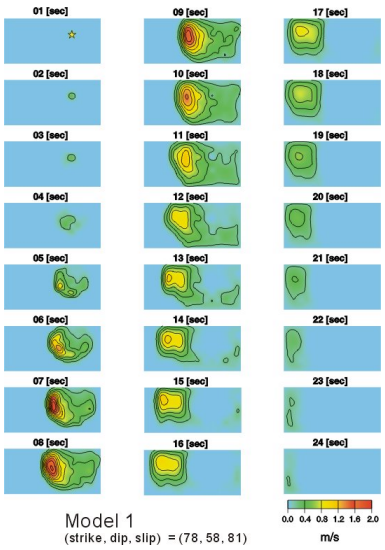

Figure 2-6: 1-second "snapshots" of slipping area on model rupture. Final slip model shown in figure 2-5. (from Yagi and Kikuchi, 2001)

"true" picture. In fact the resolution of such models needs to be evaluated quite carefully, combined with sensitivity analyses, and compared with the results from other methods before a sense of how well the data are resolving real slip on a fault can be stated.

An additional source of information about the mainshock comes from the best-fitting source-time function (or moment release rate function, Figure 2-7). We show a source time function computed by Larry Ruff at U. of Michigan. The source time function tells us how the rate of moment release changed in time. The Bhuj earthquake source-time function is very simple for an earthquake of its size. Larger earthquakes tend to have more complex source-time functions as, presumably, fault slip speeds up and slows down, and is affected by geometrical irregularities on a large rupture plane.

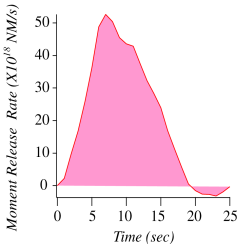

Figure 2-7: Moment release rate function of the Bhuj mainshock, (by Ruff, 2001)

All such analyses are based on teleseismic waveforms and while they may use different phases or analytical techniques, their results have common elements (See also Antolik and Draeger, 2001). The rupture started at mid-crustal depths, 20-25 km. It propagated to the west, where the largest slip (a patch with 9-12 m of slip) occurred. Within this patch, slip velocities of nearly 200 cm/s took place, which corresponds to quite high dynamic stress drops (Ruff (2001) estimates a dynamic stress drops of 10,5 MPa). Different models suggest different things about how deep slip took place. The Yagi and Kikuchi model suggests up to 3 m of slip occurred at depths below about 25-30 km. Antolik and Draeger (2001), however, suggest that little slip took place at depths greater than the mainshock.

4. Common Threads and Future Work

Pictures of the Bhuj mainshock derived from teleseismic models and aftershock locations have some common features. Primarily, the rupture was unusually deep. The rupture area was small compared for the seismic moment released, and the average stress drop and slip was high. Moreover, it appears that most of the moment was released in a relatively small patch to the northwest of the epicenter.

Future work on the rupture processes of the Bhuj earthquake will include refinements and sensitivity tests of the sort of model discussed in this chapter. However, we may anticipate that mainshock and large aftershock seismograms recorded at regional distances (i.e. from Indian broadband seismic stations) will permit us to add important observational constraints that are currently unavailable.

5. References

Antolik, M. and D. Draeger (2001) Preliminary Source Inversion of the 26 January Bhuj, India, Earthquake American Geophysical Union Spring Meeting, Boston, MA.

Ruff, L. (2001) http://www.geo.lsa.umich.edu/SeismoObs/STF.html

Yagi and Kikuchi (2001) http://wwweic.eri.u-tokyo.ac.jp/yuji/southindia/index.html

Chapter 3: Aftershock Measurements

by

Stephen Horton[1] (Research Scientist), Paul Bodin[2] (Assistant Research Professor)
and Mitch Withers[3] (Seismic Networks Director)
Center for Earthquake Research and Information, University of Memphis

1. Introduction

We deployed seismic instruments to record aftershocks of the Mw=7.7 Republic Day (26 January) 2001 earthquake in Gujarat, India. We recorded nearly 2000 events during the 18 day deployment. The largest aftershock has mb=5.2 (PDE), and several have mb>4.0. The largest acceleration recorded by our network was 108.8 cm/s^2 (0.11 g) at a station 20 km from a mb=4.7 (PDE) earthquake.

In this report we present pertinent details regarding the seismic network and instrumentation, and then results of our preliminary analysis of the aftershocks. The analysis of aftershock data occurs in stages. Our analysis to date is fairly routine. We have located a subset of the aftershocks, we have obtained a reasonable velocity model for the region, and we have generated first motion focal mechanisms. We are in the early stages of estimating magnitude of the recorded aftershocks, and we recently began to model waveforms. The analysis is ongoing and will address other issues in the future.

2. Seismic Instrumentation

We deployed 8 Kinemetrics K2 digital recorders near the main shock epicenter. A typical field set-up is shown in the picture below. Each K2 included an internal triaxial force-balance accelerometer set to full scale of 2 g and a built-in GPS timing system. An external velocity sensor (Mark Products triaxial L-28) was also attached to each K2 to insure detection of weak ground motion. All six channels were recorded at 200 samples per second. An external battery and solar panel provided power. Each K2 was operated in a STA/LTA triggered mode with a trigger ratio of 4 on all channels. Pre-event time was 10 s, and post event time was 20 s.

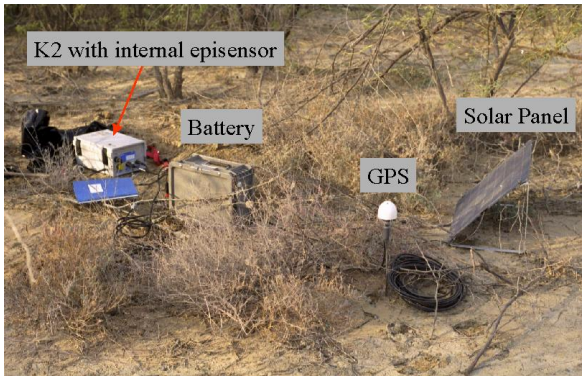

Figure 3-1: Seismic instruments deployed at station L1Q1

[1] SH, 687 Loeb St., Memphis, TN 38111 USA,
email: horton@ceri.memphis.edu
[2] PB, CERI, 3890 Central Avenue, St. 1, Memphis TN 38152-3050 USA,
email bodin@ceri.memphis.edu
[3] MW, CERI, 3890 Central Avenue, St. 1, Memphis, TN 38152-3050 USA,
email: bodin@ceri.memphis.edu, withers@ceri.memphis.edu

Event data were stored on an internal 182MB PCMCIA card. Each site was visited about every 48 hours to transfer data from the PCMCIA card to a PC. Data was ultimately written to CD for storage and transportation to the US. At CERI, data were converted into *ah* format to be compatible with the regional processing software, and into *mseed* format for incorporation into the IRIS database. Event association was performed based on trigger times at station KHA1. Events were declared when at least 3 other stations triggered within a 30 s window around trigger times at KHA1. We have nearly 2000 events satisfying this criteria.

The 8 station network was designed primarily for aftershock location. The figure below shows the location of stations and the main shock epicenter. The general intent was to surround the area of aftershock activity. The network configuration was moderately impacted by logistical constraints imposed by the location of our base of operations in Bhuj (LOT1 on map) and by the local road system. Travel time limited the extension of the network to the east. Available roads limited access to northern areas.

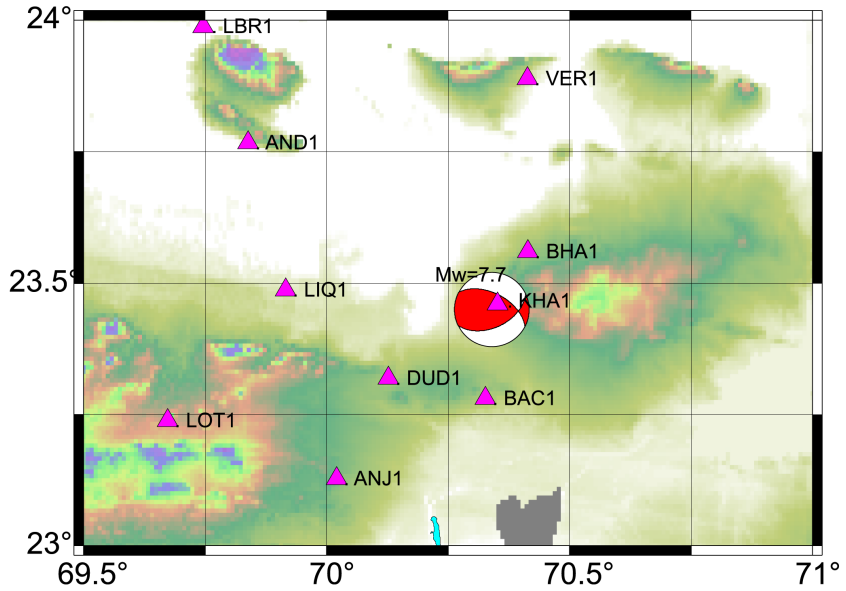

Figure 3-2: Network configuration during the aftershock deployment. Seismic stations are denoted by pink triangles. The epicenter of the main shock is shown by the focal mechanism (Harvard CMT). Colored areas are rock. White indicates deep sediments

Most stations were sited on sandstone, basalt or on a thin veneer of soil overlying sedimentary rock. LIQ1 is a notable exception. Intentionally located at the site of a large sand-blow, sediment thickness at LIQ1 is thought to be around 500 m. The thickness of sediments at KHA1 and DUD1 is also unknown.

3. Results

Approximately 300 events that triggered 6 or more stations have been located to date. XPICK was used to pick P-wave and S-wave arrival times. PQL was used to apply a 1Hz low-pass filter to waveforms for verifying or modifying arrival times. HYPOELLIPSE was used to locate the earthquakes.

We initially located 257 aftershocks using a velocity model purportedly used by the Indian Meteorological Department to locate regional events in Gujarat. For each event the velocity model is used by HYPOELLIPSE to calculate travel times of P-waves and S-waves to each station. HYPOELLIPSE then performs an iterative inversion to find the earthquake location and origin time that minimizes the root-mean-square of the travel-time residuals (observed minus predicted).

We averaged the travel-time residuals for each station over the 257 events. Stations close to the epicenter were found to have negative average residuals while stations at large distance were found to have positive residuals on average. This suggests the velocity model is too fast near the surface and too slow at depth, and that the velocity model should be modified.

We inferred a new velocity model from arrival time curves for both P- and S-waves. The figure on the left below shows our starting and favored velocity models. The aftershocks were grouped into 5 km depth bins, and the observed and predicted travel times plotted against epicentral distance, as in the adjacent figure. Predicted S-wave travel times are early at close distances, while both P-wave and S-wave travel times are late at long distances. This suggests the velocity model is too fast near the surface and too slow at depth.

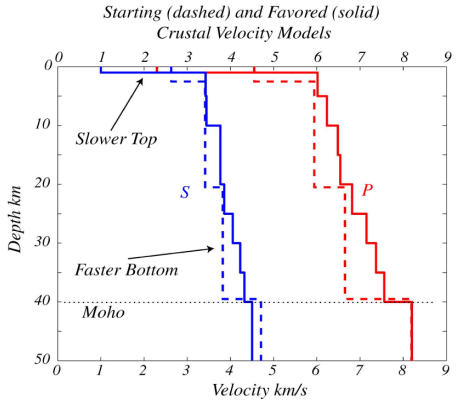

Figure 3-3: The starting velocity model (dashed lines) and the favored model (solid lines) are shown

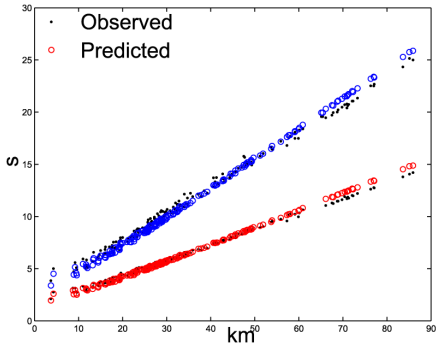

Figure 3-4: For aftershocks with depths between 20 and 25 km, predicted (circle) and observed (period) travel times are plotted

For each depth bin, we fit a 3rd order polynomial to the observed travel times, and take the derivative with respect to time. The resulting curves have units of slowness (s/km). The inverse, velocity (km/s), is plotted against epicentral distance in figure 3-5 for one depth bin. Apparent P-wave and S-wave velocities are large near the source (rays leave the source near vertical) reaching a minimum at a distance where rays leave the source horizontally. The minimum in each curve is the velocity at the depth of the source. At larger epicentral distances, rays leave the source going down and are turned at a higher velocity.

This method was used to produce the favored velocity model. Aftershocks occurred over a large depth range from around 5 to 40 km. The aftershocks were binned in 5 km depth intervals, and the velocity for that interval was obtained from the velocity curve minimum. The favored model is faster than the starting model at depth, and slower near the surface. (The slow velocity layer near the surface is discussed below.) We relocated the 257 events using the favored model and plotted predicted and observed travel times as a function of distance. An example is shown in the

figure 3-6. The systematic differences observed in the starting model are no longer observed. (Verification of the velocity model through waveform modeling is discussed later.)

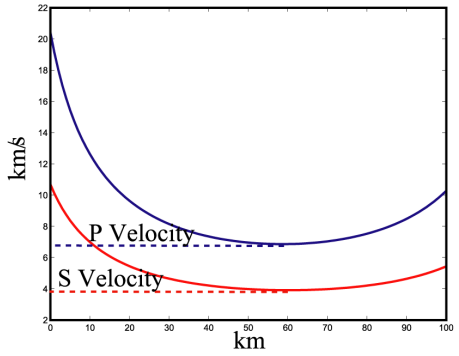

Figure 3-5: Plot of velocity obtained from observed travel times for depth range 20 to 25 km

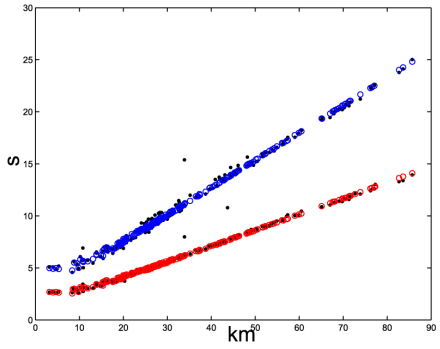

Figure 3-6: For aftershocks with depths between 20 and 25 km, predicted (circle) and observed (period) travel times are plotted

The geologic cross-section below shows that the top of the Precambrian is generally shallow in the study area varying in depth from about 1 to 3 km beneath the surface. The shallow depth to Precambrian rock explains the generally high velocities in our model. The Precambrian surface is overlain by a relatively thin veneer of unconsolidated sediment, sedimentary rock or basalt.

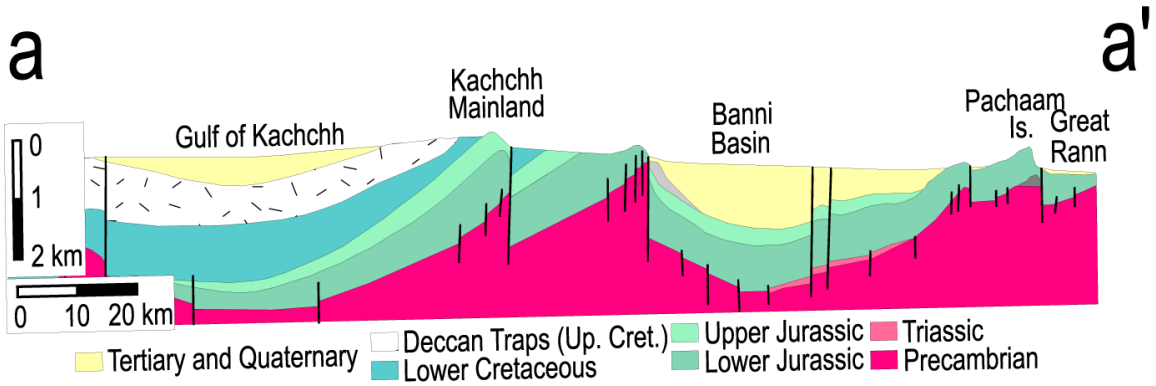

Figure 3-7: North-South geologic cross-section of the study area. The section location is shown in the epicenter figure later in this section. The section illustrates that Precambrian basement is quite shallow beneath Kachchh, overlain by one to two kilometers of indurated Mesozoic sediment, and with shallow basins of Tertiary unconsolidated sediment

The method used to determine velocity above was not applicable to the upper 5 km since aftershocks did not occur in this depth range. However, an apparent converted phase observed at most stations in the network indicates a low velocity layer at the surface overlying a much faster layer. Figure 3-8 shows an example of this converted phase at station DUD1. In this example the S-P conversion arrives 0.9 s before the S-wave arrival. The timing of the converted phase varies for each station, but it is consistent between earthquakes at any given station. The overall character of the converted phase suggests that vertical S-wave motion is converted to a P-wave at the top of the Precambrian. This energy travels at the P-wave velocity through the upper layer and so arrives earlier than the S-wave. A preliminary screening of this phase gave an average

advancement of about 0.7 s over the network. We adjusted the thickness and velocity of the surface layer accordingly.

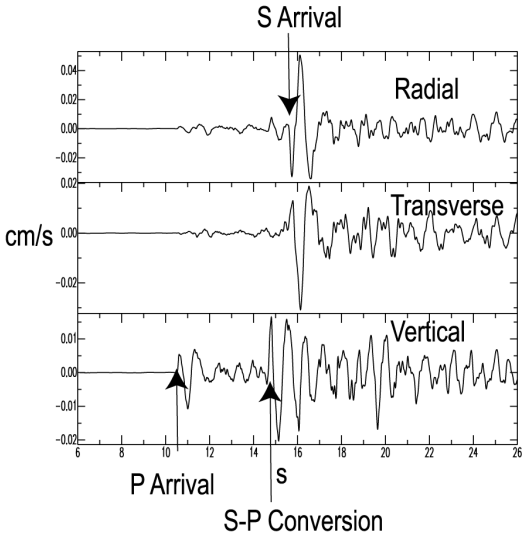

Figure 3-8: Seismograms at DUDI show an arrival on the vertical component 0.9s before the S-wave arrival on the horizontal components

Figure 3-9 shows the location of approximately 300 aftershocks. The epicenter of the main shock lies close to the center of aftershock activity. These epicenters lie well south of the Island Belt fault, and just north of the Kachchh Mainland fault. The distribution of epicenters suggests a nearly east-west fault plane approximately 40-50 km in length and would be consistent with either main shock nodal plane.

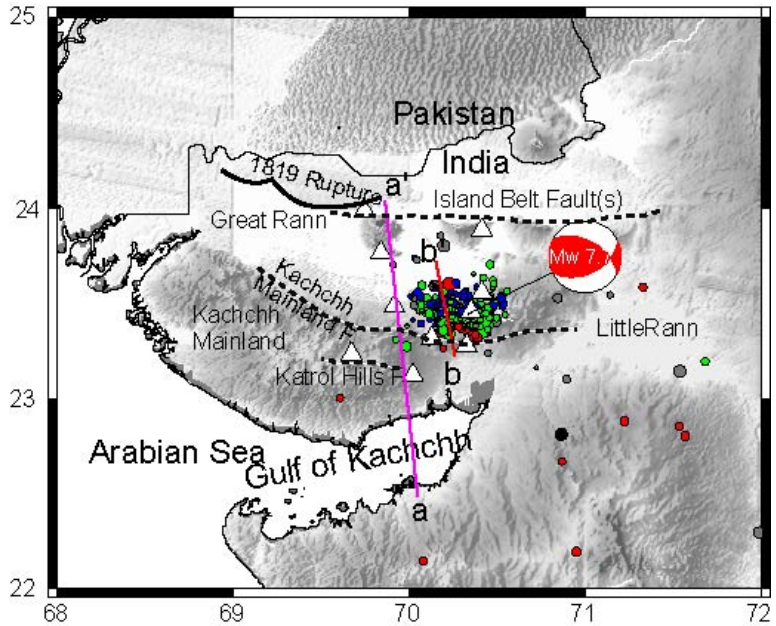

Figure 3-9: Epicenters (small circles) are shown on a shaded relief map. Triangles are locations of seismic stations. Prominent faults are labeled. Shallow geology along a-a' is shown two figures above. Depth distribution of aftershocks along b-b' is shown below

A north-south cross section below shows the depth of aftershocks. The depth distribution of aftershocks suggests a south dipping fault plane of 20-30 km down-dip length. These earthquakes are unusually deep with depths ranging from 5 to 35 km.

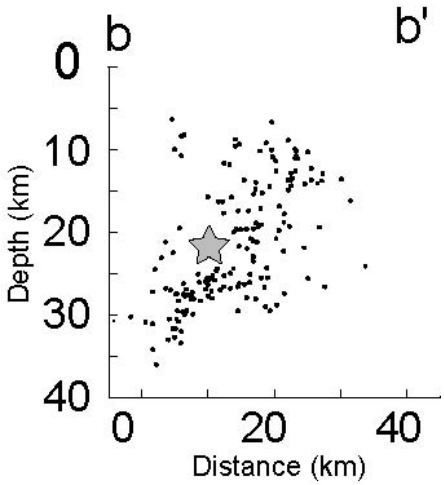

Figure 3-10: Cross section along b-b' in figure above showing hypocenters projected onto vertical plane

Focal mechanisms were generated for the 300 aftershocks using FPFIT. The focal mechanisms are plotted in figure 3-11. A large variety of fault mechanisms are observed. These mechanisms were constrained by first motions at 8 or fewer stations, and have not been evaluated in detail to determine stability. However, the focal mechanism shown in the next figure (waveform modeling) is fairly well constrained with 5 observations. The size of the focal sphere reflects a relative magnitude scale adopted for this study. The magnitude is determined from S-wave amplitude averaged across the network. We are attempting to tie the relative scale to Mw through waveform modeling. This work is in the beginning stage.

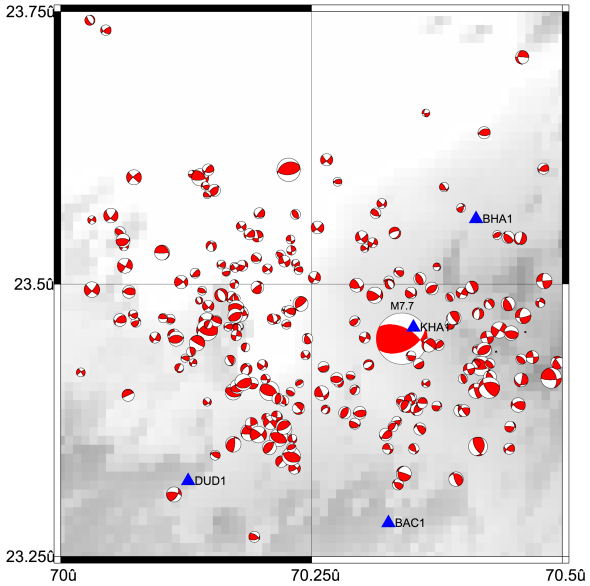

Figure 3-11: Focal mechanisms of aftershocks. These are lower hemisphere projections with the tension quadrant colored red

Waveform modeling has been started for several of the larger aftershocks. An example of the observed and synthetic waveforms is shown in the figure below. The synthetics were generated using the focal mechanism produced by FPFIT. The uncertainty in strike and dip is 13° and uncertainty in rake is 10°. The waveforms fit the general sense of motion at most stations well. The synthetics were generated using a discrete wave-number integration program with the favored velocity model discussed above. In general, timing of arrivals is good indicating the velocity model is reasonable.

In addition, the absolute amplitudes of the observed and synthetic waveforms agree very well with the exception of LIQ1. Although this event has an mb=4.5 (PDE) and a relative magnitude size of 4.6, the Mw used to generate the synthetics is 4.0. Using Mw=4.5 generates synthetics that are obviously too large at all stations, while using Mw=3.5 generates synthetics that are obviously too small. Refinement of this work will likely produce synthetics that constrain Mw to within 0.25 Mw units at least for the larger events.

At LIQ1 the observed waveform is significantly larger and later in arrival than the predicted. This suggests a slower surface velocity is needed for this station. Since LIQ1 lies atop approximately 500 m of unconsolidated sediment, it would be reasonable to introduce a lower near-surface velocity for this station. A slower surface velocity would delay the S-wave arrival time and increase its amplitude.

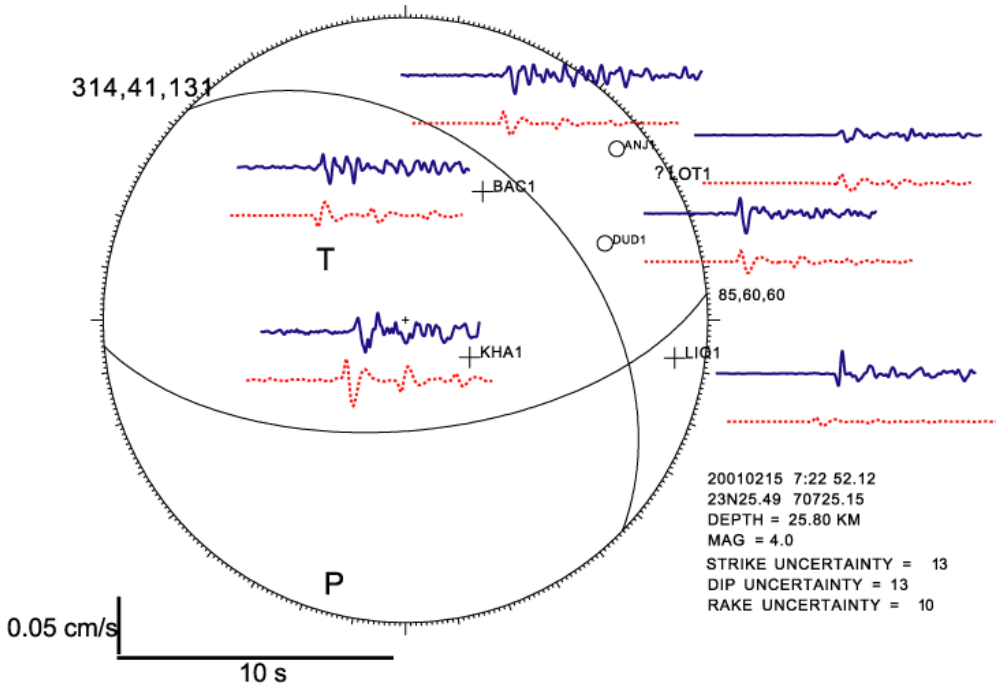

Figure 3-12: Observed and synthetic waveforms for mb=4.5 aftershock. The focal mechanism is fairly well constrained with 5 observations. The synthetics were generated for a Mw=4.0 earthquake with a 50 bar stress drop. Both synthetic and observed waveforms are bandpass filtered around 1Hz. The observed waveforms are the solid blue lines and the synthetic are the red dashed lines. The waveforms are plotted in proximity to the station location on the focal sphere

4. Summary

We present preliminary analysis of aftershocks of the Mw=7.7 Republic Day (26 January) 2001 earthquake in Gujarat, India, recorded on a network of 8 portable digital event recorders. During the 18 day deployment, this network recorded nearly 2000 earthquakes, almost exclusively M<5 events within about 100 km of all stations.

Approximately 300 aftershocks have been located to date. The distribution of epicenters suggests a nearly east-west fault plane ~40-50 km in length. The depth distribution of aftershocks suggests a south dipping fault plane of 20-30 km down-dip length. These earthquakes are unusually deep with depths ranging from 5 to 35 km.

We infer a velocity model from the arrival time curve for both P- and S-waves. The model with significant station corrections is currently used in location. Verification of the model through waveform modeling is just beginning.

First motion focal mechanisms have been generated. No preferred orientation is observed for aftershock focal mechanisms.

We are testing several options for determining earthquake size. At this point S-wave amplitude and RMS values averaged over the network are used to suggest relative size. We are attempting to use waveform modeling to determine Mw for the aftershocks.

Chapter 4: Liquefaction Features

by

Martitia P. Tuttle[1]
M. Tuttle & Associates

1. Abstract

The Mw 7.7 Republic Day earthquake in the Kachchh region of northwestern India induced liquefaction and related ground failures over an area >15,000 km^2 and possibly up to 250 to 300 km from its epicenter. Surface manifestations of liquefaction include sand blows, sand-blow craters, and lateral spreading. Lateral spreading was responsible for significant damage to water wells and pipelines in the epicentral area as well as to port facilities along the Gulf of Kachchh. In general, liquefaction features induced by the Republic Day earthquake are smaller than those produced by the 1811-1812 New Madrid earthquakes, which may be due to differences in ground motion and site conditions. Much remains to be learned from the Republic Day earthquake that would contribute to our understanding of earthquake hazards in intraplate settings, prediction of liquefaction and ground failure potential, and use of liquefaction features in paleoseismology.

2. Introduction

The Kachchh region of northwestern India was the location of a major earthquake in 1819. The 1819 event, known as the Kachchh earthquake, is one of the larger events to occur in an intraplate setting and produced widespread liquefaction (MacMurdo, 1824; Oldham, 1926; Johnston and Kanter, 1990). The recent Republic Day earthquake of moment magnitude, Mw, 7.7 also occurred in the Kachchh region. Aerial reconnaissance conducted soon after the event (Lettis and Hengesh, 2001), followed by a field survey and evaluation of satellite imagery conducted by the Mid-America Earthquake Center, has found evidence for liquefaction over an area >15,000 km^2 including parts of the Banni Plain, Great Rann, Little Rann, and Gulf of Kachchh (Figure 4-1).

The Rann of Kachchh and Banni Plain are low-lying areas underlain by a Holocene sedimentary sequence of sand, silt, and clay related to deltaic and estuarine deposition into an arm of the Arabian Sea (Malik et al., 1999). Today the Rann is flooded during the monsoon as the result of runoff from several large rivers as well as inundation by the Arabian Sea driven up the tidal estuaries of Kori Creek and the Gulf of Kachchh by strong onshore winds (Gupta, 1975). During the dry season, the surface of the Rann becomes encrusted with salt from evaporation of esturine brine. The Gulf of Kachchh is a present-day arm of the Arabian Sea and is characterized by extensive mudflats and salt pans along its margins.

According to many residents in the Kachchh region, fountains of water ranging from 1 to 2 m in height formed during and immediately following the earthquake. So much water vented to the surface in the Banni Plain and Great Rann that temporary streams of water flowed in previously dry channels. These streams, as well as the larger sand blows, are clearly visible on satellite imagery taken after the earthquake (Figure 4-2). Satellite imagery also suggests that liquefaction occurred near Naliya and Lakhpat along the coast about 180 km west of the epicenter. In addition, there are reports of ground failure indicative of liquefaction as far away as Ahmadabad, 250 km east of the earthquake epicenter, and even near Hyderabad, Pakistan, about 300 km northwest of the epicenter.

[1] MT, 128 Tibbetts Lane, Georgetown, MD 04548
email: mptuttle@eros.com

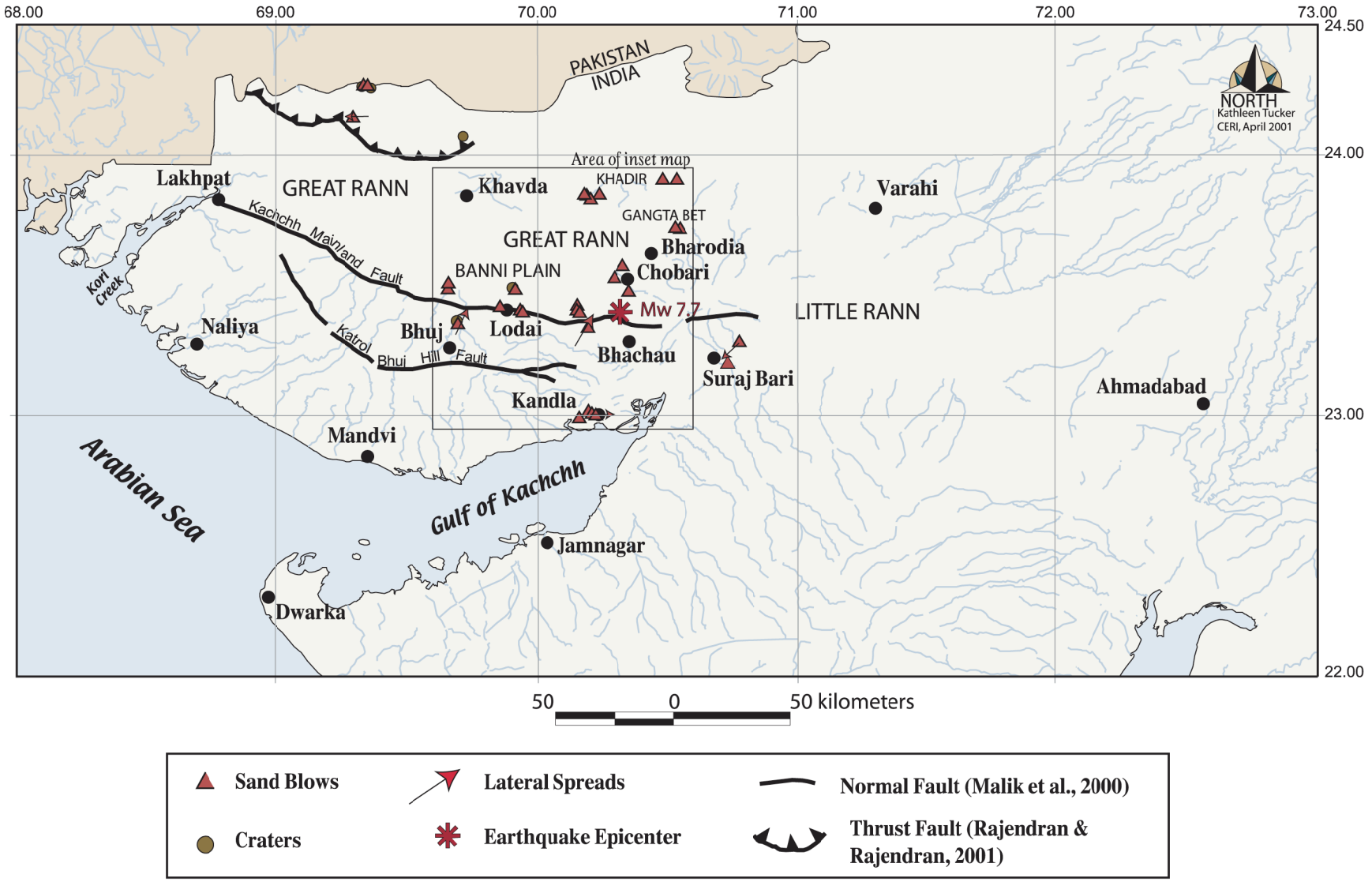

Figure 4-1: Map of the Gujarat region showing locations of documented liquefaction features relative to epicenter of January 26, 2001 earthquake

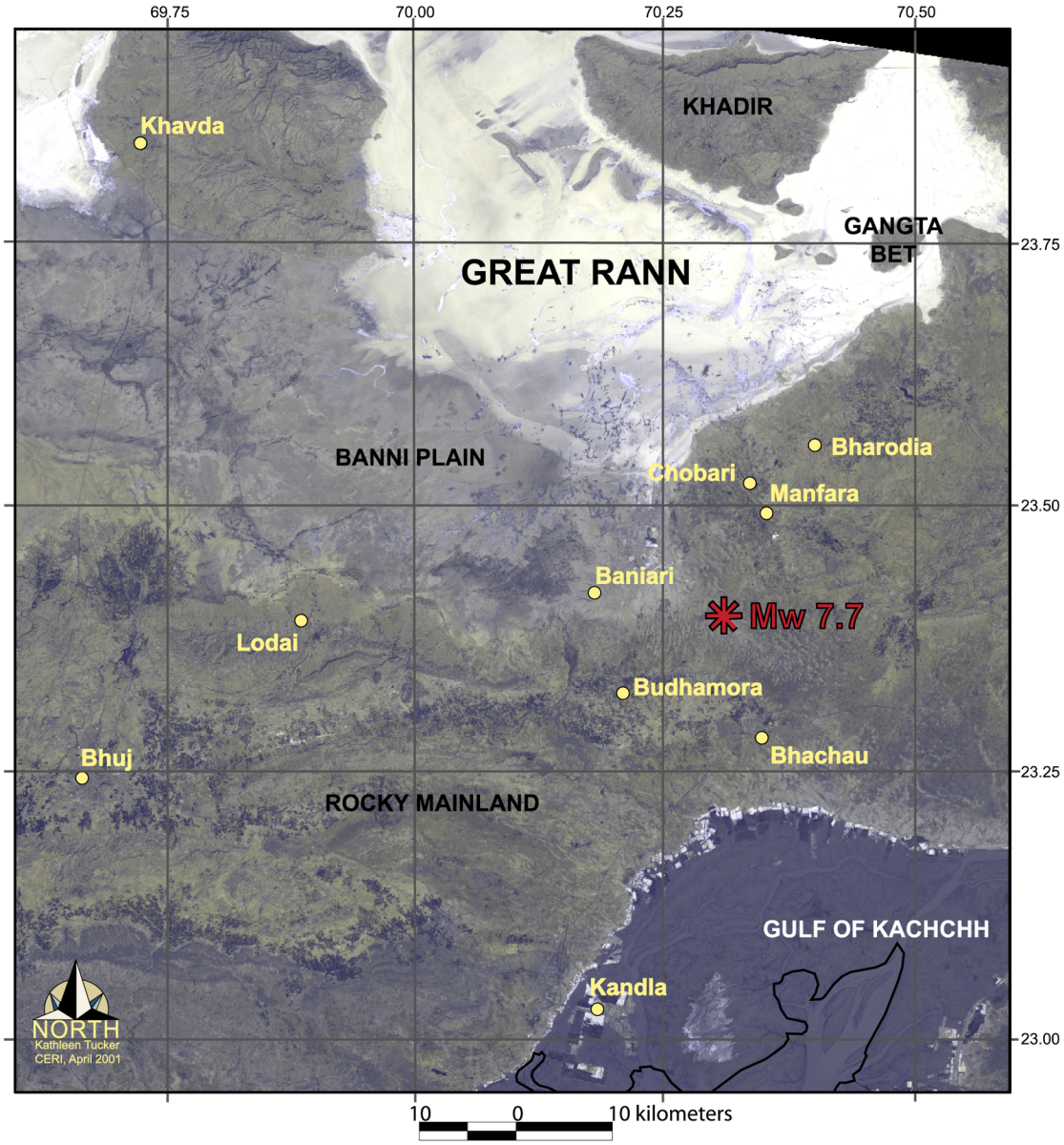

Figure 4-2: Satellite image (Thematic Mapper 7, RGB composite) of area of inset map shown in Figure 4-1. Temporary streams of vented water are purple in color and especially obvious along southern edge of Great Rann. Sand blow deposits are gray in color and often associated with temporary streams

There is considerable interest in the Republic Day earthquake as a modern analogue for the New Madrid earthquakes in the central United States. Like the very large 1811-1812 New Madrid earthquakes (e.g., Fuller, 1912; Kelson et al., 1996) and 1819 Kachchh earthquake (e.g., Oldham, 1926; Rajendran and Rajendran, 2001), the Republic Day earthquake induced widespread liquefaction, but apparently did not produce surface rupture. The New Madrid and Katchchh regions are underlain by rift basins that are currently under compressional stress. Both regions occur at more than 200 km from an active plate boundary and in stable continental crust characterized by low attenuation of ground motions (Johnston and Kanter, 1900).

The Republic Day earthquake offers a rare opportunity to study liquefaction and related ground failures generated by a large intraplate earthquake whose location and magnitude are well-known. This paper summarizes the results of a post-earthquake survey sponsored by the Mid-America Earthquake Center of liquefaction features and related ground failures in the Kachchh region.

3. Liquefaction Features in the Meizoseismal Area

During the post-earthquake survey, sand blows, sand-blow craters, and lateral spreads were documented in the epicentral area of the Republic Day earthquake, in the Banni Plain north of Bhuj, in the Great Rann of Kachchh near Gangta Bet and Khadir, near the Allah Bund and Pakistan Border, in the Little Rann near Suraj Bari, and along the Gulf of Kachchh near Kandla (Figure 4-1). The goal of the survey was to characterize the range in type, size, and orientation of liquefaction-related features in the meizoseismal area. The liquefaction survey was by no means comprehensive. However, an attempt was made to document liquefaction sites along N-S and E-W transects roughly perpendicular to and along the strike of the fault inferred from the focal mechanism of the mainshock and distribution of the aftershocks. For each site, the geomorphic setting was noted and liquefaction features measured including the length, width, orientations, and thickness (measured near vents) of sand blows; the length, width, orientations, and depth of sand-blow craters; and length, width, and amount and bearing of horizontal and/or vertical displacement of lateral spreads (Figure 4-3; Appendix). Several examples are described below.

Sand Blows

Sand blows, or constructional cones of predominantly sand vented to the ground surface through ground fissures, are the most common liquefaction features observed in the meizoseismal area. The sand blows in the Kachchh region range from 10s of centimeters to 10s of meters in length and up to a couple of decimeters in thickness. Review of satellite images suggests that a few sand blows larger than those documented during the field survey occur north of the epicenter in the Great Rann.

Along the boundary between the Banni Plain and the Great Rann, where temporary streams flowed during and immediately following the earthquake, many moderate-size sand blows formed (Figure 4-3). For example, about 20 km north of the epicenter, sand blow deposits are abundant along a 70 m-wide zone that water had occupied after the earthquake and was still wet a month after the earthquake. Sand blows in this area range up to 60 m in length, 12 m in width, and 14 cm in thickness (Figure 4-4).

Farther north in the Great Rann, near Gangta Bet and Khadir Island, sand blows are considerably smaller (Figure 4-3). For example, 50 km north-northwest of the epicenter and just a few kilometers southwest of Khadir Island, sand and silt blows range up to 13 m in length, 12 m in width, and 5 cm in thickness (Figure 4-5). The sand and silt blows documented in this area occur close to the northernmost surface projection of the seismogenic fault inferred from mainshock and aftershock data and are likely to occur on the footwall of the fault.

South of the Banni Plain in the Rocky Mainland, small sand blows, on the order of 2 to 4 m in length, occur in association with lateral spreads within 20 km of the epicenter and along river channels at greater distances (Figure 4-3). Sand blows within lateral spreads typically formed along fissures oriented parallel to head-scarp grabens and roughly perpendicular to the downslope direction (Figure 4-6).

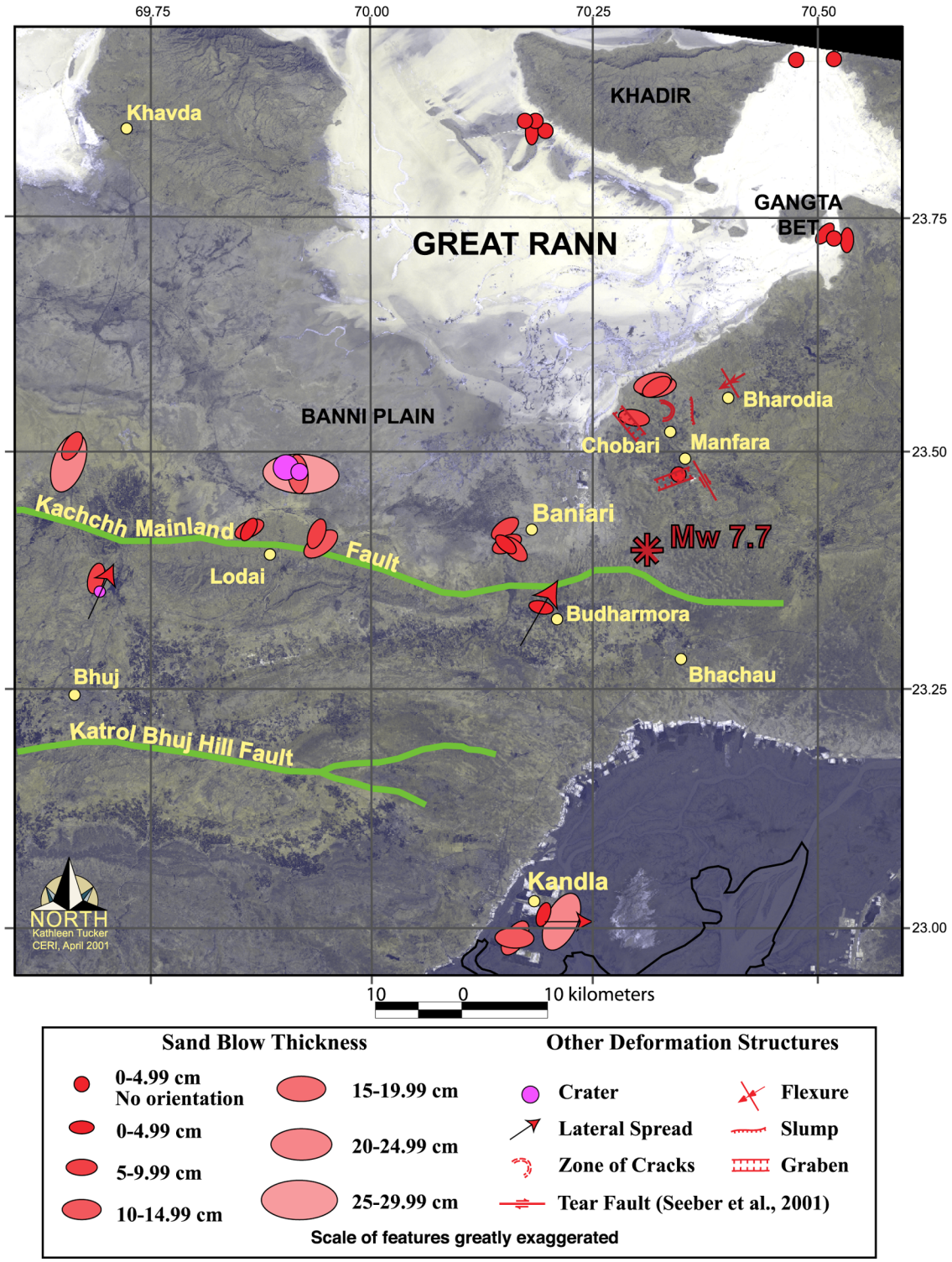

Figure 4-3: Locations of documented liquefaction features and other deformation structures superimposed on satellite image of area of inset map shown in Figure 4-1. Size and orientation of sand blows and sand-blow craters as well as direction of lateral spreading are indicated

Figure 4-4: Moderate-size sand blow in Great Rann northwest of Chobari

Figure 4-5: Silt blow in Great Rann southwest of Khadir Island. Recent deposition of salt marks area covered by vented water following the earthquake

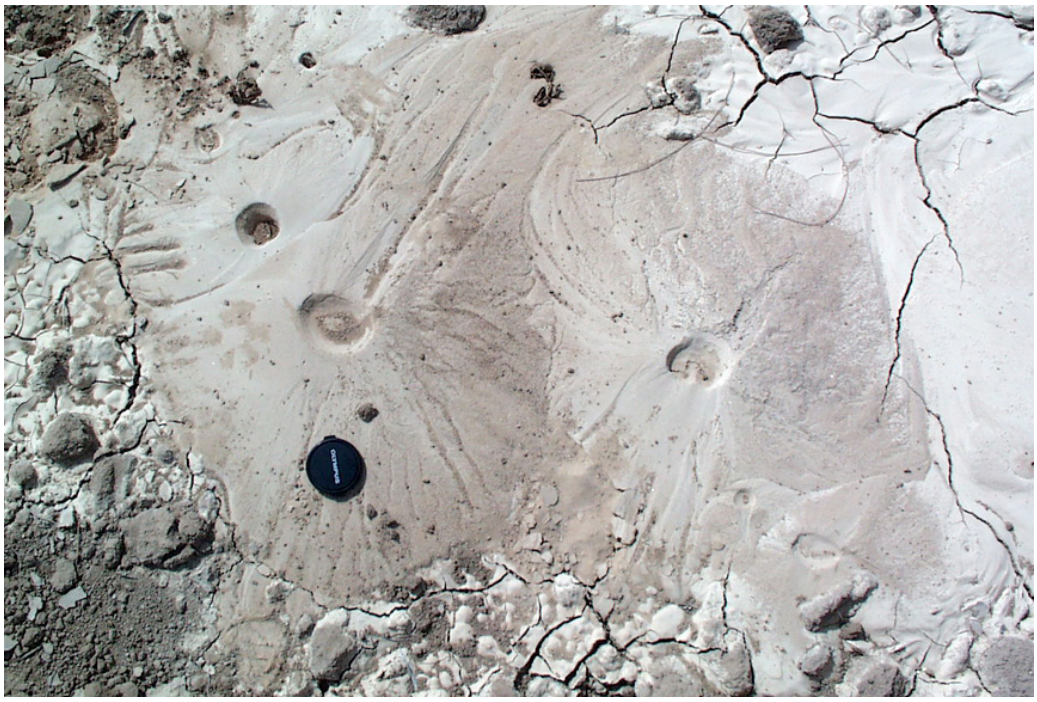

Figure 4-6: Small sand blows within lateral spread at near Budharmora about 14 km from earthquake epicenter. Camera lens for scale

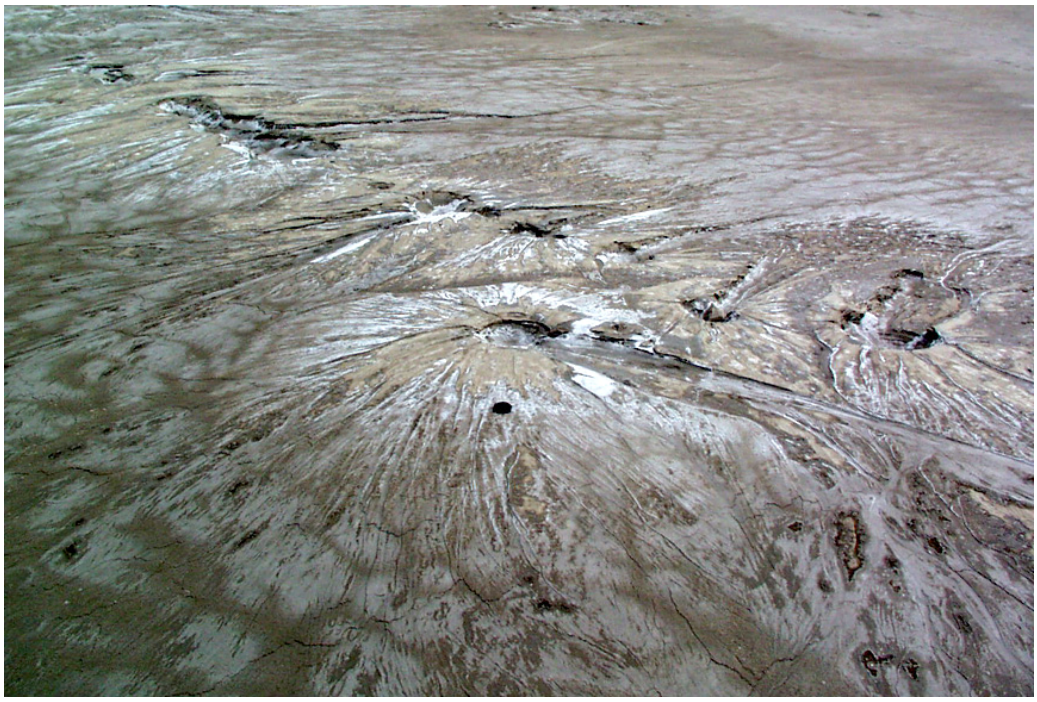

Figure 4-7: Sand blow, 12 m long, 7 m wide, and 14 cm thick, that formed in mud flats used for salt production near Kandla. Multiple vents are aligned along ground fissure through which water and sand vented. Lens cap for scale

About 50 km south of the epicenter, many small to moderate-size sand blows formed in the mudflats and salt pans along the northern margin of the Gulf of Kachchh (Figure 4-7). The largest sand blow documented near Kandla is 15 m long, 10 m wide, and 20 cm thick. Many of the sand blows in this area had similar orientations between N20°E to N50°E, subparallel to the axis of the Gulf of Kachchh. The formation of the sand blows may be related to extension perpendicular to the Gulf. Other sand blows at Kandla Port clearly formed in association with lateral spreads.

Sand-Blow Craters

Like sand blows, sand-blow craters are characterized by constructional sand aprons. Unlike sand blows, they have large central craters formed by the removal of surface soil and sediment. Sand-blow craters are not as common as sand blows and only a few sand-blow craters have been documented in the meizoseismal area so far. Their sand aprons are similar in size to those of sand blows and their central craters range from about 1.5 m to 10 m across. The largest sand-blow crater documented is located near Umedpur about 45 km west-northwest of the epicenter (Figure 4-8). The central crater, which was still filled with water a month after the earthquake, is 10 m by 5 m in plan view. The vented sand deposit is 33 m long, 32 m wide, and 26 cm thick (Figure 4-9).

Also at the Umedpur site, two unusual craters formed that are 2.4 m by 1.8 m and 1.6 m by 1.5 m in plan view and about 1.4 m deep (Figure 4-10). The craters walls are dry and irregular and did not appear to have formed by or been filled with water (Figure 4-10). A round hole dipping at about a 45° angle towards the east occurs near the base of one of the craters. The ground surface adjacent to the craters is broken and a field of ejected clasts extends 26 m towards the west.

Figure 4-8: Large sand-blow crater near Umedpur. Channels incised in sand apron filled with late phase deposition of silty clay. Back pack for scale

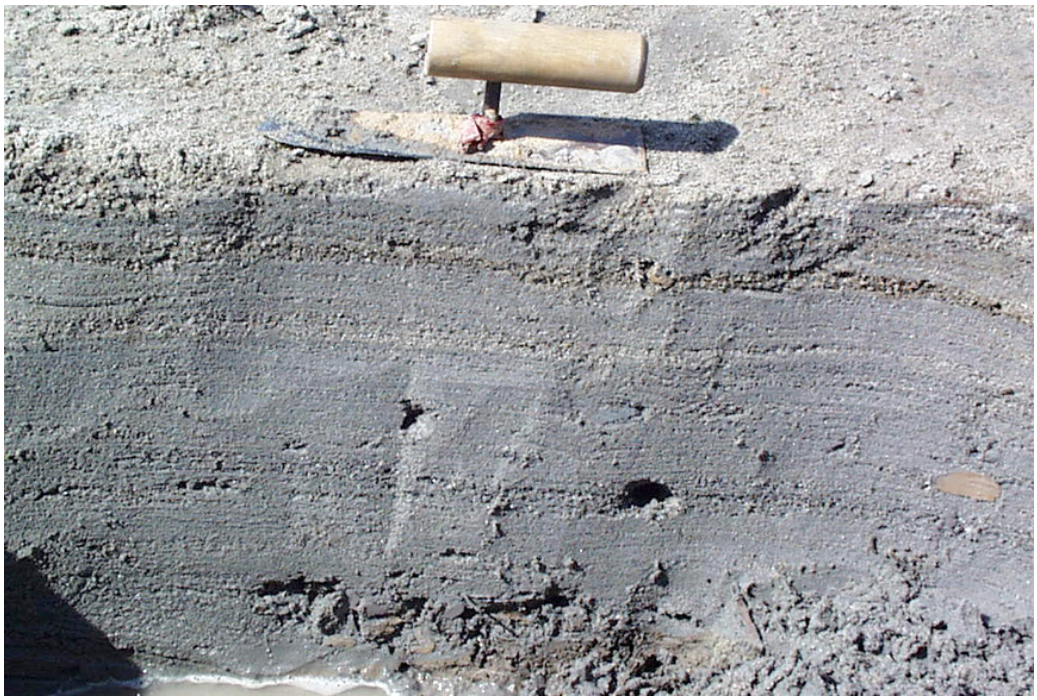

Figure 4-9: Excavation of vented sand deposit adjacent to large crater at Umedpur. Deposit is composed of medium to coarse sand containing small clasts of clay overlain by interbedded coarse, medium, and fine sand. Hand trough for scale

Figure 4-10: Unusual craters and broken ground at Umedpur site. Craters may have formed by some mechanism other than venting of water from liquefied deposit below

A silty clay deposit, interpreted as a distal portion or late phase of the vented deposit associated with nearby sand blows, was broken by the dry craters. In addition, the ejected clasts formed impact craters in the silty clay. A thin layer of silty clay was also deposited over the clasts. These observations suggest that the craters formed after liquefaction and venting of subsurface sediment but while silty water was still ponded on the surface. The mechanism of formation of these unusual features is uncertain at this time. One hypothesis is that natural gas in a reservoir at depth was released during the earthquake. This would be similar to the release of gas along fractures associated with the Clarendon-Linden fault in western New York State triggered by the 1988 Saguenay, Quebec, earthquake (Jacobi and Fountain, 1993).

Lateral Spreads

Lateral spreading occurred on gentle slopes (1 to 2°) in the epicentral area and along rivers and bays at greater distances. In the epicentral area, lateral spreading was responsible for damage to many water wells and pipelines. One such example occurs near the village of Budharmora. At the site, there is a disturbed area 140 m across and at least 400 long that trends N70 to 85°W. The pre-event ground surface slopes about 1° towards the north. A water pipe, that is roughly parallel to the downslope direction, is broken and displaced in several places. In the upslope portion of the disturbed area, ground deformation includes 0.35-m and 1-m wide grabens, extensional cracks and back-rotated blocks, and sand blows up to 3.5 m long, 50 cm wide, and 4 cm (Figures 4-11 and 4-12). The water pipe is broken and separated laterally in a N30 to 35°E direction across the two grabens. In contrast, sseveral uplifted linear features and related cracks occur in the downslope portion of the disturbed area. Here, the water pipe is broken and overlapping both laterally and vertically by at least 0.8 m. The disturbed area is clearly a lateral spread with extensional features at the head scarp and compressional features at the toe of the failure.

Figure 4-11: Graben in upslope portion of lateral spread near Budharmora. Water pipe, exposed in base of graben, broken and displaced by 1 m

Figure 4-12: Small sand blows in upslope portion of lateral spread at Budharmora. Local residents described 1-m-high water spouts issuing from ground fissures immediately following earthquake

Figure 4-13: House within graben south of Manfara titled as result of ground failure

In the epicentral area, there are numerous ground fissures and associated grabens that are associated with liquefaction features. This sort of ground deformation may be related to lateral spreading. For example, a 12-m-wide zone of N80°E oriented fissures and intervening conjugate cracks occurs south of the village of Manfara. The ground surface, which slopes about 1° toward the north-northwest, is displaced downward by 10-15 cm on the north side of the fissures and cracks within the zone, forming a stepped graben (Figure 4-13). According to local residents, water and sand had vented in the field south of the zone. Small sand blows are still present there. A trench excavated across the zone revealed sand dikes filling the fissures and cracks below the surface. Liquefaction clearly was involved in ground failure at this site. However, the orientations of the fissures and cracks suggest that roughly N-S oriented compressive stress may have played a role in the ground failure. Lettis and Hengesh (2001) attributed an east-northeast trending zone of ground cracks, bulges, and associated sand blows in the epicentral area to lateral spreading, possibly resulting from coseismic warping on the north flank of the Bauchau anticline.

4. Discussion of Observations

There is considerable variability in the size of sand blows across the meizoseismal area (Figure 4-3). However, sand blows at similar distances may be larger on the hanging wall side of the fault than on the footwall. For example, sand blows near Kandla and Lodai, on the hanging wall, are larger than sand blows near Khadir and Gangta Bet, presumably on the footwall. Could this apparent size difference be an artifact of sampling? Additional data is needed to test this possibility. If the characterization holds up with additional data, the question arises whether the size distribution of liquefaction features is related to ground motions or to liquefaction susceptibility of subsurface deposits.

The relatively large size of liquefaction features located west-northwest of the epicenter is intriguing (Figure 4-3). These large features include the sand blow-crater and dry craters at the Umedpur site described above. The large liquefaction features appear to occur in the fan-delta plains of the Kaswali and Pur Rivers. Deltaic deposits are thought to be especially susceptible to liquefaction (Youd and Perkins, 1987). Could the size of the features be related to the characteristics of the deposits that liquefied? In addition, the large features occur along the trend of one of the nodal planes of the mainshock focal mechanism. Could directivity of seismic waves have played a role in liquefaction in this area?

In general, sand blows appear to decrease in size with epicentral distance. For example, sand blows near Khadir are smaller than sand blows near Chobari and sand blows near the Pakistan border are smaller than the sand blows near Khadir (Appendix). Even less data is available for sand-blow craters, however, the largest one, 10 m by 5 m, is at Umedpur; whereas, sand blow craters near the Pakistan Border are the order of 4 m in diameter. Does the size of liquefaction features decrease in some fashion with epicentral or fault distance? Under what conditions do sand-blow craters form? What determines the size of the crater?

Only a few examples of lateral spreading and ground fissuring have been studied so far. In these cases, surface topography appears to have played an important role in their formation. However, conjugate cracks within zones of fissuring suggest that compressive force also may have influenced ground failure. Can orientations of sand dikes be used to make inferences regarding ground motions? In the geologic record, how would one differentiate sand dikes that formed as the result of gravity driven slope failures and those that reflect ground failure resulting from dynamic stress?

Liquefaction features have been verified in the field up to 150 km from the epicenter and there are reports of liquefaction 250 km, and possibly 300 km, from the epicenter. The maximum distance of liquefaction features induced by the Mw 7.7 Republic Day earthquake serves to calibrate magnitude-distance relations (Ambraseys, 1988), liquefaction severity index (Youd and Perkins, 1987), and other relations for intraplate earthquakes (Figure 4-14).

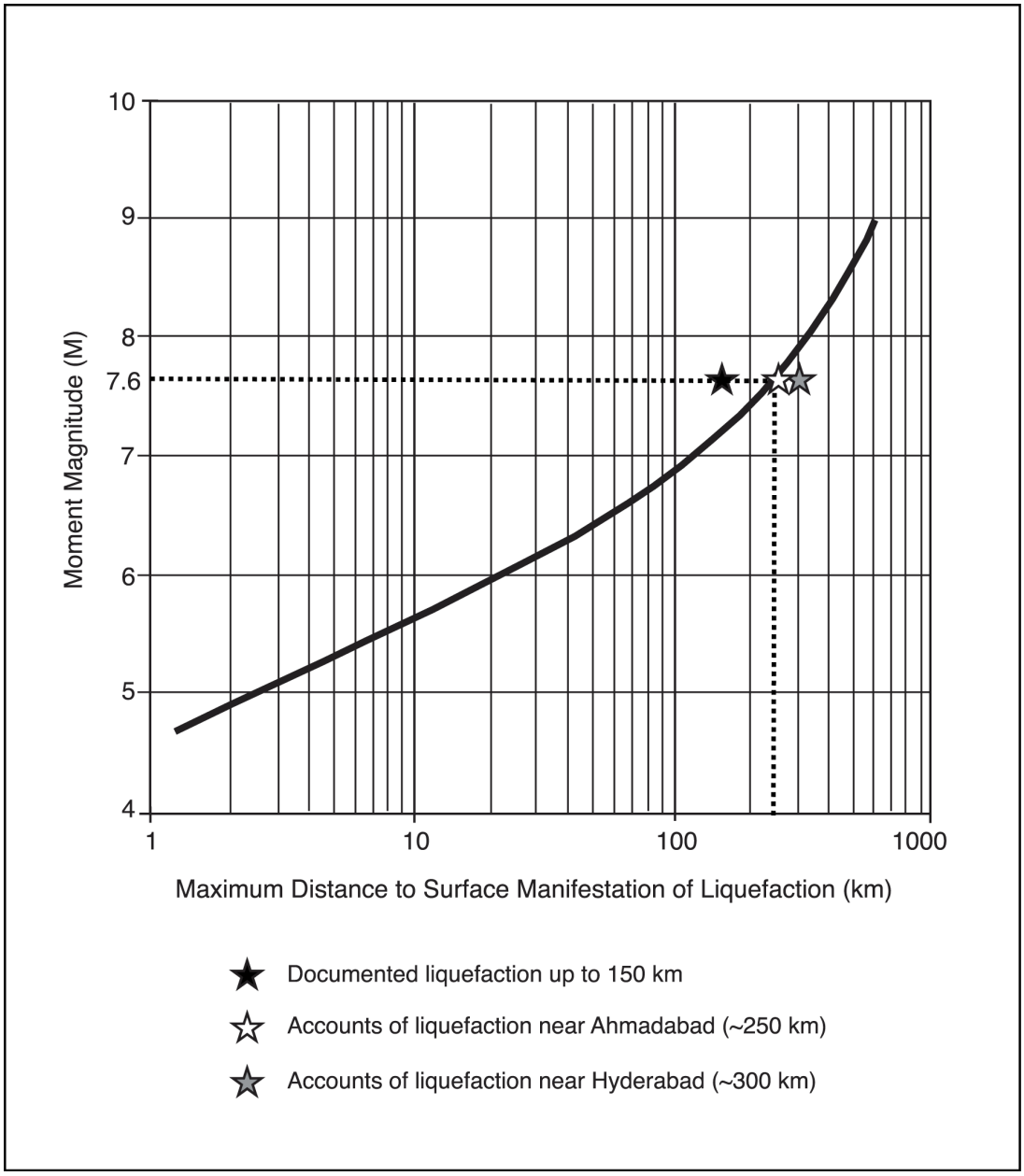

Figure 4-14: Relation between earthquake magnitude and maximum epicentral distance to surface manifestation of liquefaction (Ambraseys, 1988) shown with distances to documented and reported sites of liqufaction

5. Comparison of Kachchh and New Madrid Liquefaction Features

In general, the liquefaction features in the Kachchh region appear to be smaller than features in the New Madrid region. Most of the Kachchh sand blows are less than 60 m long, 10 m wide, and 15 cm thick. In contrast, sand blows in the New Madrid region that formed during the 1811-1812 earthquakes are commonly 100 m long, 30 m wide, and 0.5 to 1 m thick (Tuttle and Barstow, 1996). The New Madrid sand blows are unusually thick because they are compound structures composed of multiple sedimentary units related to several earthquakes (Saucier, 1989; Tuttle, 1999). Nevertheless, individual units often range from 30-60 cm in thickness. Feeder dikes of the Kachchh sand blows are typically 0.2 to 10 cm wide, occasionally ranging up to 25 cm. There are likely to be a few sand dikes on the order of 1 m in width related to lateral spreading in the epicentral area. In contrast, feeder dikes of New Madrid sand blows are commonly 0.5 to 2 m wide and can range up to 10 m. During the Kachchh earthquake, a number of sand-blow craters formed. Sand-blow craters such as these are not common in the New Madrid region but did form during the 1886 Charleston, South Carolina, earthquake of Mw 7.3 (Dutton, 1890). The Kachchh and Charleston regions both occur in the coastal zone. Perhaps the similarity in environments of deposition and resulting subsurface geology contributes to the formation of sand-blow craters during the venting of water from liquefied subsurface deposits.

Little is known about the liquefaction susceptibility of the subsurface sediments in the Kachchh region. However, Holocene river channel, alluvial fan and plain, delta and fan-delta, and esturine deposits like those in the Kachchh region are thought to have a moderate to high likelihood of liquefaction during strong ground shaking (Youd and Perkins, 1978). The water table, which affects liquefaction susceptibility of cohesionless sediment, is close to the surface of the mudflats of the Gulf of Kachchh, the Rann, and the Banni Plain, which occur at and slightly above sea level.

The New Madrid region occurs in the northern part of the Mississippi embayment. Late Quaternary sediments in the embayment are 30 to 60 m thick and are predominately Wisconsin valley train and Holocene meander belt deposits of the Mississippi, St. Francis, and White Rivers (e.g., Saucier, 1994). In general, fluvial channel deposits of this age are thought to be have a low to high likelihood of liquefaction; whereas flood plain deposits have a low to moderate liquefaction susceptibility (Youd and Perkins, 1978). In the New Madrid region, this is supported by borehole data collected for the U.S. Army Corps of Engineers for the purpose of drainage ditch design (Saucier, 1977; Obermeier, 1989) and by recent geotechnical investigations at sites of earthquake-induced liquefaction (Schneider et al., 1999). Prior to drainage of the Mississippi embayment during the 20th century, the water table was close to the ground surface much of the year.

In general, sediments in low-lying areas of the Kachchh region are probably more susceptible to liquefaction than sediments in the New Madrid region. Why then are sedimentary units attributable to one earthquake in New Madrid larger than sand blows resulting from the Republic Day earthquake? One possibility is the relative magnitude of the events. Although their magnitudes are still debated, the three largest earthquakes in the New Madrid sequence of 1811-1812 have been estimated to be of Mw 8.1 $\pm$ 0.31, Mw 7.8 $\pm$ 0.33, and Mw 8.0 $\pm$ 0.33 (Johnston, 1996). If these estimates are correct, the New Madrid earthquakes were larger than the Republic Day earthquake, and therefore, may have led to more intense liquefaction. Another possibility is the character of the deposits that liquefied. Fluvial deposits in the New Madrid region are characterized by thick (>20 m) units of channel sands overlain by silty and clayey overbank deposits (e.g., Saucier, 1994). In the Kachchh region, there may be more vertical and lateral variability of sandy units due to interfingering of marine, deltaic, esturine, and alluvial deposits.

A comparison of liquefaction induced by the Kachchh and New Madrid earthquakes would benefit from mapping of geologic deposits and geotechnical testing of liquefaction sites.

6. Conclusions

The Mw 7.7 Republic Day earthquake produced liquefaction and related ground failures in Holocene alluvial, esturine, and deltaic deposits from at least the Pakistan Border on the north to the Gulf of Kachchh on the south and from the Little Rann on the east to possibly Kori Creek on the west (Figure 4-1). Accounts of liquefaction near Ahmadabad and Hyderabad, Pakistan, suggest that there may be more distant sites of liquefaction. Surface manifestations of liquefaction in the meizoseismal area of the earthquake include sand blows, sand-blow craters, and lateral spreading. The latter, with displacements of >1 m, was responsible for significant damage to water wells and pipelines in the epicentral area and to port and other coastal facilities along the Gulf of Kachchh.

The Republic Day earthquake offers a unique opportunity to study a very large earthquake in an intraplate setting that induced liquefaction but apparently did not produce surface rupture. This event underscores the potential usefulness of liquefaction features in paleoseismology. Only a relatively small amount of data pertaining to liquefaction resulting from the Republic Day earthquake has been collected to date. Nevertheless, initial observations regarding the size, orientation, and spatial distribution of liquefaction-related features suggest certain trends and raise a number of questions worthy of additional research. Additional study of the Republic Day earthquake could provide valuable insights relevant to the assessment of liquefaction and ground failure potential and the interpretation of paleoliquefaction feature in the New Madrid seismic zone, the Kachchh region, and elsewhere around the world.

7. Acknowledgments

The research presented in this report was funded by the Mid-America Earthquake Center. The MAE Center is supported primarily by the Earthquake Engineering Research Centers Program of the National Science Foundation under Award Number EEC-9701785. C.P. and Kusala Rajendran and Mahesh Thakkar facilitated and participated in the field survey. Gary Patterson and Arch Johnston contributed additional data. Many thanks to Kathy Tucker who processed TM imagery and made the maps for this report and to David Nelson and David Diner at JPL who shared MISR imagery. Also, this report benefited from exchanges with Arch Johnston, Bill Lettis, David Nelson, Buddy Schweig, and Nano Seeber.

8. Appendix

Liquefaction features and deformation structures related to the Republic Day earthquake.

Site Name	Latitude N (degrees)	Longitude E (degrees)	Type of Deformation Structure	Length, Width, Amount of Displacement[2] (m)	Length,Width, Thickness or Depth[3] (m)	Structural Trend or Slip Direction[4]	Geomorphic Setting
Bachasar Reservoir	23.53881	70.36751	Slump	>30, >10, ~ 1_H		~W	Banni Plain
Baniari North	23.42578	70.15440	Sand blows		25.2, 7.5, 0.06	N55°E	Banni Plain
Baniari	23.40771	70.15693	Sand blows		14, 0.84, 0.03 11, 2, 0.06	N50°W N65°E	Great Rann/ Banni Plain
Baniari Village	23.40130	70.16465	Sand blows		15.2, 3, 0.08	N46°W	Banni Plain
Bharodia	23.57308	70.41320	Flexure	61, 23, 0.72 $_V$		N30°W	Banni Plain
Budhar-mora	23.34291	70.19341	Lateral spread[5] Sand blows	>400, 142, 1.35 $_H$	 3.5, 0.5, 0.04	N30-35°E N70-85°W	Mainland
Chobari; NW	23.53676	70.29948	Fissure/graben Sand blows	>100, 18.6, 0.1 $_V$	 2.84, 1.36, 0.06	N40°W N80°W	Chang River Alluvial Plain
Chobari; Monya-wadi 1	23.54176	70.34196	Fissure/graben	>100, 11, 0.12 $_V$		N20°E to N65°W to N89°W	Chang River Alluvial Plain
Chobari; Monya-wadi 2	23.57675	70.32486	Sand blows		24, 12, 0.14	N80°E	Great Rann/ Banni Plain
Chobari; Monya-wadi 3	23.57933	70.32578	Sand blows		60, 10, 0.13 21, 8, 0.08	N75°E to N85°W N60°E to N82°W	Great Rann/ Banni Plain
Dhrang	23.42296	69.86001	Sand blows		15, 12, 0.06 4, 1.6, 0.03	N65°E N30°E	Banni Plain
Gangta Bet 1	23.72565	70.52915	Sand blows		10.5, 8.5, 0.03	N38-40°E	Great Rann
Gangta Bet 2	23.72041	70.54420	Sand blows		0.9, 0.7, 0.03 0.35, 0.3, <0.03	 N2°E	Great Rann
Kandla Port 1	23.02040	70.20001	Sand blows		0.9, 0.5, 0.02	N20°E	Mud Flats
Kandla Port 2	23.01050	70.21160	Sand blows		15, 10, 0.2	N20-50°E	Mud Flats
Kandla-Subash Gate	23.00796	70.22268	Lateral spread Sand blows	>60, >40, 0.19 $_H$	 20, 0.7, disturb	~E N20°E to N40°W	Mud Flats
Kandla-Salt Pans	22.99433	70.16366	Sand blows		11.5, 7.2, 0.14 7, 6, 0.12	N88°W N35°E	Mud Flats
Khadir 1	23.84143	70.18808	Sand blows		13.2, 11.6, 0.03 1.4, 1.3, <0.03	 N-S	Great Rann
Khadir 2	23.84153	70.20143	Sand blows		11.6, 5, 0.05 3, 3, <0.05		Great Rann
Khadir 3	23.85141	70.23915	Sand blows		6, 6, <0.05		Great Rann
Khadir 4	23.91048	70.53328	Sand blows		4, 2, <0.05		Great Rann
Khavda 1	23.49433	69.66133	Sand blows		18, 12, 0.20	N20°E	Banni Plain
Khavda 2	23.51166	69.66233	Sand blows		47, 25, 0.08	N30°E	Banni Plain
Khavda 3	24.06667	69.71667	Crater		4.1, NA, 1.2		Allah Bund

[2] H = horizontal displacement; V = vertical displacement
[3] Depths are for craters
[4] Slip directions are for mass movements
[5] Also interpreted as a lateral spread by Seeber et al., 2001

Appendix Continued.

Site Name	Latitude N (degrees)	Longitude E (degrees)	Type of Deformation Structure	Length, Width, Amount of Displacement (m)	Length, Width, Thickness or Depth (m)	Structural Trend or Slip Direction	Geomorphic Setting
Kharoi	23.46510	70.38015	Tear fault;[6] right-lateral		0.16 H 0.15 V	N30°W	Chang River Alluvial Plain
Lodai 1	23.40998	69.93911	Sand blows		7, 5.5, 0.07	N22°E	Banni Plain
Lodai 2	23.40333	69.94666	Sand blows		106, 8, NA[7]	~E-W	Banni Plain
Lodai 3	23.40233	69.94276	Sand blows; alluvial fan		11.5, 4, 0.1	N54°E	Banni Plain
Manfara	23.47591	70.35325	Fissure/graben Sand blows	>120, 12, 0.15 V	 0.5, 0.4, <0.05	N60-80°E	Chang River Alluvial Plain
Rudra Mata Bridge	23.35795	69.69386	Lateral spread Sand blows	350, >40, 0.8 V	 2.5, 2.3, 0.08	N25°E N15°E	Reservoir on Pur River
Suraj Bari 1	23.20000	70.73333	Sand blows				Little Rann
Suraj Bari 2	23.28333	70.00500	Sand blows				Little Rann
Suraj Bari 3	23.24000	70.76000	Lateral spread			SW	Little Rann
Umedpur	23.48716	69.91600	Sand blows Crater Dry craters		33, 32, 0.26 18.5, 8, 0.11 14.5, 11.5, NA 10, 5, NA 2.4, 1.8, ~1.4 1.6, 1.5, ~1.0	N85°W N5°W N85°W	Banni Plain/Rann
Vigakot 1	24.14683	69.29616	Lateral spread Sand blows	200, NA, 0.05 V	 1.6, 0.8, 0.2	W N20°E	Allah Bund
Vigakot 2	24.27483	69.33316	Sand blows Craters		1.5, 0.4, 0.15 4.5, 3.2, NA 3, 2.5, NA	NA	Great Rann
Vigakot 3	24.27166	69.34250	Sand blows Craters		2, 1.2, 0.06 1.6, 1.39, 2	N-S N80°E	Great Rann

9. References Cited

Ambraseys, N. N., 1988, Engineering Seismology: earthquake engineering and structural dynamics, *Journal of the International Association of Earthquake Engineering*, **17**, 1-105.

Dutton, C. E., 1890, The Charleston earthquake of August 31, 1886, *U.S. Geological Survey Extract from the 9th Annual Report of the Director, 1887-88*, 528 pp.

Fuller, M. L., 1912, The New Madrid earthquake, *U.S. Geological Survey Bulletin 494*, 119 pp.

Gupta, S. K., 1975, Silting of the Rann of Kutch during Holocene, *Indian Journal of Earth Sciences*, **2**, 163-175.

Jacobi, R. and Fountain, J., 1993, The southern extension and reactivation of the Clarendon-Linden fault system, *Geographie Physique et Quaternaire*, **47**, 285-302.

Johnston, A. C., and Kanter, L. R., 1990, Earthquakes in stable continental crust, *Scientific American*, **262**, 68-75.

[6] Interpreted as a tear fault by Seeber et al., 2001
[7] NA = not available

Johnston, A. C., 1996, Seismic moment assessment of stable continental earthquakes, Part III: 1811-1812 New Madrid, 1886 Charleston and 1755 Lisbon, *Geophysical Journal International*, **126**, 314-344.

Kelson, K. I., Simpson, G. D., VanArsdale, R. B., Harris, J. B., Haradan, C. C., and Lettis, W. R., 1996, Multiple Holocene earthquakes along the Reelfoot fault, central New Madrid seismic zone, *Journal of Geophysical Research*, **101**, 6151-6170.

Lettis, W. R., and Hengesh, J. V., 2001, Preliminary observation on the origin and effects of the January 26, 2001 Republic Day earthquake, India, *Seismological Society of America*, **72**.

MacMurdo, J., 1824, Papers relating to the earthquake which occurred in India in 1819, *Philosophical Magazine*, **63**, 105-177.

Malik, J. N., Sohoni, P. S., Merh, S. S., and Karanth, R. V., 2000, Palaeoseismology and neotectonism of Kachchh, western India: *In* Okumura, K., Goto, H., and Takada, K., eds., Active Fault Research for the New Millennium, *Proceedings of the Hokudan International Symposium and School on Active Faulting*.

Obermeier, S. F., 1989, The New Madrid Earthquakes: An engineering-geologic interpretation of relict liquefaction features, *U.S. Geological Survey Professional Paper 1336-B*, 114 pp.

Oldham, R. D., 1926, The Cutch (Kachh) earthquake of the 16th June, 1819 with a revision of the great earthquake of the 12th June, 1897, *India Geological Survey Memoir*, **28**, 71-147.

Rajendran, C. P., and Rajendran, K., 2001, Characteristics of deformation and past seismicity associated with the 1819 Kutch earthquake, northwestern India, *Bulletin of the Seismological Society of America*, in press.

Saucier, R. T., 1977, Effects of the New Madrid earthquake series in the Mississippi alluvial valley, *U.S. Army Corps of Engineers Waterways Experiment Station Miscellaneous Paper S-77-5*, 10pp.

Saucier, R. T., 1989, Evidence for episodic sand-blow activity during the 1811-1812 New Madrid (Missouri) earthquake series, *Geology*, **17**, 103-106.

Saucier, R. T., 1994, Geomorphology and Quaternary geologic history of the lower Mississippi, *U.S. Army Corps of Engineers Waterways Experiment Station*, **I** and **II**, 364 pp.

Seeber, N., Ragona, D., Rockwell, T., Babu, S., Briggs, R., and Wesnousky, S., 2001, Field observations bearing on the genesis of the January 26, 2001 Republic Day earthquake of India resulting from a field survey of the epicentral region, *Web report http://neotectonics.seismo.unr.edu/Bhuj/Report.html*.

Tuttle, M., and Barstow, N., 1996, Liquefaction-related ground failure: A case study in the New Madrid seismic zone, *Bulletin of the Seismological Society of America*, **86**, 253-256.

Tuttle, M. P., 1999, Late Holocene earthquakes and their implications for earthquake potential of the New Madrid seismic zone, central United States, *Ph.D. Dissertation*, University of Maryland, 250 pp.

Youd T. L., and Perkins, D. M., 1978, Mapping liquefaction-induced ground failure potential, *Journal of the Geotechnical Engineering Division*, **104**, 433-446.

Chapter 5: Geotechnical Observations

by

Scott L. Deaton[1] (Graduate Research Assistant) and J. David Frost[2] (Associate Professor)
School of Civil Engineering
Georgia Institute of Technology

1. Introduction

Geotechnical features including lateral spreading, sand blows, settlement and ground cracking were widely distributed in the free field after the earthquake. Conversely in towns or villages, geotechnical related foundation failures were not commonly observed. Typically residential and commercial structures in these population centers were poorly engineered and failed due to structural inadequacies. However, port facilities, dams and a number of bridge components, showed significant damage due to geotechnical related failures. Not withstanding the type and extent of damage observed, the consequences of the poor performance was, in many cases, not as significant as it might have been since the period of drought prior to the earthquake resulted in smaller hydraulic forces on many of these structures. An overview of the geotechnical failures is included herein.

2. Lateral Spreading

A typical lateral spread observed near the Varahi Village is depicted in Figure 5-1. Similar lateral spreads were observed adjacent to small stream channels and other gently sloping areas throughout the region (Figure 5-2). However, minimal damage to manmade structures occurred due to their rural location.

Figure 5-1: Lateral spreading near Varahi Village (N23.6373, E71.4306)

[1] SLD, 790 Atlantic Dr., Atlanta, GA 30332-0355
email: scottdeaton@yahoo.com
[2] JDF, 790 Atlantic Dr., Atlanta, GA 30332-0355
email: david.frost@ce.gatech.edu

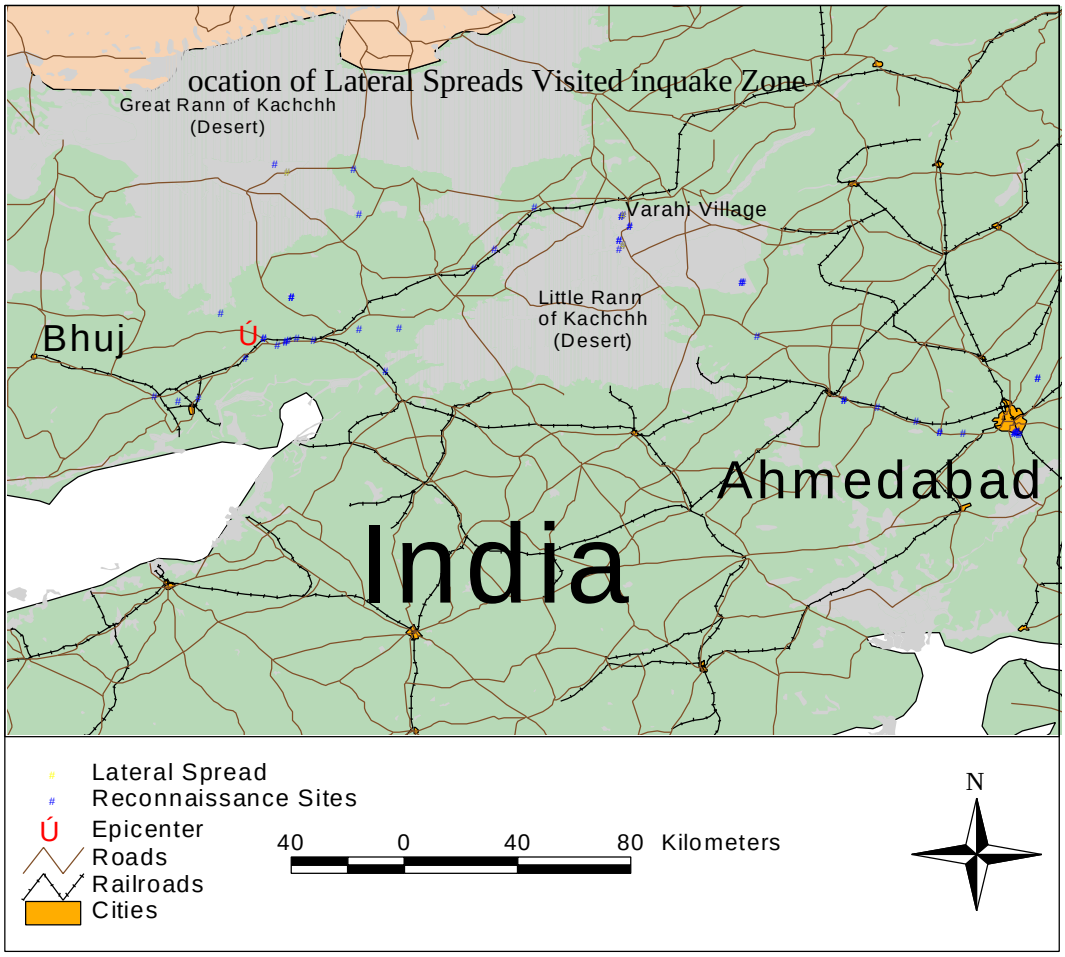

Figure 5-2: Location of lateral spreads visited in earthquake zone

3. Sand Blows

Of the geotechnical features observed after the earthquake, sand blows observed at large distances from the epicenter had the most significant relevance on related studies for the mid-America region. Sand blows similar to that shown in Figure 5-3 were prevalent at distances up to 135 kilometers from the epicenter. Locals reported water sprayed into the air up to 2 meters from sand blows in this area. In contrast, geotechnical related damage at this distance was non-existent and structural damage at this distance was very isolated. Closer to the epicenter, very large sand blows up to a meter in diameter were observed as depicted in Figure 5-4.

The region where many of the sand blows were observed is primarily agricultural and is located directly adjacent to the Little Rann of Kachchh or desert. The extent of the sand blows in this region was too widespread to perform a complete mapping unless it could have been performed from the air. However, due to the regions close proximity to Pakistan, such an alternative was not available

Figure 5-3: Linear sand blows 135 km from epicenter (N23.7345, E71.4278)

Figure 5-4: Large sand blows in dry river bed south of Chang Dam (N23.45530, E70.43787) (Photo Courtesy of J.P. Bardet)

because of the imposed “no-fly” zone. Several sand blow locations were visited and are illustrated as yellow circles in Figure 5-5.

Throughout this region the sand blows were typically linear features. They ran parallel and tended to step laterally by as much as 10 meters. Typically, there was no evident vertical or horizontal displacement for these features and there was no predominant directionality evident either. The lack of directionality led us to hypothesize that the ground cracking and sand blows were attributed to regional subsidence or settlement of the basin. Other examples of regional subsidence were observed in the Great Rann of Kachchh exhibited by extensive ground cracking with and without sand ejection and no consistent directionality.

In this region the brackish groundwater table is located approximately 8 meters below ground surface. As water expelled from the blows evaporated, white salt residue was left behind, which permitted the identification of sand blows over large distances.

Figure 5-5: Location of sand blows visited in earthquake zone

4. Ground Rupture

Ground rupture was also evident throughout the earthquake region. Significant cracking was evident at distances up to 135 kilometers from the epicenter as depicted in Figure 5-6. Concentrations of parallel ground cracks were evident in the Rann of Kachchh over distances of several hundred meters. These cracks originated in the vegetated area depicted in Figure 5-7 and extended out into the desert in multiple locations. There was no evident directionality associated with any ground cracks observed as they changed directions what appeared to be randomly at multiple locations. Many cracks were offset vertically, with the offsets varying from 0-15 cm in this region.

Figure 5-6: Location of ground rupture visited in earthquake zone

Figure 5-7: Parallel ground cracking in the Rann of Kachchh (N23.3997, E70.2275)

Figure 5-8: Settlement of backfill surrounding natural gas pipeline (N23.6220, E71.0472)

5. Settlement

Significant settlement of the backfill above a natural gas pipeline was observed over many kilometers in a stretch of desert between the Little Rann of Kachchh and the Great Rann of Kachchh as shown in Figure 5-8. It was evident the contractor simply backfilled the soil without compacting it after the pipeline had been placed. The extent of settlement was between 20 and 30 cm. In Figure 5-9 the settlement of the pipeline backfill is depicted. The white residue is the remnants of brackish groundwater that surfaced at the time of the earthquake, indicating liquefaction may have occurred. The ground in the immediate vicinity of the pipeline was very soft also indicating the large quantity of water still present in the soil 18 days after the earthquake. As mentioned previously, the depth to the brackish groundwater was reported throughout this region as approximately 8 meters.

Figure 5-9: Location of pipeline settlement in earthquake zone

6. Dam Failures

This region of Gujarat contains approximately 180 dams. At the time of the earthquake, the region was experiencing a severe drought and consequently the dams were retaining minimal amounts of water. Typically, the dams are used to retain water and decrease the flooding during the monsoon or rainy season, which lasts several months beginning in July. Even though the dams were at low pool states, there were numerous large dam failures throughout the region. The most significant dam failures visited were Shivlakha, Chang, Fategadh, Kaswati, Rudramata, Suvi and Tapar. The locations of these dams are shown in Figure 5-10 and a detailed description of the Shivlakha dam failure follows. The performance of the other dams was remarkably similar.

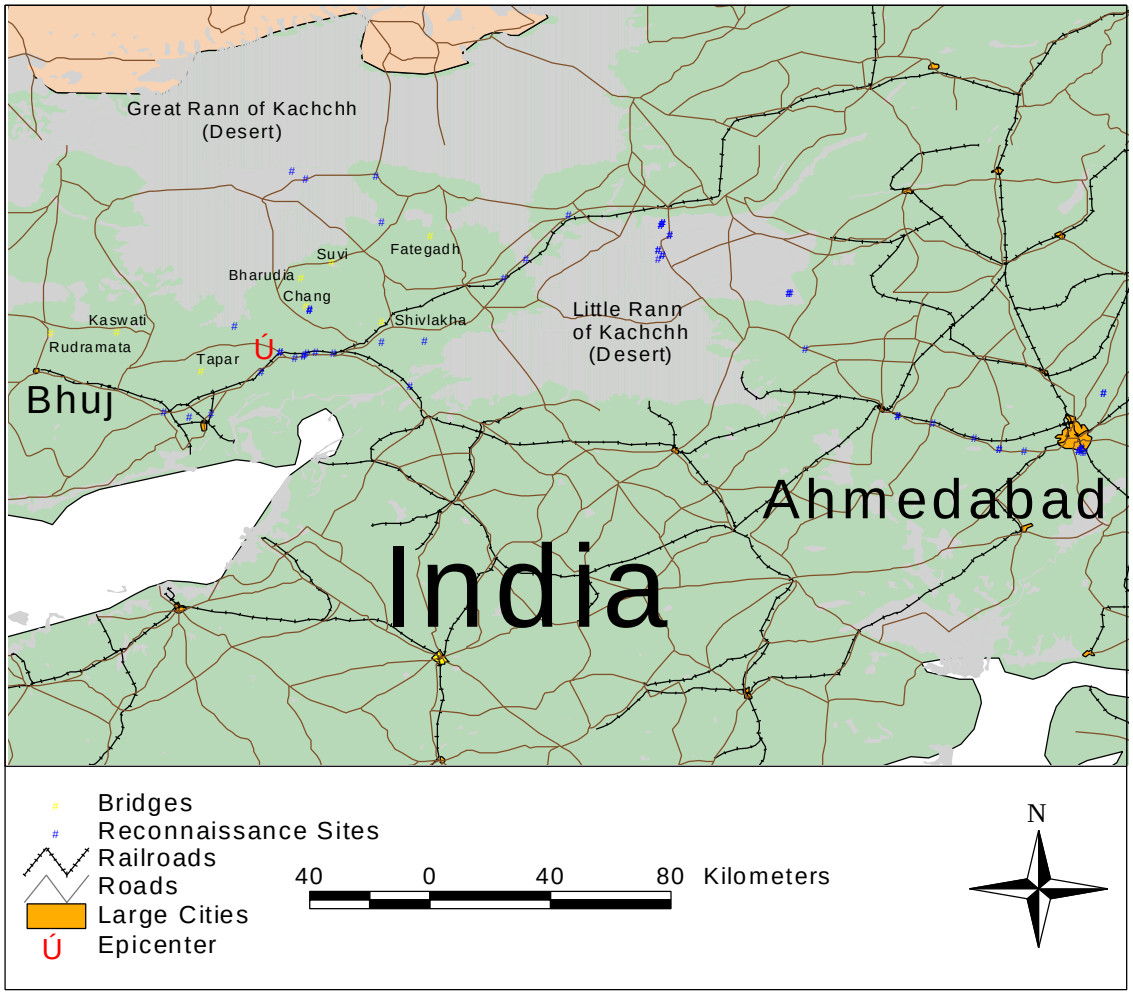

Figure 5-10: Location of dams visited in earthquake zone

Shivlakha Dam

Shivlakha Dam slumped significantly in the upstream direction. Extensive cracking was observed on the upstream face depicted in Figure 5-11. Longitudinal cracking was evident at the crest as well as on the downstream slope. A large toe bulge occurred at the upstream toe as a result of the rotational nature of the upstream slope stability failure (Figure 5-12). The scarp on the upstream crest was approximately 3 meters in both vertical and horizontal directions as seen in Figure 5-13.

Figure 5-11: Upstream slope failure at Shivlakha Dam (N23.3467, E70.6406)

Figure 5-12: Toe bulge along upstream slope of Shivlakha Dam (N23.3467, E70.6406)

Figure 5-13: Scarp at crest of Shivlakha Dam (N23.3467, E70.6406)

7. Bridge Damage

Damage to bridges ranged from abutment settlement and lateral spreading to lateral displacement of piers. The location of the significant bridge damage is illustrated in Figure 5-14.

Figure 5-14: Location of bridges visited in earthquake zone

Highway 8A Bridge

A four-span, two lane reinforced concrete bridge on Highway 8A that was under construction at the time of the earthquake was severely damaged. Significant damage occurred at the east abutment to the support bent and wing walls as depicted in Figure 5-15. This could be attributed to possible liquefaction near the abutment that resulted in overturning failure of the abutment. A similar mechanism occurred at the first pier where rotation resulted also depicted in Figure 5-15. The combination of these movements resulted in a span shortening of approximately 46 cm for the easternmost span. Measurements indicated the eastern span had the most lateral movement as the second and third spans shortened by approximately 8 and 10 centimeters, respectively.

Figure 5-15: Damage to Highway 8A bridge east abutment and first pier (N23.3039, E70.4203)

Surajbari Bridges

The Surajbari bridges are located across a tidal flat and provide a critical link from central India to the Gujarat region. There are two vehicular bridges and one rail bridge at this crossing. The length of these bridges is approximately 1300 meters.

The new vehicular bridge was still under construction at the time of the earthquake and it sustained mostly structural damage. However, the access road embankments and the abutment settled as much as 70 cm (Figure 5-16). Longitudinal cracking up to 1 meter wide was also noted on these access roads. Sand blows were observed throughout the tidal flats indicating significant liquefaction in the area as well.

The old vehicular bridge had two predominant types of geotechnical related damage. Significant tilting and/or lateral displacement of bridge piers occurred along its length. A lateral offset in the guardrail

indicated that the bridge had shifted approximately 1 meter laterally after the earthquake as shown in Figure 5-17.

Figure 5-16: Settlement of abutment on new Surajbari Bridge (N23.19143, E70.71940) (photo courtesy of J.P. Bardet)

Figure 5-17: One-meter lateral offset of old Surajbari Bridge (N23.19461, E70.71702) (photo courtesy of J.P. Bardet)

8. Port Damage

The ports in the Gujarat region suffered moderate to significant damage during the event. Lateral spreading, settlement and sand blows were common causes of features observed at these ports. The locations of the damaged ports are illustrated in Figure 5-18.

Figure 15-8: Location of port facilities visited in earthquake zone

Kandla Port

The Kandla Port was nominally damaged during the earthquake. The tower of the port tilted due to lateral spreading along the waterfront. The free-field portions of the port tended to settle uniformly with occasional sand blows and evidence of lateral spreading. The most significant geotechnical damage was to most of the 2500 hollow reinforced concrete piles supporting a jetty. These piles were cracked approximately 30 centimeters below the pile cap as illustrated in Figure 5-19. Overall, the more modern pile-supported jetties performed well within minimal lateral displacement and damage to piles. Figure 5-20 illustrates modern hybrid steel and concrete piles which suffered minimal damage during the earthquake.

Figure 5-19: Cracking of hollow reinforced concrete piles at Kandla Port (N22.9980, E70.2240) (photo courtesy of J.P. Bardet)

Figure 5-20: No damage to modern hybrid piles at Kandla Port (N22.98824, E70.22404) (photo courtesy of J.P. Bardet)

Navlakhi Port

Navlakhi Port is a small peninsula extending from the eastern end of the Gulf of Kachchh. The soils composing the peninsula are primarily soft, silty clays with interbedded sand (Bardet). The most significant damage to the port was caused by large lateral spreads and slope failures along the southern portion of the port, although moderate ground cracking was observed along the northern edge of the peninsula, which eventually resulted in slope stability failures and the closure of the access road and rail line to the port.

Once again, modern pile-supported wharfs performed well; however, a recently constructed wharf on shallow foundations underwent significant lateral displacement as a result of the slope failure at the end of the peninsula. This failure was initiated by earthquake shaking, but was propagated at high tide (Figure 5-21). Approximately 2.5 meters of vertical and 2.5 meters of horizontal displacement were reported by J.P. Bardet for the final configuration. Lateral spreads at the port resulted in deformations up to 6 meters as reported by Bardet.

Figure 5-21: Ground deformation at Navlakhi Port (photo courtesy of J.P. Bardet)

9. Summary

The Gujarat earthquake provided the opportunity to observe a wide range of geotechnical failures as indicated above. Seismic impacts on both man-made and natural earth systems were evident at distances of up to at least 135 km from the epicenter. The consequences of the inadequate performance in many cases were mitigated by: (a) the drought conditions which preceded the earthquake resulting in substantially lower loads on the earth structures at the time of the event; (b) the poor quality of the superstructure systems which resulted in structural failure prior to foundation failure; and (c) the remoteness of the region and thus lower potential for human losses.

Chapter 6: Indian Standards for Building Construction

by

John Nichols[1]
Lecturer
Department of Civil Engineering
Curtin University of Technology, Perth, Australia

1. Abstract

The 2001 Gujarat Earthquake (moment magnitude 7.9) occurred near the Rann of Kachchh in northwestern India. The Gujarat earthquake demonstrates again the devastation wrought on buildings that are subjected to a major earthquake. The damage in the town of Bhuj was consistent with a felt intensity of MM X or greater. This level of energy release destroys most concrete, steel and masonry buildings within the meizo-seismal area. This paper reviews the Indian Standards for earthquake engineering, repair of buildings, plain and reinforced concrete, steel, and masonry construction. The Indian codes are compared to the United States codes of practice to determine whether any lessons can be learned from the earthquake in relation to these Indian and the United States codes of practice. The specific area of interest in the code review was the methods for estimating seismic demand and the seismic capacity. This earthquake falls in the same region as an 1819 earthquake. There was a short repeat time between events. Should be considered in code development?

Figure 6-1: Collapse of historic wall in Ahmedabad

2. Introduction

The purposes of this paper were threefold, to provide an overview of current codes, to illustrate the seismic hazard maps for India, and to show the methods for estimating seismic demand and seismic capacity within the codes.

The late Prof. Jai Krishna of the University of Rookee headed the development of the earthquake engineering codes of practice issued by the statutory institution the Bureau of Indian Standards. The standards that are applicable in the earthquake-engineering field in India are IS 13935: 1993 Repair and Seismic Strengthening of Buildings – Guidelines, IS 1893: 1984 Criteria for Earthquake Resistant Design of Structures, IS 456: 2000 Plain and Reinforced Concrete Code of Practice (Fourth Revision, IS 13920: 1993 Ductile Detailing of Reinforced Concrete Structures Subjected to Seismic Forces - Code of Practice, IS 800: 1984 Code of Practice for General Construction in Steel (Second Revision) and IS : Masonry Structures.

---

[1] JN, GPO Box U1987, Perth, WA, Australia 6845,
email: nicholsj@vesta.curtin.edu.au

3. Seismicity and Damage

The interesting feature of this earthquake was the repeat damage to structures repaired after the 1819 earthquake (Figure 6-1). Investigators have made similar observations after recent eastern Mediterranean earthquakes. This point on repeated damage was raised after the 1989 Newcastle earthquake and recently for the Charleston, South Carolina area with the public buildings repaired after the 1886 Charleston earthquake. This problem of the repeated damage raises the question as to the design life for some structures and the accumulation of damage in structures that are subjected to multiple earthquakes such as occur in California (Nichols, 1999; USGS, 1977: Algermissen, 1972.)

Figure 6-2: Damage at Bhuj, Gujarat State

The town of Bhuj in the State of Gujarat suffered almost complete destruction in the 2001 Gujarat earthquake (Figure 6-2.) There was little doubt that this damage level represents a felt intensity MMI X to XII zone. The high death toll suggests that it was MMI XI+ (Shiono, 1995).

IS 1893: 1984 Criteria for Earthquake Resistant Design of Structures was the standard used for the earthquake design of structures in India. The Sectional Committee who prepared the standard made a number of observations that are relevant to this work. These observations were:

"*It is not intended with this standard to lay down regulations so that no structure shall suffer any damage during earthquakes (sic) of all magnitudes. It has been endeavored to ensure that as far as possible structures are able to respond without structural damage to shocks of moderate intensity and without collapse total collapse to shocks of heavy intensity.*" This condition is in line with the methods being developed through the Federal Emergency Management Agency for seismic design in the United States (FEMA 273, 1997).

"*Though the basis for the design of different types of structures is covered in this standard, it is not implied that detailed dynamic design analysis shall be made in every case. There might be cases of less importance and relatively small structures for which no analysis need be made, provided certain simple precautions are taken in the design… Similarly in highly seismic areas, construction of a type which entails heavy debris and consequent loss of life and property such as masonry, particularly mud masonry and rubble masonry should be avoided in preference to construction of a type which is known to withstand seismic effects better, such as construction in lightweight materials and well braced timber-framed structures.*"

This frank statement of intent of the code committee recognizes the problems of poor quality masonry construction in highly seismic zones. The continuing difficulty that the code committee grapples with is the political reality of the existing construction and the economics of future construction. The Code Committee had no intention of permitting the inadequate design of structures in the higher seismic zones, although this was not expressly stated.

The Committee defined the seismic zones using five categories numbered I to V. Figure 6-3 shows the seismic zone map for the State of Gujarat reproduced from the code's Figure 6-1 (IS 1893: 1984, pg 7-8 and Appendix E). The key cities in the area are Bhuj that was clearly in Zone V, and Rajkot and Ahmedabad that were clearly in Zone III.

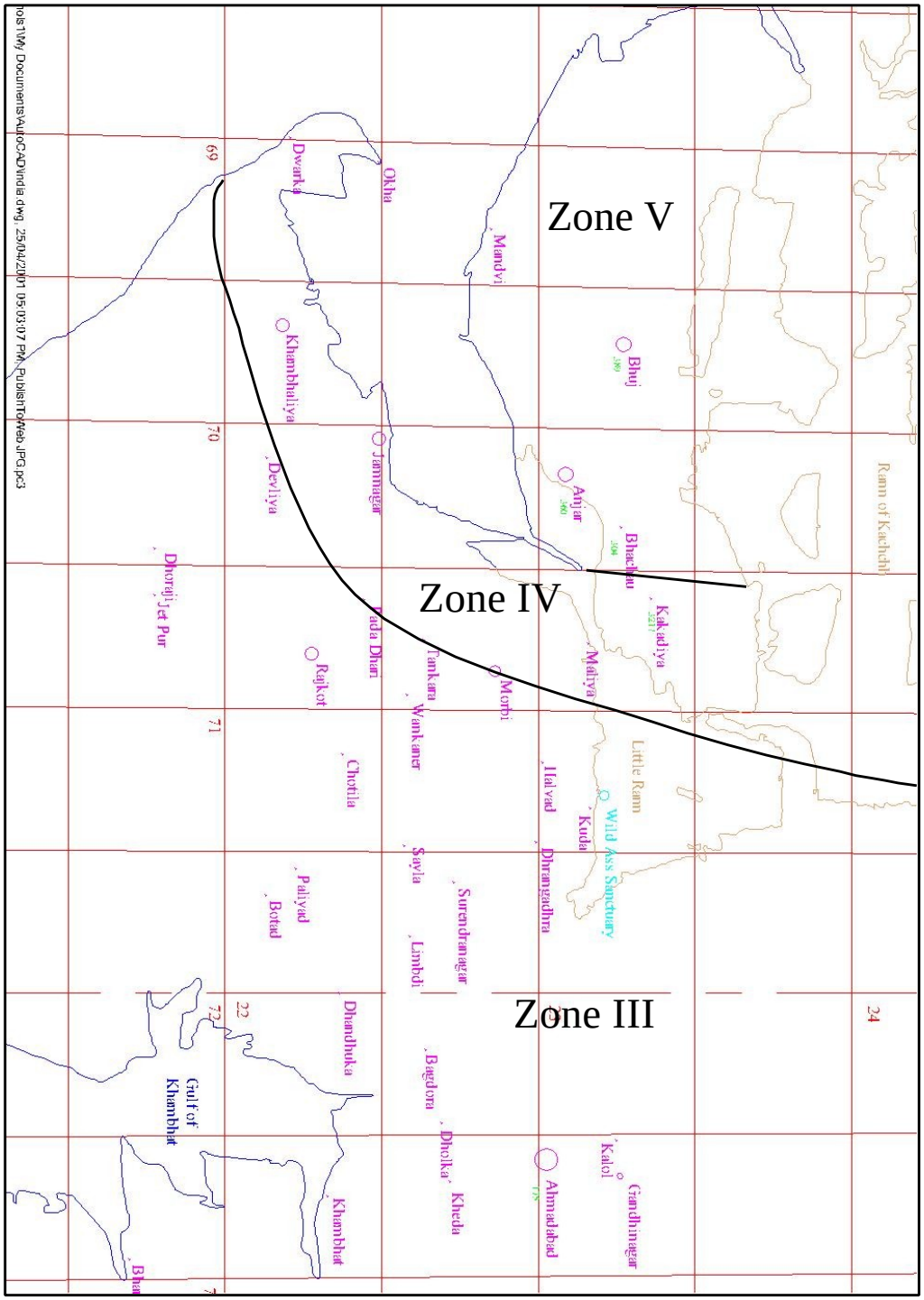

Figure 6-3: Gujarat State seismic zonation

The committee provided the following correspondence between the Modified Mercalli Intensity and the Indian Zonation (Table 6-1).

Table 6-1: Definition of the Indian zonation standard

Zone	Mod. Mercalli Intensity	Basic Horizontal Seismic Coefficients a_0	Town (Distance to epicenter)	Seismic Zone factor F_0 for average acceleration spectra	Abrams' Estimate of the MMI[2]
I	V or less	0.01		0.05	
II	VI	0.02		0.10	
III	VII	0.04	Ahmedabad (255)	0.20	VI
IV	VIII	0.05	Morbi[3] (100)	0.25	VII
V	IX to XII	0.08	Bhuj (40) Dudhai (14)	0.4	IX at 40 kms and XII at 12 kms.

The attenuation of the felt intensity for the Gujarat earthquake was not as rapid as observed in Tangshan for equivalent distances. The difference may be due to a difference in construction standards, ground conditions and at distance in Tangshan the ground has thinner sediments over coal bearing rock. The MMI data collated by Abrams has been plotted against the Tangshan data collated by Shiono (Figure 6-4). A polynomial has been fitted through the Gujarat data. The point at 130 kilometers will require further investigation.

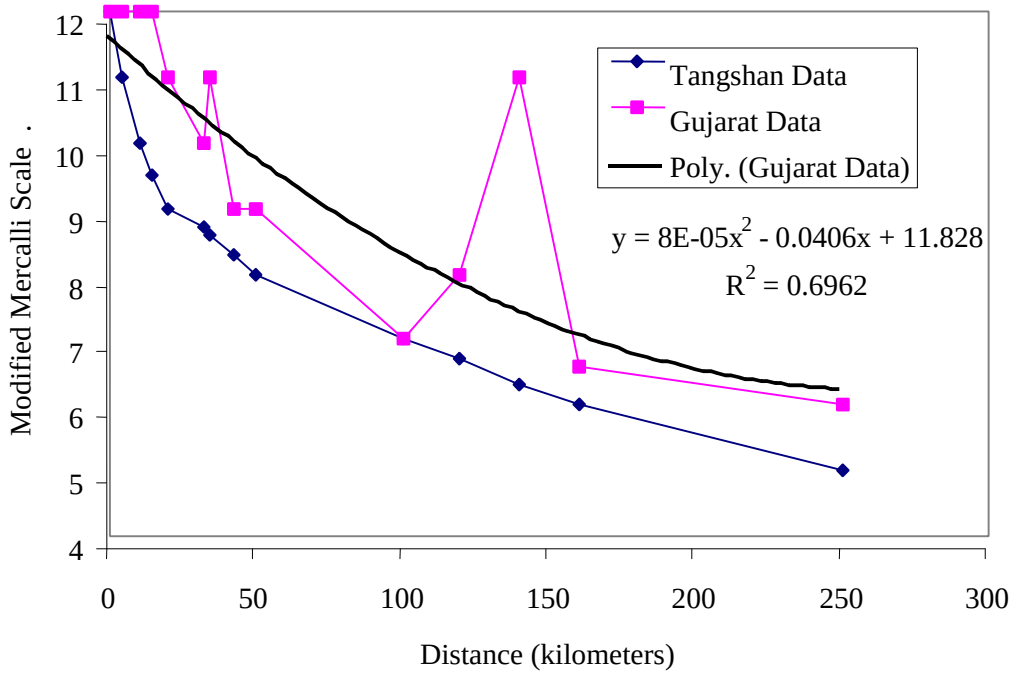

Figure 6-4: Gujarat and Tangshan attenuation of felt intensity

[2] Chapter 7.
[3] Interpolation of the Indian Standard figure would appear to place Morbi in Zone IV.

Rossetto noted "*that together with the increased damage potential of the ground motion due to possible site amplification and earthquake duration effects, bring the structures to exhibit a higher vulnerability than would be expected in a population of typical European buildings*." The difficulty in reaching conclusions based on this limited data set was in determining what were the problems.

1. Are the buildings more vulnerable than equivalent European and American buildings?

2. Has the earthquake energy attenuated at a lower rate than for an equivalent European setting?

3. Did a lower attenuation rate couple with the duration of the earthquake to cause the increased damage?

The rapid attenuation in the 1915 Avezzano earthquake in Italy in the east west direction underscores the difference in the interplate and intraplate areas (Nichols and Beavers, 2000). The attenuation rate in the New Madrid Seismic Zone and the Gujarat State will need to be the subject of further study.

The clear conclusions that can be reached from the examination of the Indian Earthquake Standard are that the Code Committee has adequately addressed the question of estimating the likley intensity of shaking, at least from the perspective of the Modified Mercalli Scale. The code has addressed the issues of minor buildings in a sensible manner, although one could suggest that the note was subject to intrepretation. The code committee has recommended against the common practice of poor quality masonry construction, which conforms with the very specific and detailed conclusions drawn by Abrams.

The issue of the intraplate attenuation rate that has arisen in the last few years with the research on the New Madrid Seismic Zone and from the Tangshan data strongly suggests that this point will continue to require significant and ongoing research in India, China, and the United States. The economic impact from failure to address this issue in the central and eastern United States will be significant. The Standards committee would have been unaware of the magnitude of this problem at the time of preparation of the standard.

4. Seismic Code (IS 1893: 1984 Criteria for Earthquake Resistant Design of Structures)

The IS 1893: 1984 Criteria for Earthquake Resistant Design of Structures has been compared to the requirements of FEMA 273 and 356 for the design of structures subjected to earthquake loading.

Three source documents for the development of the Indian and American standards are used in this comparison (Newmark and Hall, 1968, 1978; Veletsos and Newmark, 1964). The original documents are used to confirm the applicability of the selected methods and whether change or additional research is warranted. The work by Veletsos and Newmark (1964) includes pulse waves, which are of interest in near field analysis for great earthquakes (Richter, 1958) and Fast Fourier transform methods (Brigham, 1988).

Veletsos and Newmark[4] (1964) noted the limited seismic data of the time. The FFT procedure was not available to these researchers, although they use the Fourier mathematics in their analysis.

IS 1893: 1984 provides the design criteria for multi-storied buildings that was based on the estimation of the equivalent static base shear:

$$V_B = KCa_h W \tag{1}$$

where W represents the dead load and a fraction of the live load depending on the Load Class being either 25 percent or 50 percent; a_h was the design seismic co-efficient; C represents the flexibility of the structure related to the number of stories and the fundamental period T ; K represents the performance factor depending on the structural framing system and the ductility level for construction; V_B represents the base shear load on the structure.

The fundamental period was estimated for moment resisting frames without bracing or shear walls using:

$$T = 0.1n \tag{2}$$

where n defines the number of storys. The equation for all other structures was:

$$T = 0.09H/\sqrt{d} \tag{3}$$

where H represents the height of the building in meters; d represents the maximum base dimension in meters in the direction parallel to the applied seismic load.[5]

The equation provides an estimate that was equivalent to a Finite Element analysis of a degrading structure on a soil. The equation for the frequency f was:

$$f = \frac{10}{n} \quad or \quad f = 11\sqrt{d}/H \tag{4}$$

Figure 6-5 presents factor C determined from the IS graph (IS 1893: 1984, pg 22).

[4] These documents use the frequency as the standard unit for expressing dynamic structural response. This method will be used in this document to be consistent with the work of Newmark and to avoid the inversion problem associated with use of period. The seismic community records earthquakes in the time domain and reports results as a function of time and frequency. Inversion to period introduces a distortion to the graphing of the results. While the conversion is trivial, its use should be discouraged in code documents and in the education of young engineers, who will increasingly work directly with seismic data and Fast Fourier transforms.

[5] Equation (3) estimates a period for a 20-meter masonry tower with a base dimension of 4.5 meters at 0.84 seconds or a frequency of 1.2 Hertz, and for a 15-meter structure at 0.46 seconds or 2.1 seconds.

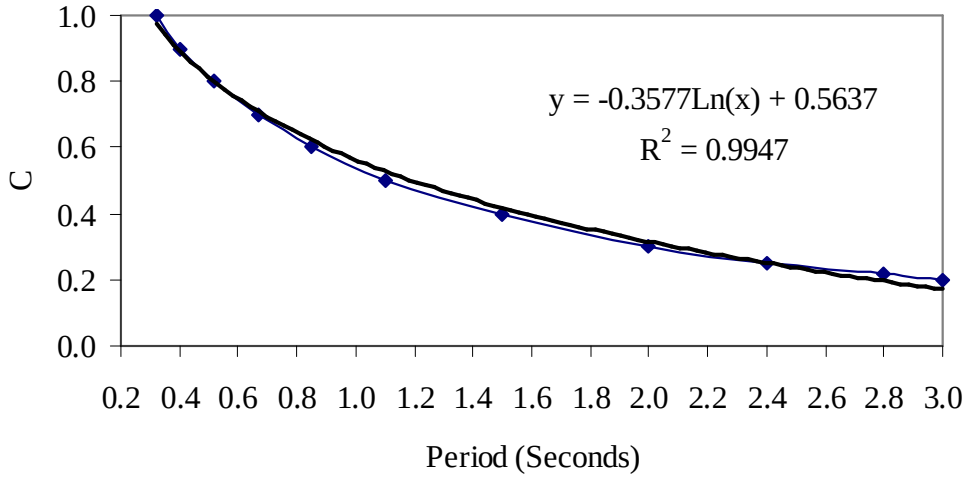

Figure 6-5: The factor C against period T

The data has been expressed in terms of frequency, as that was relevant for masonry structures (Figure 6-6).

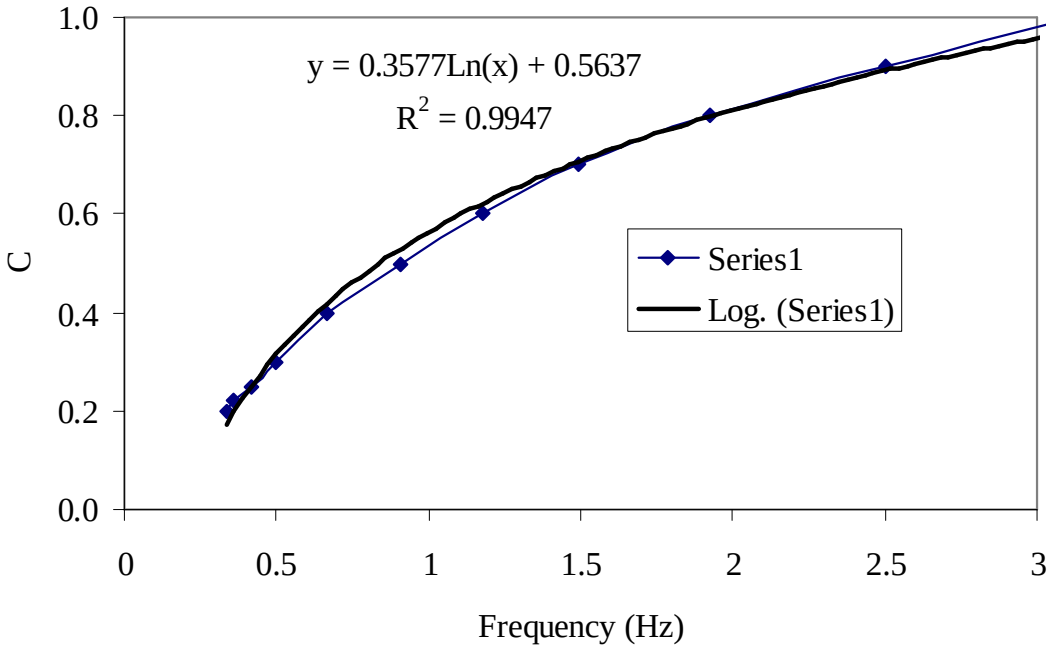

Figure 6-6: The factor C against period F

This result shows that the code provides a higher base shear for shorter structures such as low masonry buildings.[6] This results imply that:

$$C = (0.3577 Ln(f)) + 0.5637 \quad (5)$$

The Indian equations for determining the period can be traced to ATC 3-06 (1978) except that the moment resisting frame (steel and concrete) in ATC 3-06 had the equation for period of:

$$T = C_T h_n^{0.75} \quad (6)$$

where the values for C_T for ATC 3-06 and the values from FEMA 302 (1997) are presented in Table 6-2.

Table 6-2: Coefficients for the determination of period of a structure

	C_T			Period	Frequency
Frame Type	ATC 3-06	FEMA 302	Metric[7] co-efficient	20 meter height	20 meter height
Steel – moment resisting	0.035	0.035	0.0853	0.80	1.23
RC – moment resisting		0.030	0.0731	0.69	1.44
Reinforced Concrete	0.025		0.0609	0.57	1.73
Eccentrically braced steel frame		0.030	0.0731	0.46	2.16
All other framing systems		0.020	0.0488	1.38	0.72
Wood frame (2 to 3 stories		0.060	0.1462	0.80	1.23

FEMA 302 (1997) allows the use of equation (2) provided that the buildings were less than or equal to twelve stories and has minimum story height of 3 meters. A finite element analysis of the earlier detailed masonry tower provided a period of 0.46 seconds and a frequency of 2.2 Hz. This result represents a higher frequency or lower period than the results calculated using equation (3). Chopra and Goel (2000) comment in detail on the derivation of these types of equations and the intentions of the code committees.

The selection of factor C depends on the calculated frequency. There is a conceptual difficulty in selecting a bounding function such as equation (2) or (6). The form of two equations depends on the researchers original data set, the selection of the type of the fitted equation and the fitting method[8] used in the analysis. The equations give reasonably comparable answers. Chopra and Goel (2000) provide a range of solutions to this problem of selecting a natural frequency equation. The issue of building response frequency will need to be reviewed in both the IS and FEMA 302 based on the recent work of Chopra and Goel.

---

[6] The example masonry tower would have a C of 0.6.

[7] These metric co-efficients are used in the nomenclature for the subsequent figures.

[8] The three fitting methods could be the least squares, robust or bounding functions. The least squares provide a mean answer that can be distorted by extreme outliers, the robust has the problem of equal weight for points and the bounding will introduce systematic errors as identified by Chopra and Goel.

Two methods are provided in the IS 1893: 1984 for calculating the design seismic co-efficient. The first method was the seismic co-efficient method (equation 7a) and the second is the response spectrum method (equation 7b).

The forms of the equations for the two methods are:

$$a_h = bIa_0 \tag{7a}$$

$$a_h = bIF_0 \frac{S_a}{g} \tag{7b}$$

where b defines different soil-foundation systems (Table 6-3) and $\frac{S_a}{g}$ was defined from an average acceleration spectra (Figure 6-7), and I defines the importance factor (Table 6-4).

Table 6-3: Values for b for different soil-foundation systems[9]

Sl No.	Type of soil mainly forming the foundation	Piles passing through any soil but resting on Soil Type 1	Piles not covered under Column 3	Raft Foundations	Combined or isolated RCC Footings with tie beams	Isolated RCC Footings without tie beams or unreinforced strip foundations	Well foundations
(1)	(2)	(3)	(4)	(5)	(6)	(7)	(8)
i	Type I Rock or Hard Soils	1.0	-	1.0	1.0	1.0	1.0
ii	Type II Medium Soils	1.0	1.0	1.0	1.0	1.2	1.2
iii	Type III Soft Soils	1.0	1.2	1.0	1.2	1.5	1.5

Table 6-4: Values for I for structures

SL No.	Structure	Value of Importance Factor
(1)	(2)	(3)
i	Dams (all types)	3.0
ii	Containers of inflammable or poisonous gases or liquids	2.0
iii	Important service and community structures, such as hospital, water towers and tanks, schools, important bridges; important power houses; monumental structures; emergency buildings like telephone exchanges and fire stations; large assembly halls and subway stations	1.5
iiii	All others	1.0

[9] The value of b for dams shall be 1.0.

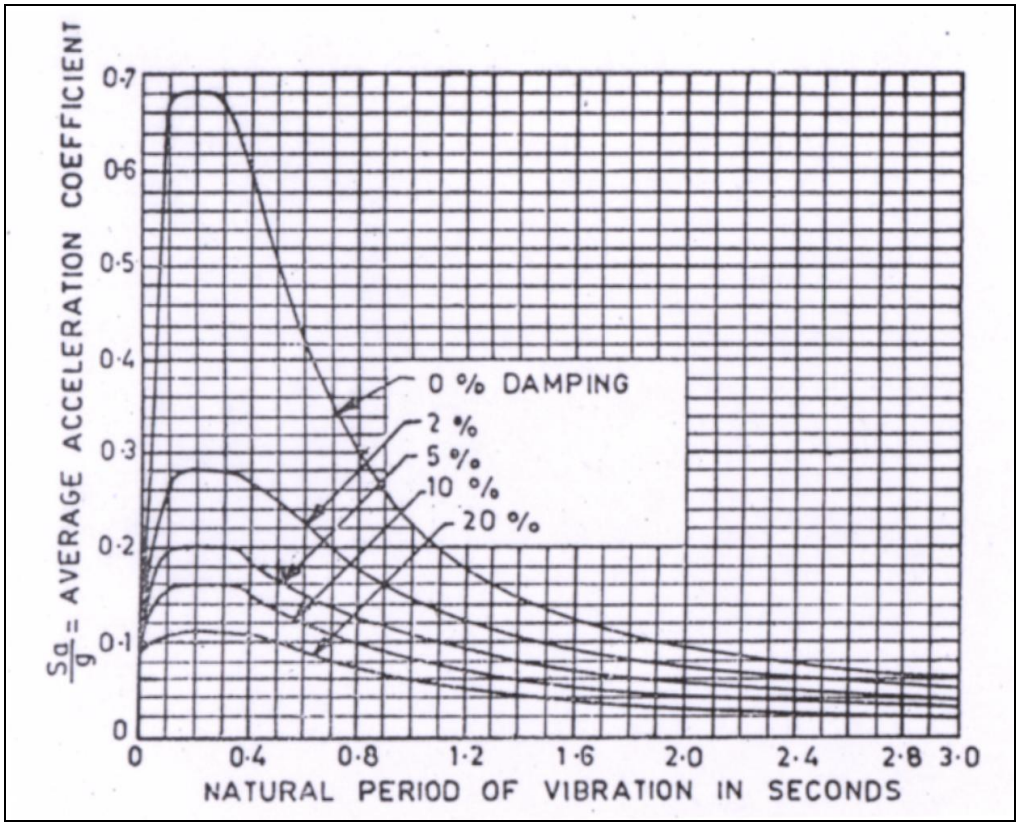

Figure 6-7: Average acceleration spectra (after IS 1893: 1984, Figure 2, pg. 18)

K represents the performance factor depending on the structural framing system and the ductility level for construction (Table 6-5).

Table 6-5. Values for *K* for structures

SL No.	Structural Framing System	Value of Factor	Remarks
(1)	(2)	(3)	(4)
i (a)	Moment resistant frame with appropriate ductility details as given in IS: 4326-1976	1.0	--
i (b)	Frame as above with RC Shear walls or steel bracing members designed for ductility	1.0	These factors will apply only if the steel bracing members and the infill panels are taken into consideration in stiffness as well as lateral strength calculations provided that the frame acting alone will be able to resist at least 25 percent of the design seismic forces.
ii (a)	Frame as in (i) (a) with either steel bracing members or plain or nominally reinforced concrete infill panels	1.3	
ii (b)	Frame as in (i) (a) in combination with masonry infills	1.6	
iii	Reinforced concrete framed buildings (Not covered above)	1.6	

The distribution of forces in the code uses:

$$Q_i = V_B \frac{W_i h_i^l}{\sum_{j=1}^{j=n} W_j h_j^l} \tag{8}$$

where Q_i represents the lateral forces at the roof of floor i, W_i represents the dead and live load (portion) of the roof and any floor i *' the weight of the walls and columns in any story is assumed to be shared half and half between the roof or floor at top and the floor or ground at the bottom, and all weights are assumed to be lumped at the level of the roof or any floor* i. h_i represents the height measured from the base of the building to the roof or any floor i and n represents the number of stories including the basement floors, where the basement walls are not connected with ground floor deck or the basement walls are not fitted between building columns, but excluding the basement floors where they are so connected. l represents an exponent that for this IS code was two for all periods.

The original development of this force distribution in ATC 3-06 (1978) has a variable for l (Table 6-6).

Table 6-6: Values for l for structures

Period (Seconds)	Frequency (Hz)	Value of l
0.25	4	1
0.5	2	1
1.0	1	1.25
1.5	0.67	1.50
2.0	0.5	1.75
2.5	0.4	2
5	0.2	2
10	0.1	2

The effective quasi-static limit for masonry has been estimated from experiment and a theoretical analysis of the errors in Newton's equation of motion at 0.4 Hz (Nichols, 2001).

The Average Acceleration Spectra provided in the Indian Standard (Figure 6-7) has been converted to the frequency spectra for the two percent damping (Figure 6-8). The relative paucity of points in the one to ten hertz region was considered to reflect the significant problem of translating the seismic data from the frequency domain into the inverted period form. The use of the period represents a carry-over from the twenties and electric circuit theory (Hall, 2001).[10]

One earthquake that has been used in developing the seismic standards for the CEUS was the Nahanni Earthquake[11] (Figure 6-9). This M6.8 event occurred in the Northwest Territories. The Nahanni earthquake has a series of spikes in the acceleration record. Veletsos and Newmark (1964) in the analysis of shock loading generated by bomb blast have considered the analysis of such pulse loading. This method is considered applicable to these large short duration pulse loads.

[10] Hall, W. (2001) personal conversation dated 26 April 2001 on the development of the period formula.
[11] Station 1, Iverson, Canada: 23 Dec, 1985.

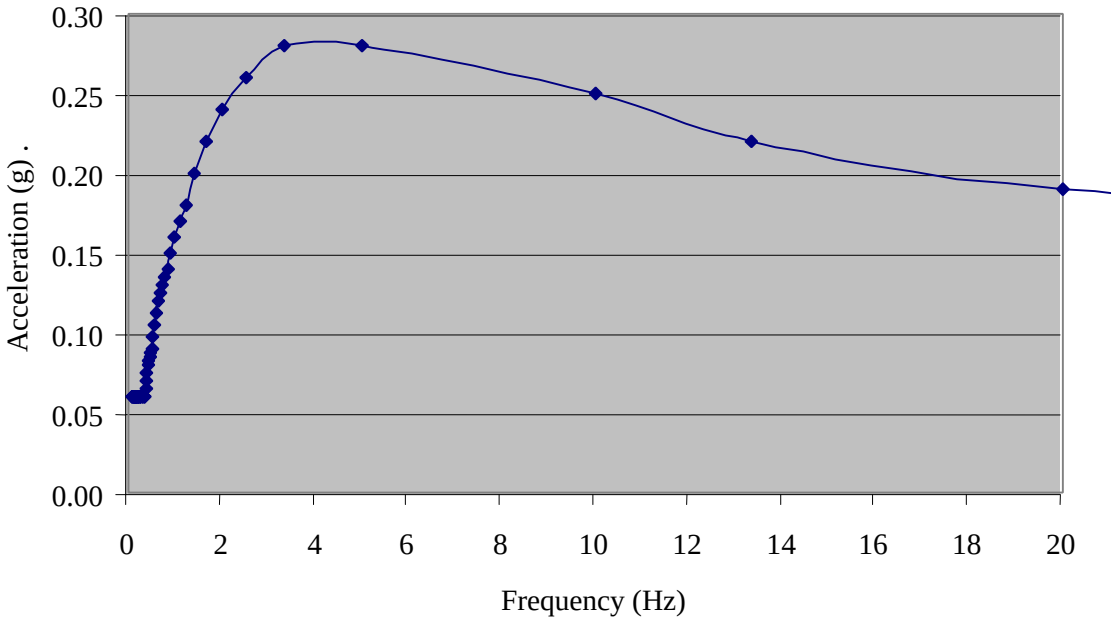

Figure 6-8: Average acceleration spectra in frequency domain

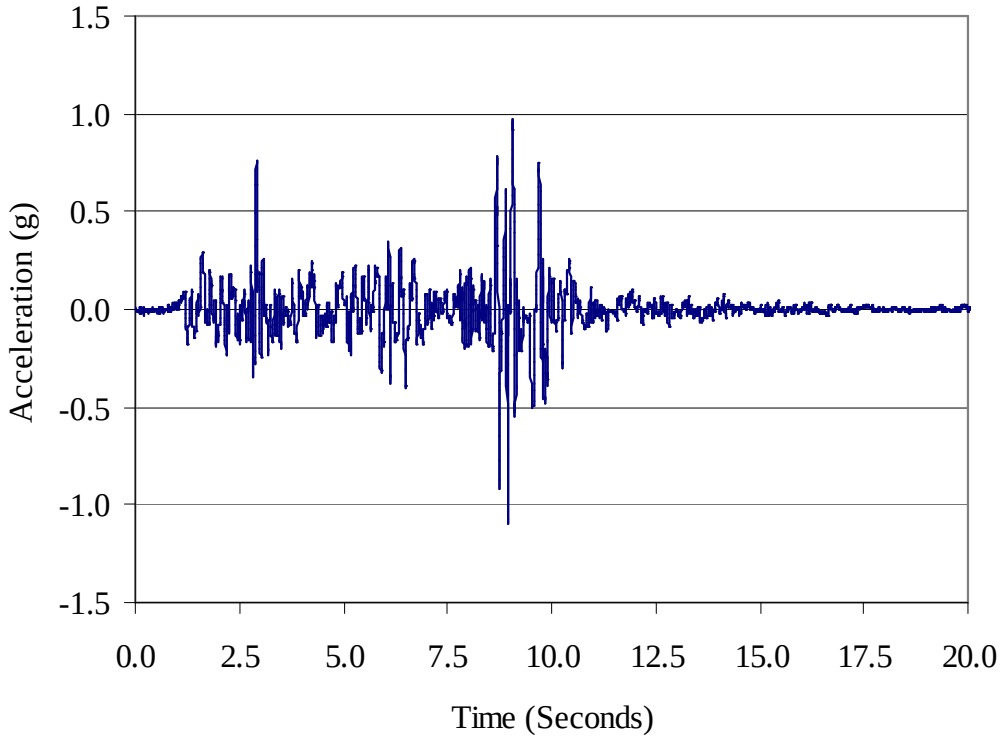

Figure 6-9: M6.8 Nahanni earthquake longitudinal time trace

The work of Atkinson and Boore (1995) for Eastern North America (ENA) provides one interesting seismic data set. The two specific earthquake events that were used in this work, were at Saguenary, Quebec (1988) and Nahanni, Northwest Territories, both located in Canada. The new ground motion relations provided by Atkinson and Boore cover the peak ground motions and response spectra for Eastern North America events in the range of M 4 to 5. Atkinson and Boore noted that this analysis was consistent with the data from the Nahanni and Saguenary earthquakes. Whilst the trace (Figure 6-9) was instructive, it does little to provide guidance as to the frequency relationship for the earthquake trace.

This data on the frequency component is instructive when it is matched with building data and the modal frequencies. The pulse analysis technique of Veletsos and Newmark (1964) can be applied to the low frequency peaks in the FFT. The same trace (Figure 6-9) was transformed using the procedure from Numerical Recipes in Fortran[12] in a program named CONVERT. The discrete Fourier transform programs were checked using the exponential function routine and the square wave routine from Brigham (1988, Chapter 9). The resultant frequency domain trace for the time-domain acceleration trace has been competed with frequency as the dependent variable (Figure 6-10) and using the period as the dependent variable (Figure 6-11). Note the point density differences in Figure 6-11, the fact that one third of the graph represents the quasi-static region; one third represents the region from 0.4 to 1.0 Hz and one third the region from 1.0 Hertz to the recorded limit. The FFT limit from typical time traces is 25, 40 or 100 Hertz.

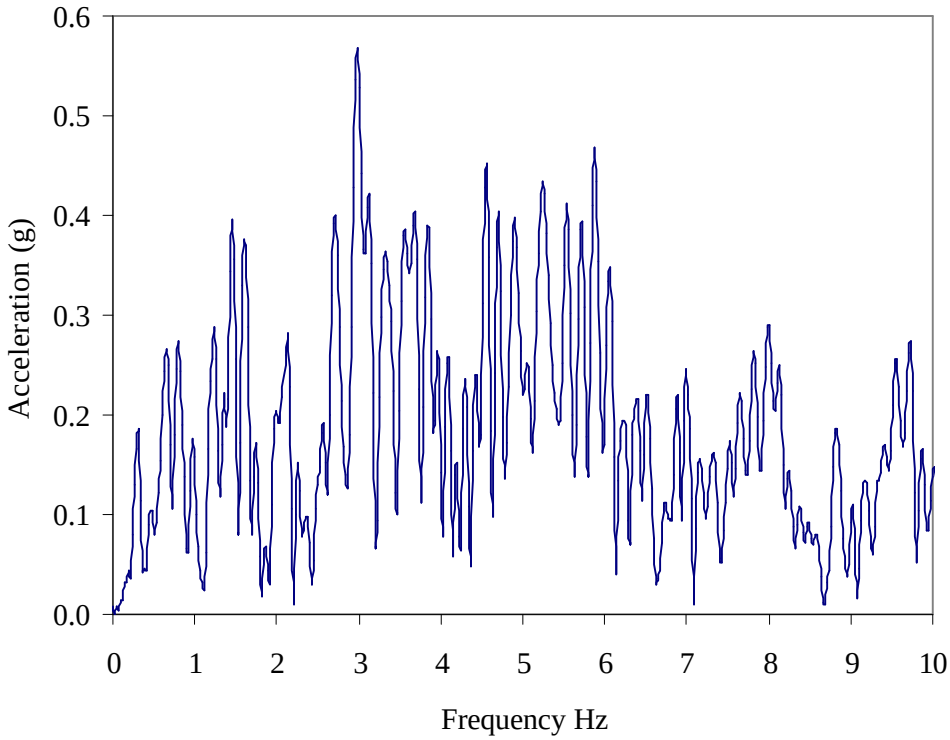

Figure 6-10: FFT of the Nahanni earthquake

[12] Press *et al.*,(1994), *Numerical Recipes in Fortran* (Cambridge: Cambridge UP), DFOUR Routine.

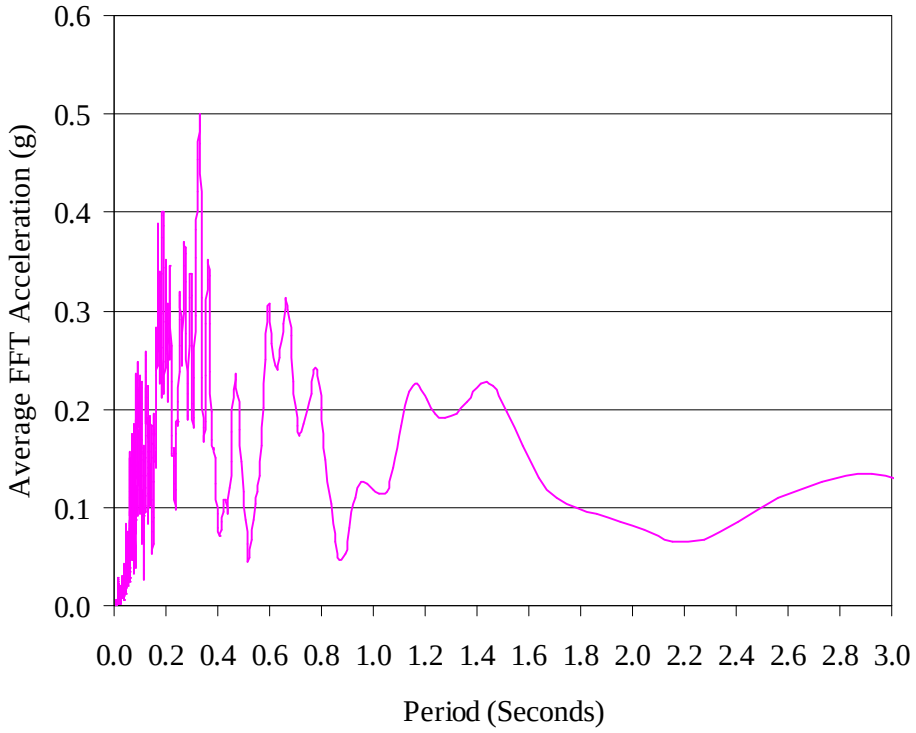

Figure 6-11: FFT of the Nahanni earthquake (period)

At Memphis, one has access to the work of Horton, Barstow, and Jacobs [13] who have generated synthetic earthquakes of varying M r combinations and stress drops for the LAMB project (Abrams and Shinozuka).[14] Jacobs[15] noted that in the production of these records that "*natural records are always 'holey' or peaked and troughed, but to various degrees. This spectral roughness is pronounced when you make Fourier spectra or undamped response spectra, but diminishes of course with increasing damping of the SDoF resonator for response spectra. The latter is what happens really in damped structures. Occurrence of spectral roughness is a strong function of the site conditions: i.e. of the impedance (shear-wave velocity times density) profile with depth for the site. The Nahanni and El Centro records have less contrast-rich soil/rock profiles, while the sites for Memphis we modelled have very soft soils overlying denser sands, and eventually hard rock, therefore being very ringie and full of holes and peaks. We start out in the synthetics with a smooth Brune spectrum, which becomes a bit more ringie after the crustal wave-propagation scattering function is applied (and the Earth does that also, that's why we mimic it); but once we add in the soil response we really get site-specific 'holiness'. That is the reason why you sometimes get surprising damage for certain structures at certain sites: double resonance*

[13] Horton, S.P., Barstow, N., and Jacobs, K., (1997), Simulation of earthquake ground motion in Memphis, Tennessee, Proceedings of the Eleventh World Conference on Earthquake Engineering, June 23-28, 1997, Acapulco, Mexico, Elsevier Science, Paper 1302, passim.

[14] Abrams, D.P., and Shinozuka, M., (1197), Final Report Loss Assessment of Memphis Buildings, Technical Report NCEER-97-00, (Urbana, Illinois: UIUC), passim.

[15] Jacobs, K., Lamont Doherty Observatory, Columbia University, personal communication, November 1997.

between site peak and fundamental period of the structure. The most famous case for this is of course the Mexico City effect in 1985 (?): 1- 2 second 10-20 story high rise buildings located on the clayey Old Lake bed (site resonance's peaked near 1 - 2 seconds) collapsed, while people in adjacent old colonial masonry buildings 2 or 3 stories high did not even realize there was an earthquake (totally detuned). If you are interested in a generic study, then you must use several of the records from different site conditions, and average the effects, so that you never have structural performance for a given building height or fundamental period influenced by the peaks or troughs of just one site condition. I do not think that the use of artificially smoothed spectra is a valid substitute. Rather the smoothing of performances over real site conditions seems to me a more valid approach, at least if you are not only interested in the mean response, but also want to get a measure for the variability of response, which highly depends on whether double resonance's of sites and structures do or do not occur under region-specific site conditions and their respective variability." The Nahanni earthquake tolerably matches the undamped average acceleration spectra from the Indian Standard 1893: 1984. The Nahanni earthquake has a spike of 1.5 g's and a short time at about 12-15 seconds. The Gujarat earthquake was a larger, longer event. The Indian Standard 1893: 1984 was based on the work from ATC 3-06 (1978) that was largely developed at the University of Illinois by Newmark, Hall and Souzen. The current FEMA documents related to the design of new structures are derivatives of the ATC manual. The two standards IS and FEMA have diverged in the base equations that have been selected from the ATC work. It was instructive to compare the calculated results from the two derived documents for a typical range of building sizes. The building has been assumed to have three depths ten, twenty and thirty meters and heights ranging from three meters in increments of three meters. The analysis was completed for Zone V, or MMI XI-XII. The building period was determined against the height for the varying type of structure (Figure 6-12).[16]

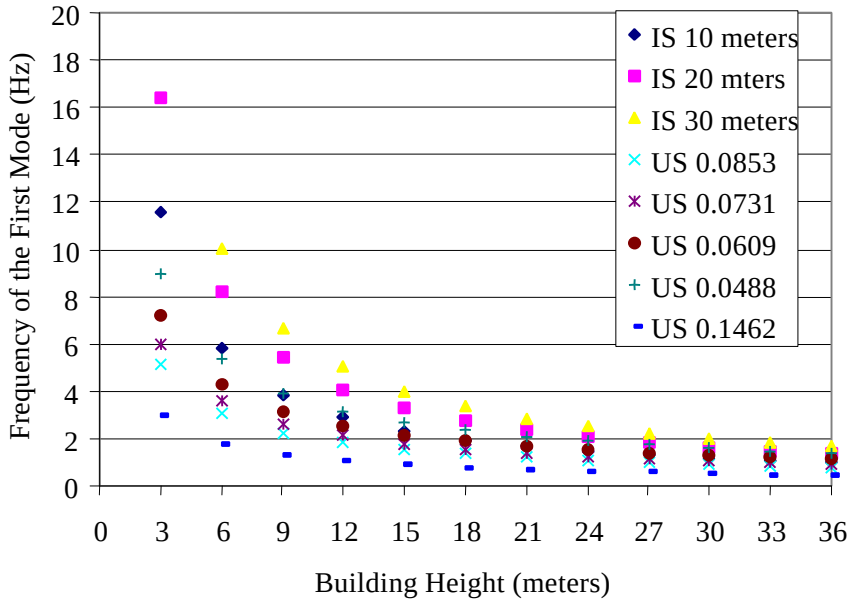

Figure 6-12: Varying building frequency for different structural systems

[16] The IS represents the IS analysis for three building depths and the US represents the various metric constants used in equation (6).

The mean building period was determined against the height for IS and US data (Figure 6-13).

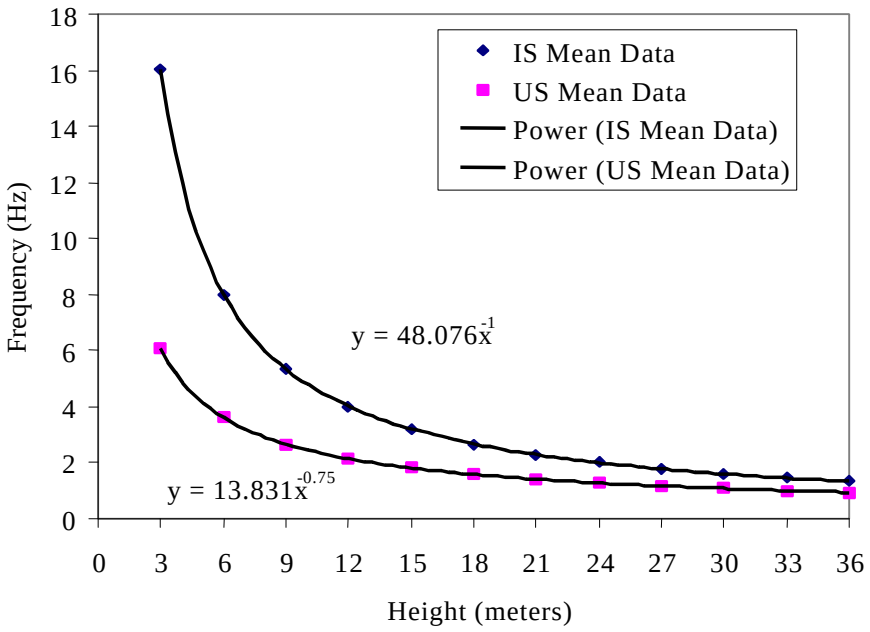

Figure 6-13: Mean building frequency for IS and US systems

The clear result was that the Indian standard provides a higher estimate for the frequency of the first mode than the United States equivalent codes. The difference was not significant for the taller structures, but is significant for short structures. The relationships for the two data sets are shown on the figure. The Indian Standard C coefficient relates the stiffness of the structure to the loading from the earthquake. A stiffer structure attracts proportionally higher load (Figure 6-14).

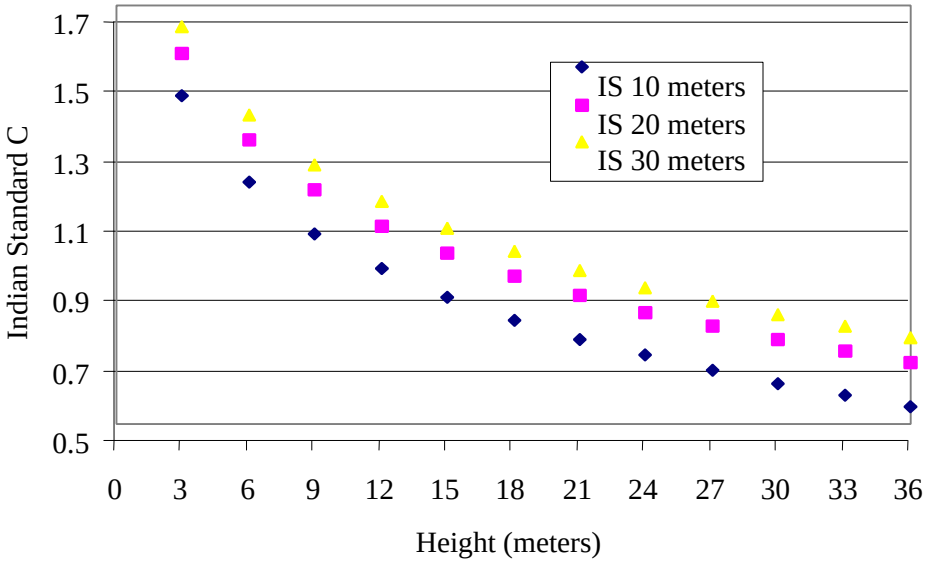

Figure 6-14: Co-efficient C versus the building height for different building depths

The composite factor for the Indian Standard KCa_h was calculated for the buildings (Figure 6-15).

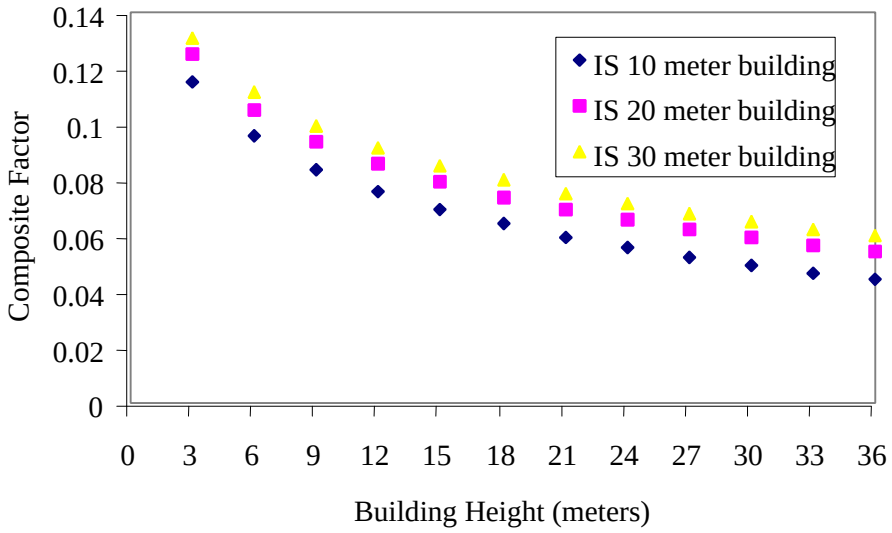

Figure 6-15: Composite factor for the three building depths

The composite factor was established for the response spectrum method (Figure 6-16).

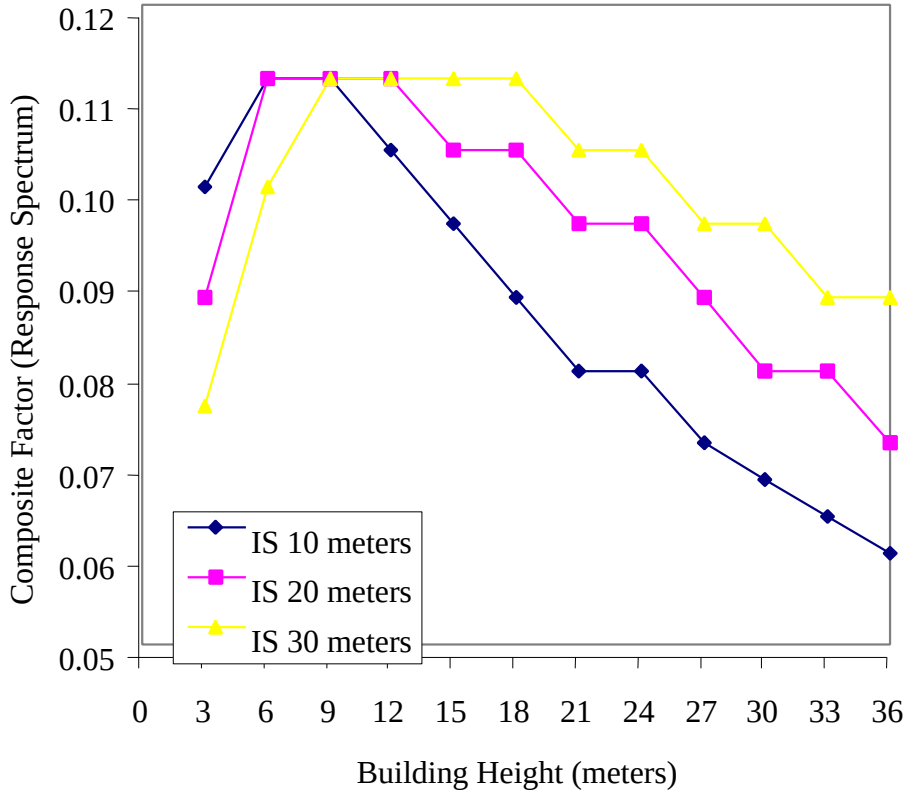

Figure 6-16: Indian standard composite factor response spectrum method

The composite factor was established for the response spectrum method for the US data (Figure 6-17).

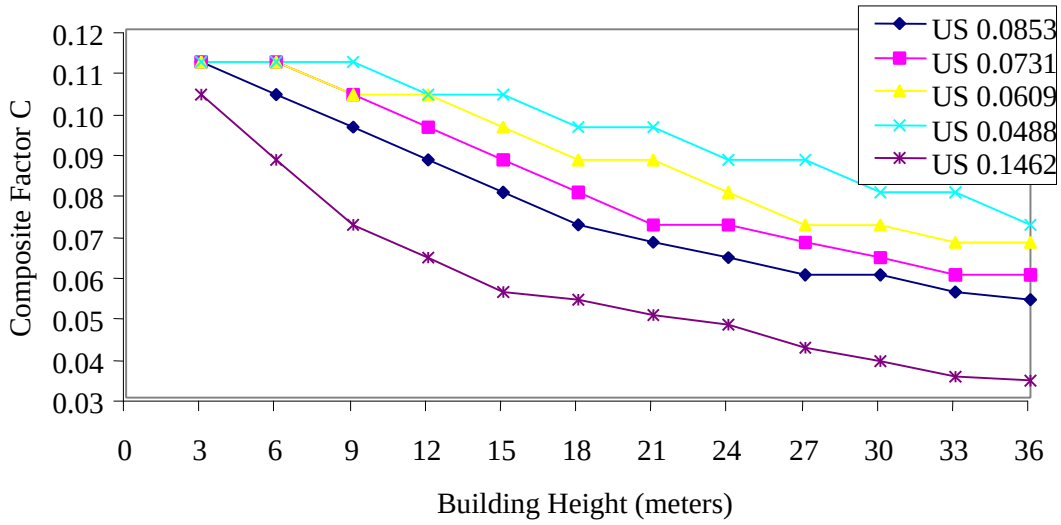

Figure 6-17: Indian standard composite factor response spectrum method US data 2 % damping

The base shear equation from ATC 3-06 has the form:

$$V_B = C_s W \tag{9}$$

The composite C_s factor presented in ATC 3-06 Equation 4-1 was calculated assuming a Zone 7 area (equivalent to California at the time) for a response modification factor of 8 and the acceleration factors both 0.4 (Figure 6-18).

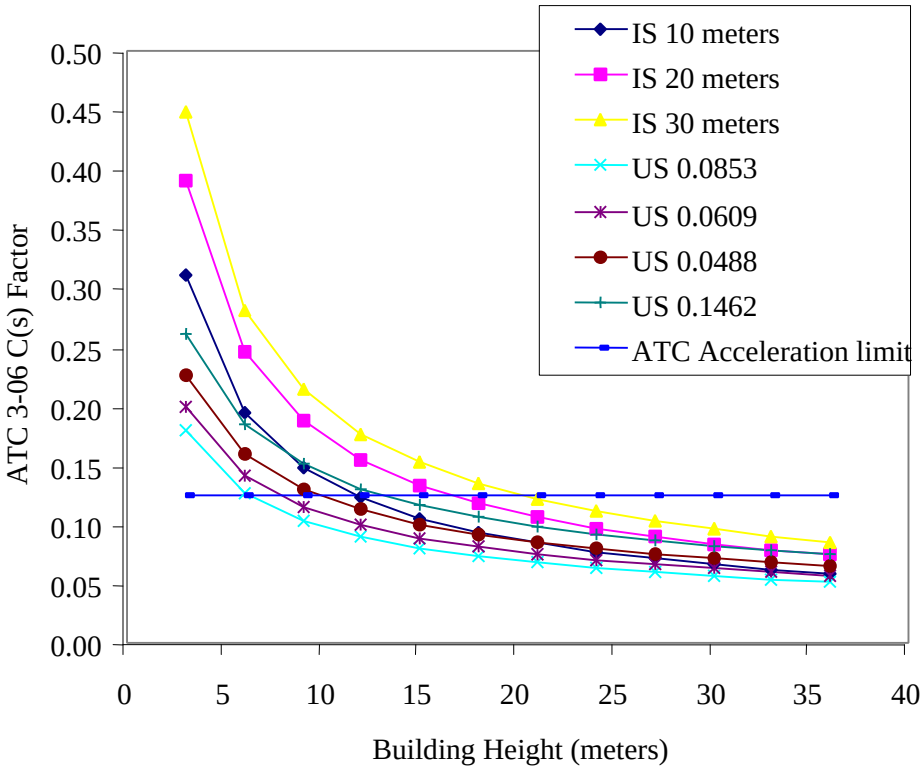

Figure 6-18: ATC 3-06 composite C_s factor and the ATC acceleration limit

The two controlling features of the ATC method are the acceleration limit that for standard conditions was set by the developers of the method at three Hertz.[17] The FFT of the Nahanni earthquake does not suggest that the limit was inappropriate; however, the two limiting equations in ATC 3-06 are extremely sensitive to the value of R and certainly the value of R selected at eight would appear high simply to bring the composite C_s factor into the range of the results of the other methods. The acceleration limiting composite C_s factor was inversely proportional to R. The base shear equation from FEMA 273 has the form:

$$V = C_1 C_2 C_3 S_a W \tag{10}$$

Where W represents the dead load and the anticipated dead load; C_1 was modification factor to relate expected maximum inelastic displacements to the displacements calculated for an elastic analysis; C_2 represents the modification factor to represent the effect of stiffness degradation and strength deterioration on maximum displacement responses; C_3 represents $P-\Delta$ factor; V represents the base shear load on the structure and S_a represents the response spectrum acceleration at the fundamental frequency of the structure for that direction. The methods for determining the natural frequency of the buildings are based on either modal analysis, equation (4) or for a single story building a special purpose equation related to displacements of the walls and diaphragm.

[17] Calculation using ATC 3-06 equations 4-2 and 4-3 pg. 55.

The New Madrid Seismic Zone is equivalent in seismic form to the Gujarat State. A review of the NMSZ data can assist in considering the current status of the IS and whether revisions are required to the American Standards. The key points to consider are the results from the Nahanni earthquake, the typical synthetic trace results developed for the NMSZ and the development work by Veletsos and Newmark on the additive impact of pulse in seismic events. The estimated spectral response data for the New Madrid Seismic Zone was determined from the USGS maps in FEMA 273 (Table 6-7).

Table 6-7: Spectral accelerations NMSZ

Description	Period 0.2 sec (5 Hz)	Period 1 sec (1 Hz)
MCE 5 % ? Class B	3	1.23
2 % probability in 50 years 5 % ? Class B	3	1.23
10 % probability in 50 years 5 % ? Class B	0.43	0.092

The adjustment of the site class allows for the soil classes A to F. The site class in the NMSZ was assumed D for the purpose of this analysis (Table 6-8).

Table 6-8: Spectral accelerations site class adjusted NMSZ

Description	F_a	Period 0.2 sec (5 Hz)	F_v	Period 1 sec (1 Hz)
MCE 5 % ? Class B	1.0	3	1.5	1.84
2 % probability in 50 years 5 % ? Class D	1.0	3	1.5	1.84
10 % probability in 50 years 5 % ? Class D	1.45	0.60	2.4	0.221

The general response spectrum can be calculated using the FEMA 273 (equations 2-8 and 2-9). Two response spectra are relevant for the New Madrid Seismic Zone; these are the Maximum Credible Earthquake[18] and the 475-year return period.[19] The response spectrum (Figure 6-19) for the NMZS MCE has developed estimated natural frequencies for the various combinations of building height and type. These spectral accelerations are developed from the USGS data contained in FEMA 273.

[18] The two-percentile event was the MCE.

[19] The return period was used in this chapter as we are discussing characteristic or singular points in the probability space functions that were developed to model the probability of occurrence of the earthquakes. The trivial conversion for this return period was ten percent in fifty years. The difficulty at least for this author from this definition was the building life of five decades. The thought that structures will have a failure of two percent in fifty years or ten percent in fifty years fails to account for the characteristic earthquakes that dominate the fatality counts in earthquakes; that we have general failure in an earthquake of buildings as in the 1988 Spitak earthquake must be considered intolerable in this century. The anomalous situation that occurs in some interplate areas can be explained and the issue of fifty years in these few locations can be considered a trivial issue. It was not considered a trivial issue for areas with characteristic events and one that may fail to account for the basic life safety issues under these specific circumstances.

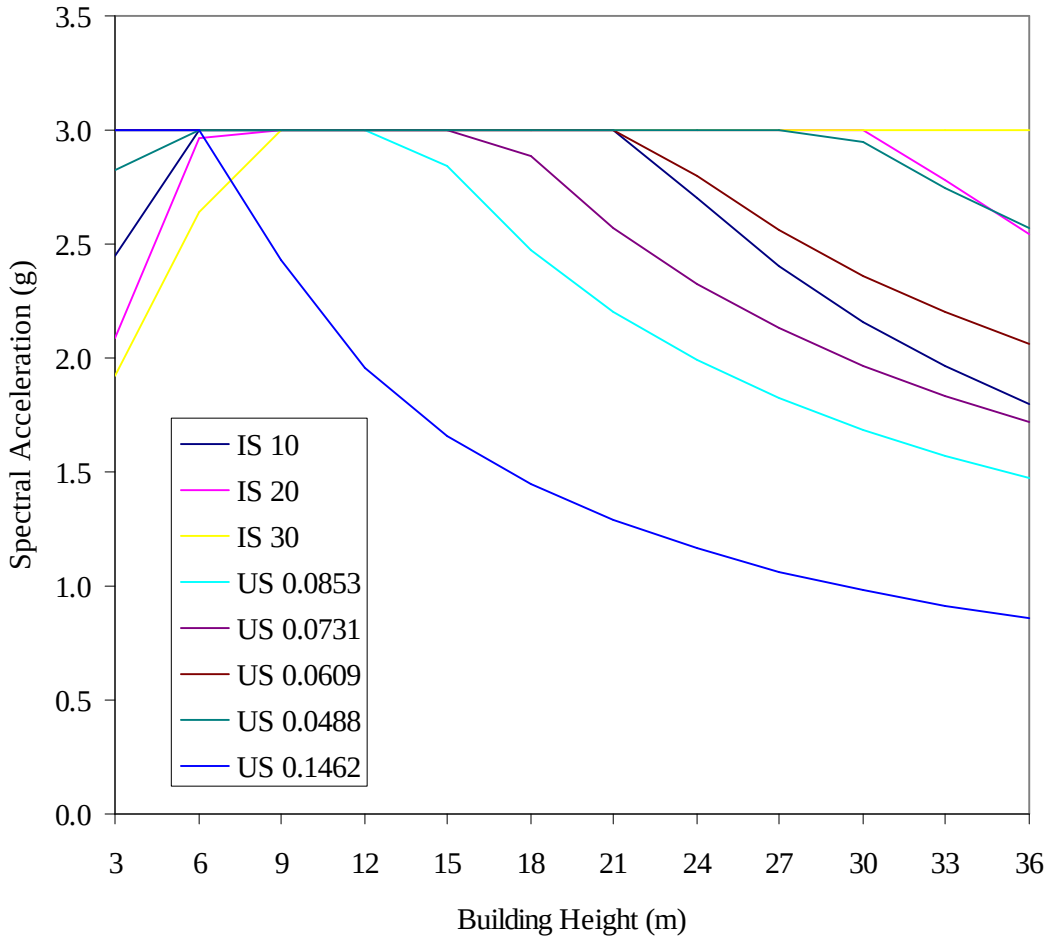

Figure 6-19: NMSZ MCE spectral accelerations for the standard building range

The problem that can be identified in the use of the standard spectral acceleration shape relates to the occurrence of a tuned structure and FFT for a particular earthquake or simply an earthquake with a spread of energy through the power spectrum. The results demonstrate the scatter in using the different building periods. The collapse of reinforced concrete buildings at a distance of 250 km in Ahmedabad points clearly to the design issue of soft story as the cause of failure, however without an accurate estimate of the frequency of the building then the base shear can be in error. This underscores the interrelated issues of tuned buildings, systematic errors in building frequency and the problem of spikes in the traces of great earthquakes. The purpose of using the NMSZ data was to consider these issues and determine whether the existing analysis methods developed from the earlier work of Veletsos and Newmark (1964) requires changes for great or characteristic events.

The response spectrum (Figure 6-20) for the NMZS 475 year return period has been developed for the various combinations of building height and type. These spectral accelerations are developed from the USGS data contained in FEMA 273.

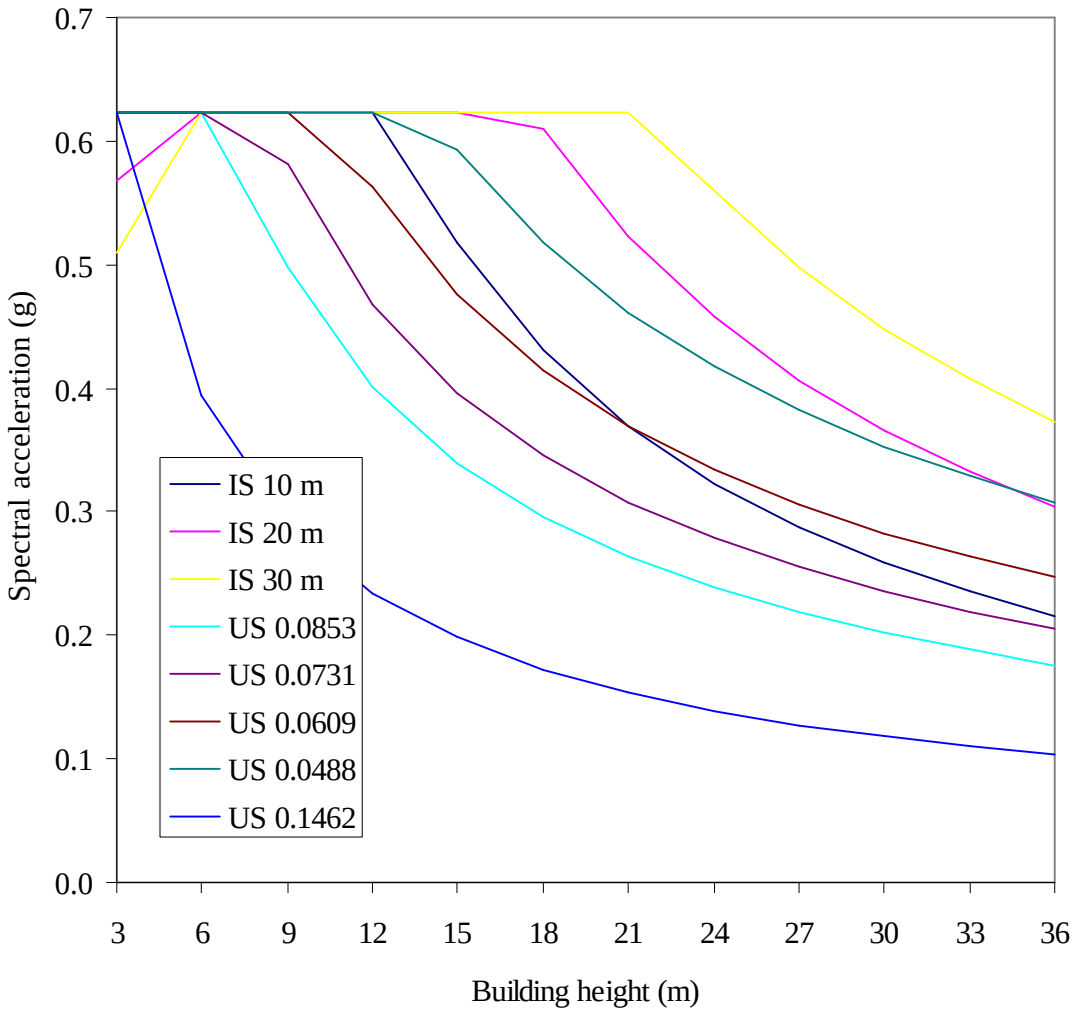

Figure 6-20: NMSZ 475 year spectral accelerations for the standard building range

The range in the results between the two codes was interesting. The paleo-seismological data for the NMSZ would suggest that the MCE and the 475-year return period event should be a great event as defined by Richter. Green and Hall (1994), and Krinitzsky (2000) discussed in detail the problem of hazard analysis methodologies. The conclusions of these authors are that there are shortcomings in the current analysis techniques.

The method being developed by Kafka and Ebel (2000) provides an alternative method to estimate the seismicity of a regional area. The clear point is 35 percent of all seismic activity occurs in areas that have not recorded prior activity.

The next step was to consider the differences between the Nahanni earthquake and the various spectra formula.

Veletsos and Newmark (1964) provide the mathematical and numerical derivation of design spectra (shown in their Figure 2.23). The adoption of a constant velocity component to the design

spectra represents for their analysis a simple and pragmatic limit to the zero gradient on the spectra for the varying pulse forms. This limit was based on their analysis (Veletsos and Newmark, 1964, *§ 2.9.2 Presentation and Discussion of Results, a. Characteristics of the Representative Spectra*) of the form of the design spectra for a range of pulse shapes.

The choice made by Veletsos and Newmark was appropriate for their analysis, of course noting their lack of strong motion data for intraplate earthquakes. The limited strong motion data available now provide data to use the Veletsos and Newmark techniques to allow for acceleration spikes within a normal earthquake trace.

The Nahanni earthquakes FFT and a number of the standard spectral shapes are plotted on Figure 6-21. The spectral shapes include data from Newmark and Hall (1978, Figure 6-5) that were developed for the nuclear regulatory agency, the standard NMZS 475 year, a newly developed bounding spectra[20] and the Newmark and Hall spectra scaled to 0.6 g's. The frequency has been plotted in the range of zero to ten Hertz as this represents the region of interest for masonry and soft story RC structures.

The bounding spectrum has been developed to essentially encase the NMSZ earthquakes. The bounding function has been scaled to twenty percent of the normal limits. The function has been developed for comparison purposes only and was not developed for any design purpose and should not be used for that purpose.

[20] The bounding spectra has not been based on previous models.

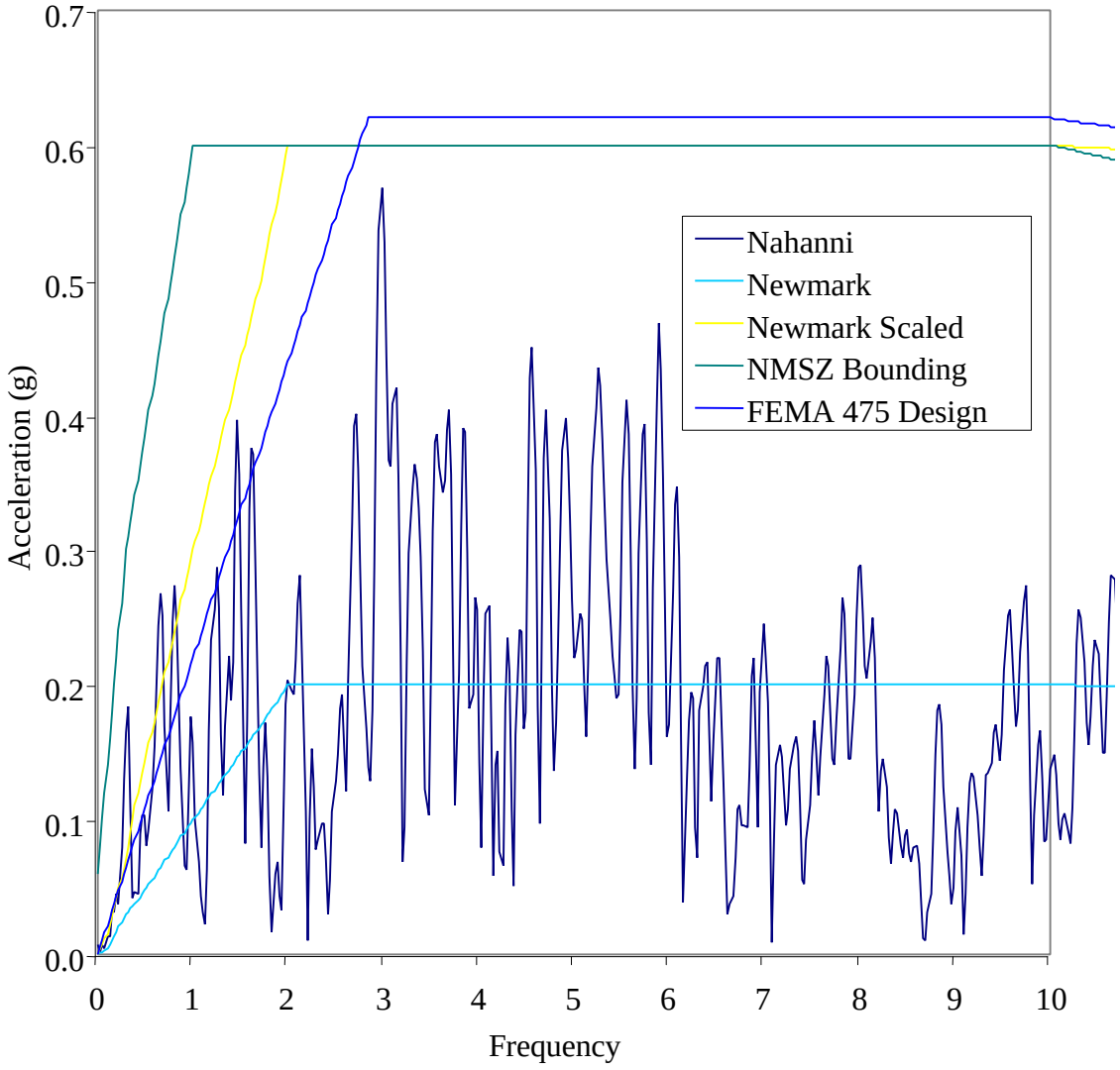

Figure 6-21: Nahanni earthquake FFT and standard spectra (0 to 10 Hz.)

Only the bounding function does not have peaks in the FFT that exceed the design spectra. The Nahanni earthquake was a M6.8 event of short duration. The data have been recast in the frequency range of zero to two Hertz (Figure 6-22).

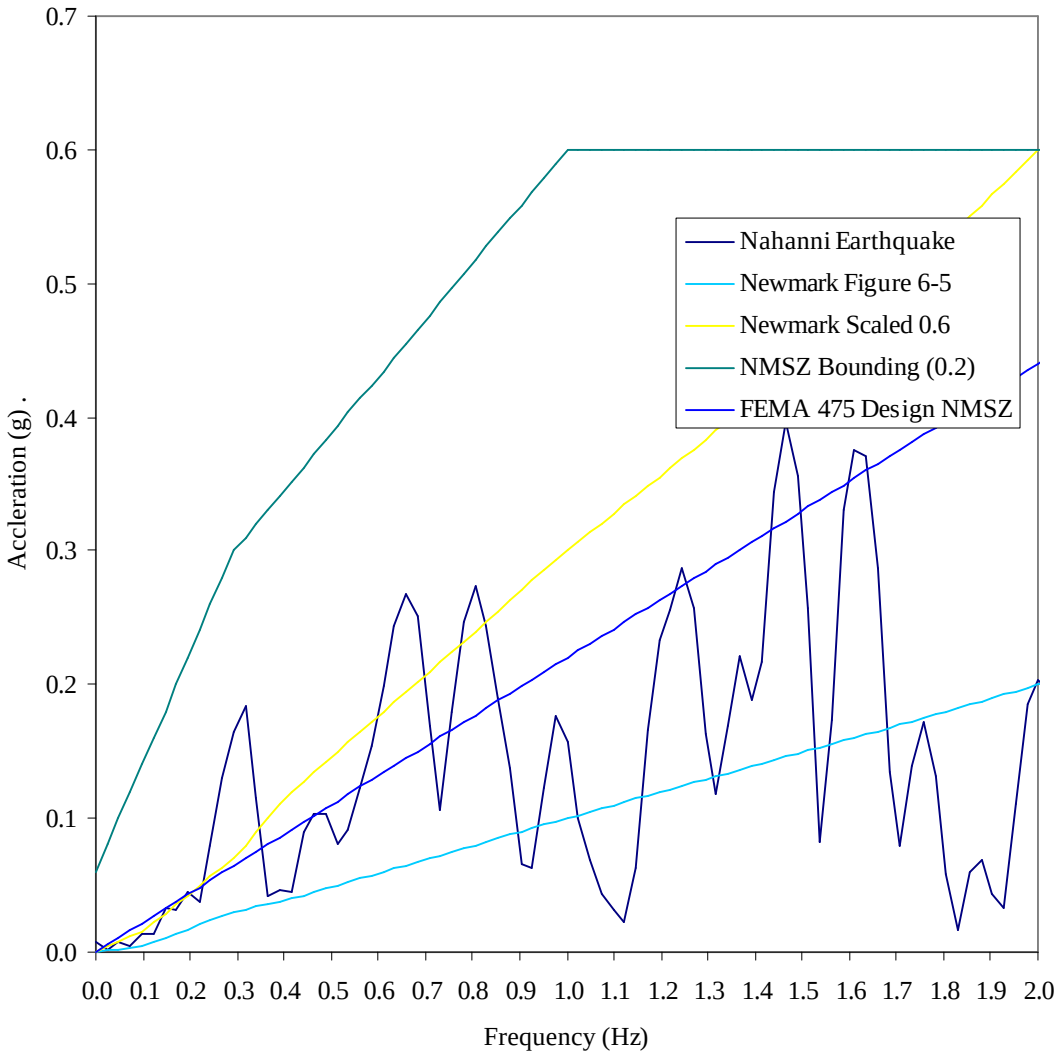

Figure 6-22: Nahanni earthquake FFT and standard spectrums (0 to 2 Hz.)

The Nahanni earthquake has several peaks in the FFT trace (Figure 6-22) with numerical values greater than the design spectra. The design spectra are based on the constant velocity region from about 0.2 to 2.0 Hertz (Newmark and Hall, 1978, Figure 6-5). The Nahanni FFT provides spikes that exceed the design spectra in the range from 0.2 to 2.0 Hertz. What are the impacts of these spikes?

The study into the loss assessment in Memphis buildings had a number of synthetic traces prepared for the Marked Tree region in the NMSZ. The M7.25 earthquake time trace has been converted to the frequency domain using the standard FFT technique. The use of the M7.25 was purely arbitrary. The FFT trace (Figure 6-23) was approximately damped using the factors derived by Newmark and Hall (1978). The earthquake had a peak intensity of about 3.2g's.

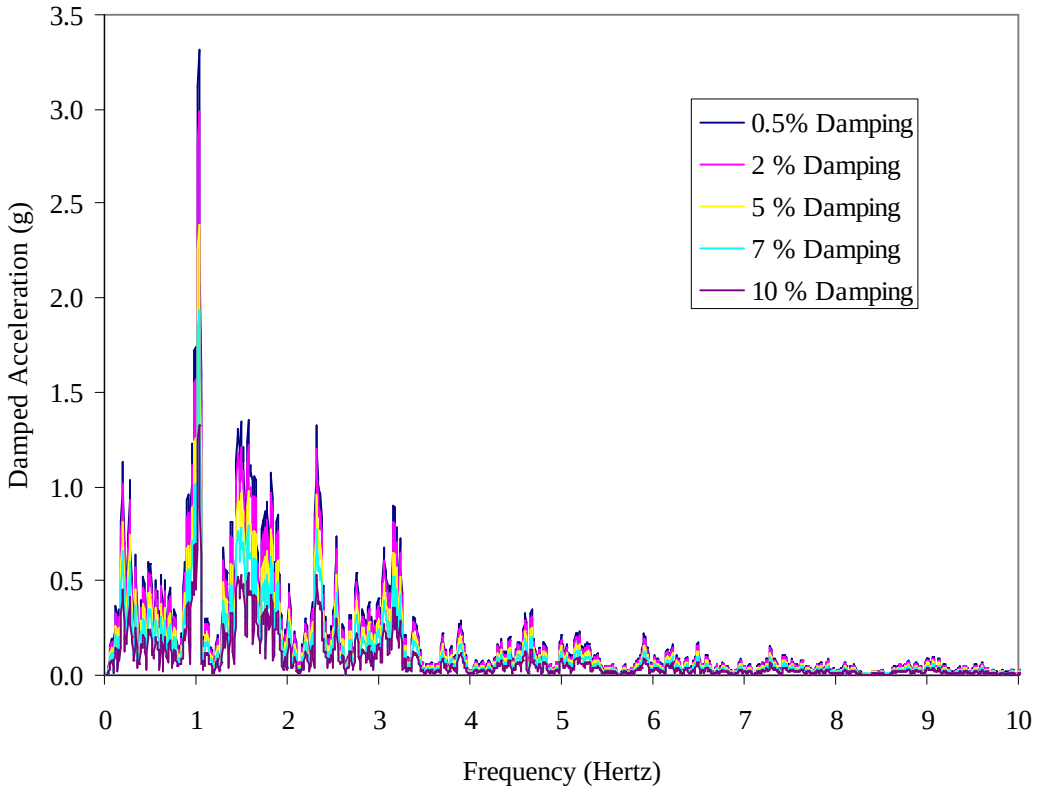

Figure 6-23: M7.25 Marked Tree earthquake FFT (with damping)

The M7.25 Marked Tree earthquake FFT and a number of the standard spectral shapes are plotted on Figure 6-24. The spectral shapes include data from Newmark and Hall (1978, Figure 6-5) that was developed for the nuclear regulatory agency, the standard NMZS MCE, the full bounding spectra[21] and the Newmark spectra scaled to 0.6 g's. The frequency was plotted in the range of zero to ten Hertz as this represents the region of interest for masonry and RC structures. The FFT for the M7.25 breaks the design spectra at a number of low frequencies. The NMSZ MCE will require significant damping in the building to ensure that demand does not exceed capacity.

The data have been recast in the frequency range of zero to two Hertz (Figure 6-25) and with the dependent variable the period (Figure 6-26). The spectral shapes have been tabulated for the standard spectra and the estimated bounding spectra (Table 6-9). Figure 6-27 and Figure 6-28 show the period versus frequency graph, and the various design spectra used in this report for the ranges of 0-100 Hz and 0-10 Hz. The purpose of showing the period graph was to demonstrate the rapid slope changes in this function in our region of greatest interest.

Queste (2000) has shown a method to allow for the variation in the peaks in the SDOF operator for the earthquake record CH85VALP.070. The method uses a shift in the curve and the intersection frequency (Figure 6-29). This method for allowing for the spike represents the same mathematical procedure as the development of the bounding function in the frequency plots.

[21] The bounding spectra has not been based on previous models.

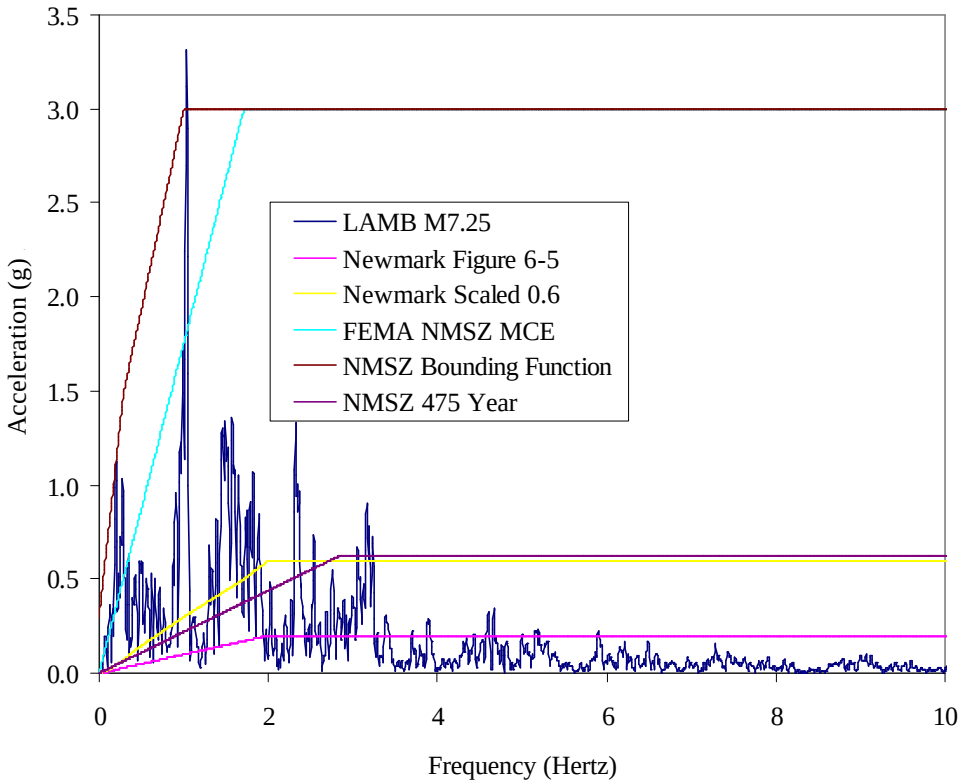

Figure 6-24: M7.25 Marked Tree earthquake FFT with standard spectral shapes

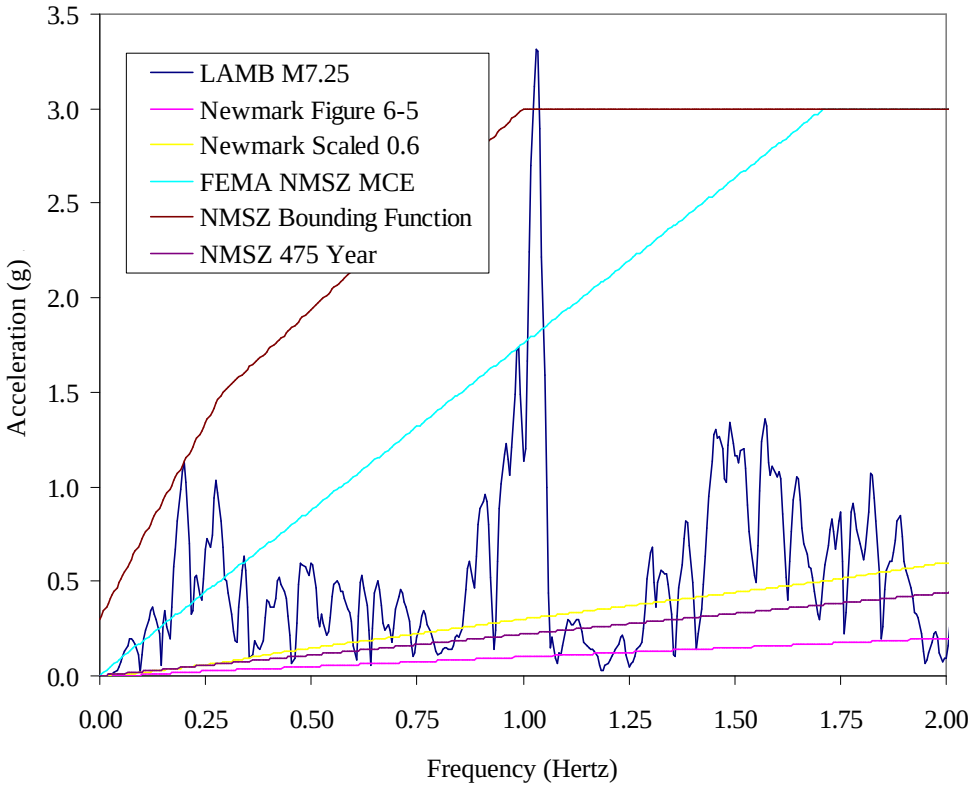

Figure 6-25: M7.25 Marked Tree earthquake FFT with standard spectral shapes 0 to 2 Hz.

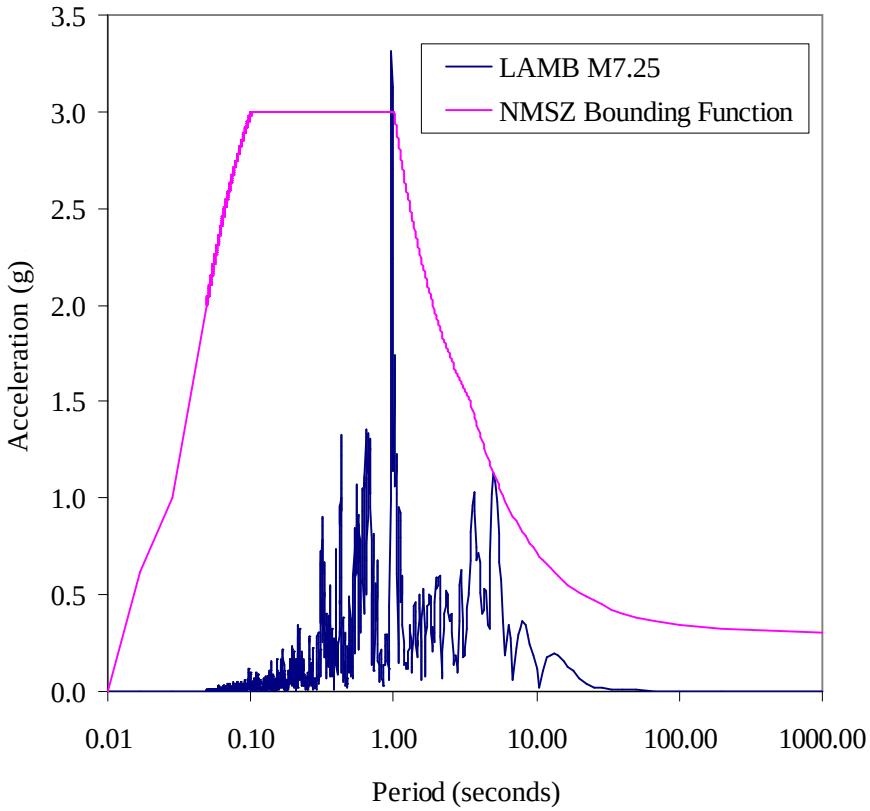

Figure 6-26: M7.25 Marked Tree earthquake FFT with the bounding shape

Table 6-9: NMSZ tabulated spectral points

Frequency Hertz	Period seconds	Acceleration (g)					
		Newmark Figure 6-5	Newmark scaled 0.6	NMSZ MCE	LAMB NMSZ Bounding	LNB (0.2)	NMSZ 475 year
0.000	1000.000	0.000	0.000	0.000	0.30	0.06	0.00
0.098	10.204	0.004	0.015	0.172	0.70	0.14	0.02
0.293	3.413	0.030	0.070	0.514	1.50	0.30	0.06
0.415	2.410	0.040	0.120	0.728	1.76	0.35	0.09
0.610	1.639	0.060	0.180	1.071	2.17	0.43	0.13
1.001	0.999	0.100	0.300	1.757	3.00	0.60	0.22
1.709	0.585	0.170	0.500	3.000	3.00	0.60	0.38
2.002	0.500	0.200	0.600	3.000	3.00	0.60	0.44
2.82	0.355						0.62
10.010	0.100	0.200	0.600	3.000	3.00	0.60	0.62
35.010	0.029	0.170	0.500	1.580	1.00	0.20	0.38
60.010	0.017	0.170	0.170	1.340	0.62	0.12	0.21
100.000	0.010	0.000	0.000	1.200	0.00	0.00	0.00

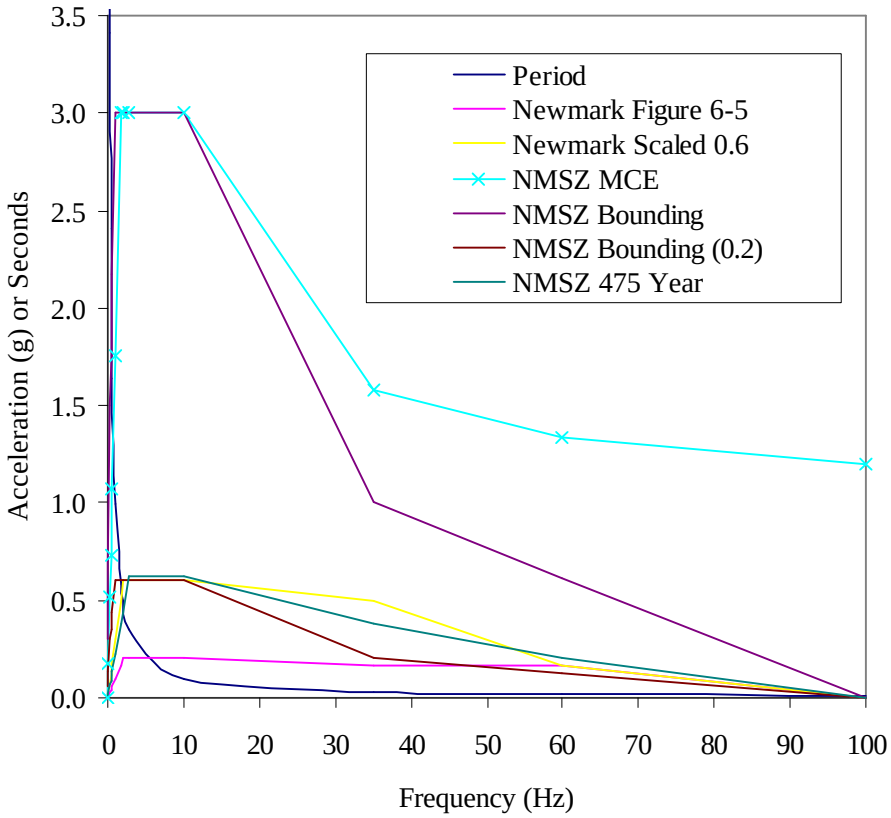

Figure 6-27: Period versus frequency and the various design spectra

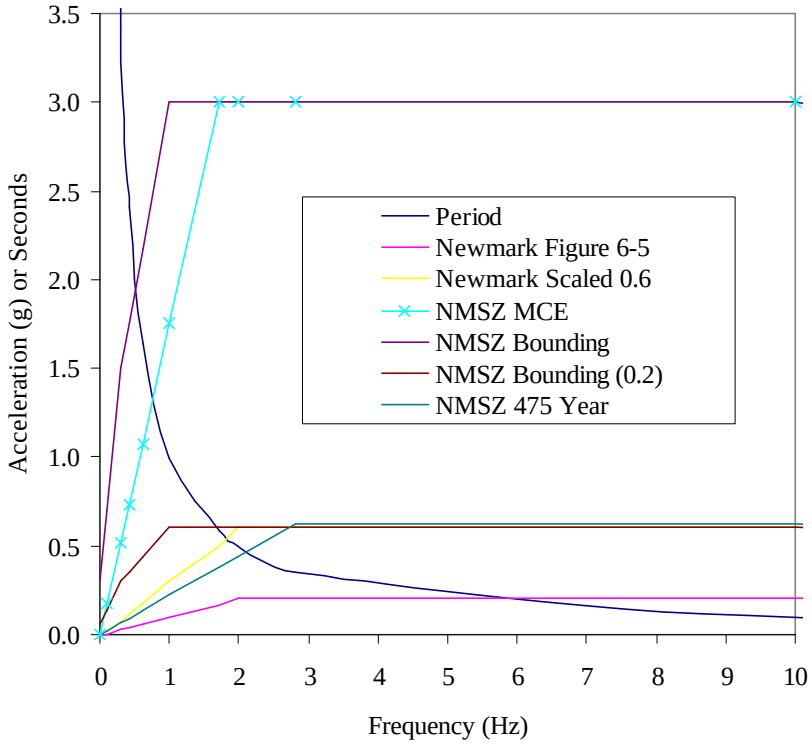

Figure 6-28: Period versus frequency and the various design spectra 0-10 Hz.

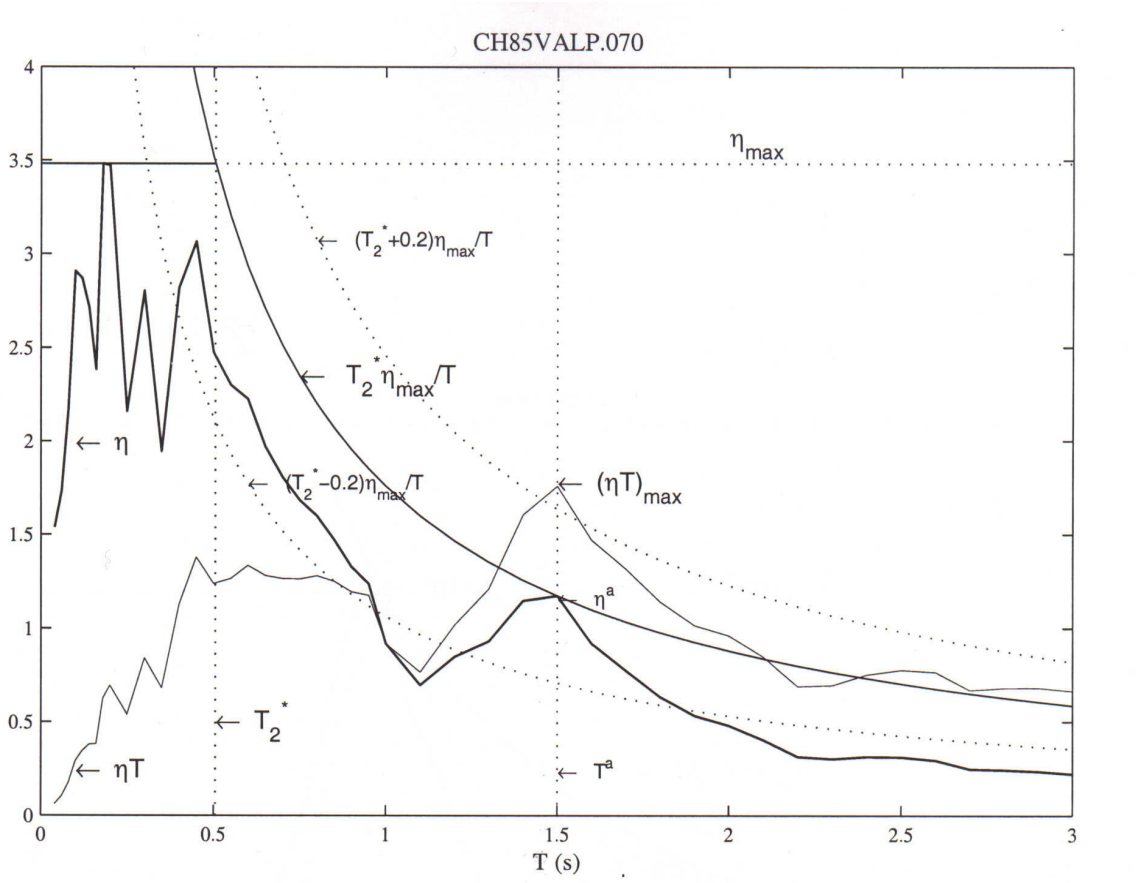

Figure 6-29: CH85VALP.070 Method to adjust for a spike in the record

A number of earthquake details are provided in Table 6-10. These events are typical design earthquakes used in the development of standards.

Table 6-10: Earthquakes, location, date, magnitude, and duration

Earthquake Location	Recording Location	Date of the event	Magnitude	Duration
Marked Tree Arkansas	Synthetic		7.25	40
Nahanni (1)	Station 1,Iverson, Canada	23 Dec, 1985	6.8	12
Nahanni (2) St 3	Battlement Creek, Canada	23 Dec, 1985	6.8	20
Saguenary (1) St 8	La Malbaie, Canada	25 Nov, 1988	5.4	20
Saguenary (2) St 16	Chicoutimi Nord PQ, Canada	25 Nov, 1988	5.4	15
Irpinia Calatrini	Italy	23 Nov, 1980		70
Newcastle Australia	Synthetic	28 Dec, 1989	5.5	6
Miramichi Loggie Lodge	Canada	6 May, 1982		1
Imperial Valley (1)	El Centro, USA	18 May, 1940	7.1	30
Imperial Valley (2)	El Centro Peknold, USA	18 May, 1940	7.1	28
Miyagi-Ken-Oki	Sensai City, Japan	12 June, 1978		35
Parkfield California		27 June 1966		20
San Francisco	Cholame St., California	22 March, 1957		10
Kern County	Taft High, California	21 July, 1952	7.6	40

The first peak and the maximum peak in the FFT spectra for the earthquakes listed in Table 6-10 are shown in Figure 6-30.

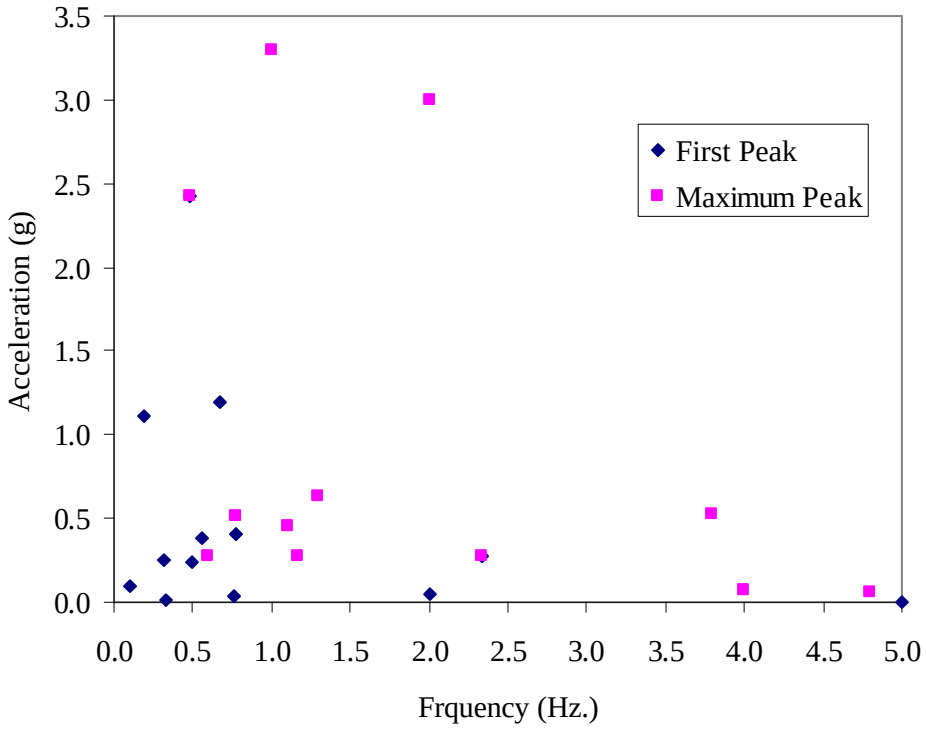

Figure 6-30: First and maximum peaks in the frequency spectra

Veletsos and Newmark (1964) investigated the spectra for a variety of pulse loadings for bomb blasts. The research work of Veletsos and Newmark included a comparison of the results to the El Centro and the Eureka[22] earthquake SDOF spectral shape. These two researchers commented on the area of constant peak velocity as being the controlling feature from about 0.3 to 3 Hertz. This comment was true for the interplate earthquakes that were studied at the time for their report. Additional data having been collated since that time (1964) provide some further guidance as to the controlling features in the range of 0.3 to 3 Hertz. The frequency range of real interest for our work was the 1 to 2 Hertz range.

Veletsos and Newmark (1964) provide extensive guidance on handling the types of responses that were recorded for the Nahanni earthquake and that have been synthetically generated for the Marked Tree event. The first and maximum peaks in the FFT spectra have been plotted in Figure 6-30 for the earthquakes listed in Table 6-10. The frequency range of 0 to 1 Hertz has been plotted in Figure 6-31 to show the large earthquakes that have a high acceleration in the frequency range of 0 to 1 Hertz.

[22] Eureka earthquake of December 21, 1954 S11E Component.

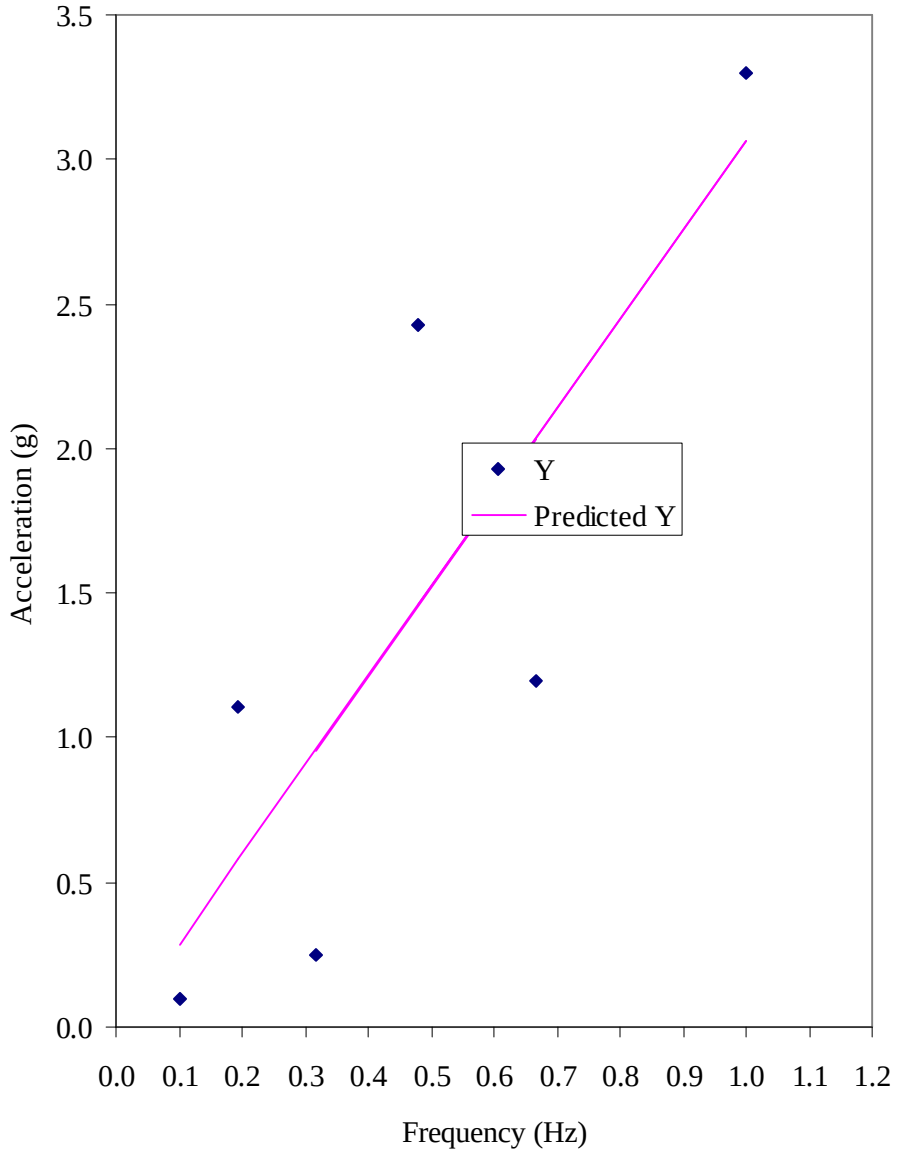

Figure 6-31: First and maximum peaks in the frequency spectra 0 to 1 Hertz

While there were limited data to make any firm observations, the analysis completed by Veletsos and Newmark (1964) and the further data on these larger intraplate events provide some guidance on the applicability of the standard spectra shapes. The applicable comments are:

1. The interplate earthquakes such as El Centro contain a range of frequencies that provide for a series of peaks in the spectrum for the 0.3 to 3 Hertz region creating the constant velocity section of the standard spectrum. Veletsos and Newmark (1964) clearly show that this region was dominated by the acceleration and the velocity components rather than the velocity component alone.

2. The Nahanni and similar earthquake events include large pulses in the time trace that dominate the spectral shape. These pulses in the Nahanni earthquake are a 1 Hertz underlying pulse with a non-damped acceleration of about 0.6 g's which will not be significantly reduced by low damping levels (0.02 to 0.05), and a 6-Hertz pulse at about 10 seconds with a peak acceleration of 1.5 g's. This pulse at 6 Hertz will be damped out in the sample damping range (0.02 to 0.05).

3. There are no physical reasons that the spectral shape from 1 to 3 Hertz has a constant velocity component and the FFT data provided in Figures 6-30 and 6-31 suggest that the asymptote can be reached in these larger intraplate events at 1 Hertz. The region of constant velocity was simply an overlapping area of asymptotes for the El Centro and other earthquakes. The large intraplate earthquakes may contain pulses. The analysis from Veletsos and Newmark (1964) for pulses provides a simple method to deal with pulses in an otherwise fairly standard earthquake signal.

4. The Figure 6-5 from the Newmark and Hall report (1978) and all derivative curves developed since then should be reexamined in detail to consider the potential impact in intraplate areas of these large low frequency and higher frequency pulses.

5. The standard curve with a constant velocity component will require modification to return to the asymptote form.[23]

In conclusion, the Indian Standard 1893: 1984 while generally maintaining the principles outlined in ATC 3-06, has selected different base equations for the natural frequency of the structures; the IS method would appear to provide more conservative answers for the frequency of the structure.

Estimation of the composite C_s factor that directly and linearly relates the mass of the structure to the base shear has been established using two methods in the IS. The two methods are the seismic co-efficient method and the response spectrum method. These two methods provide peak acceleration for Zone V of the Indian continent of 0.13 g's for a two percent damped structure and about 0.38 g's for zero damped structure.

The Indian Standard 1893: 1984 will require amendment after the Gujarat earthquake as the equivalent Australian standard was amended after the Newcastle earthquake and the US Standards after the Northridge earthquake and to permit incorporation of the seminal work completed by FEMA, NSF and others in the past decade. The main amendments will need to include a revision to the method of calculating the composite C_s factor that for the Zone V in the Indian Standard would appear to provide for rapid attenuation and to require amendments to the spectrum response data that form the basis of the code. The US data for the New Madrid Seismic Zone appear the applicable data to use to supplement the data obtained from the Gujarat earthquake.

That the engineering community in the United States uses period and US customary units in the day-to-day analysis of structures would appear in the long run to be an untenable position. In completing this analysis between the two standards, the translations and chances for error were significant simply because the base data for seismicity is collected in the SI units and is measured in units of seconds. This data has a linear translation to frequency, whereas the period provides an

[23] Thanks to Professor W. Hall for suggesting where to look in this data and for the helpful comments on the constant velocity region of the standard spectra.

inverse measure that squash the collected data in an untenable form. The chance for error grows in this continued use of these methods and fundamentally breaches the ASCE Code of Ethics Canon One for preservation of life. The suggestion that the method is that preferred by the contractors raises an interesting argument heard frequently in this matter, which self-evidently fails the Code of Ethics test.

The work of Veletsos and Newmark (1964) should be examined with the additional data to determine if there are suitable changes to the standard spectral shape for these larger intraplate events. Finally the natural frequency formula should be reviewed to determine the appropriate set of standard equations. The use of a method of artificially changing the frequency to provide some conservatism to the base shear estimates should be stopped and if further conservatism was warranted it should be addressed at the appropriate equations and not through the period formula.

The use of US customary units and period should be discouraged in earthquake engineering. The simple reasons are to be in line with seismological practice and general world practice.

5. Building Repair Standards

IS 13935: 1993 Repair and Seismic Strengthening of Buildings – Guidelines The Bureau of Indian Standards is responsible for the preparation of the standard documents. This code provides practical guidelines on the retrofitting of buildings constructed prior to the introduction of seismic codes. The guidelines follow the standard deemed to comply provisions present in such codes in the US and Australia.

6. Concrete Standards

IS 456: 2000 Plain and Reinforced Concrete Code of Practice (Fourth Revision), and IS 13920: 1993 Ductile Detailing of Reinforced Concrete Structures Subjected to Seismic Forces - Code of Practice provide limit state codes based on world wide practice. The code provides an alternative of using the working stress method for some designs. The principal issue to be addressed in a future revision of the code is the design of soft story buildings both in the retrofitting and in the subsequent design of new structures. Collapse of a RC concrete structure at 250 km from the epicenter clearly breaches the intention of the code developers. The structure is to be designed as stable under earthquake loads. This problem is not unique to India.

7. Steel Construction

IS 800: 1984 Code of Practice for General Construction in Steel (Second Revision) was developed in parallel with the equivalent AS 1280 Steel Structures Code from Australia. This code draws on an extensive body of work by Trahair and Hawkins from the University of Sydney in the late 1960s. The code simply requires revision to bring it in line with modern codes of practice.

The code by way of example limits compressive stresses to a level determined from geometrical properties.

8. Masonry Standards

IS: Masonry Structures was not reviewed as it was not available at the time of production of the report.

9. Conclusions

The Indian Codes of practice are generally in line with accepted practice. The seismic design methods will require revision to account for the new knowledge gained from the Gujarat earthquake and also the equivalent work being developed in the New Madrid Seismic Zone. The corrections required to the concrete code are minor in terms of the state of the codes development. The steel code should be redeveloped to be in line with recent research results from Californian experience.

10. References

Abrams, D.P., and Shinozuka, M., (1997), Final Report Loss Assessment of Memphis Buildings, Technical Report NCEER-97-00, (Urbana, Illinois: UIUC).

Algermissen, S.T., (1972), A study of earthquake losses in the San Francisco Bay Area Data and Analysis, US Dept. of Commerce, NOAA: SF, (Algermissen, S.T.; PInvest), 220.

Atkinson, G.M., and Boore, D.M., (1995), Ground motion relations for Eastern North America, *Bulletin of the Seismological Society of America*, 85, 1, 17-30

Benedetti, D., (1997), Letter to the author, including Irpinia earthquake trace.

Benedetti, D., and Pezzoli, P., (1996) *Shaking table tests on masonry buildings - results and comments*, Milano: Politecnico di Milano.

Boore, D., (1997), Letter to the author.

Brigham, E.O., (1988), *The fast Fourier transform and its applications*, Englewood Cliffs: Prentice.

Brigham, E.O., (1974), *The Fast Fourier Transform*, Englewood Cliffs: Prentice. 252.

Chopra, A.K., (1995), *Dynamics of Structures Theory and Application to Earthquake Engineering*, NJ: Prentice Hall.

FEMA, (1997), *NEHRP Guidelines for the Seismic Rehabilitation of Buildings*, no. 273, FEMA: Washington.

Halliday, D., and Resnick, R., (1974), *Fundamentals of Physics*, NY: Wiley.

Horton, S.P., Barstow, N., and Jacobs, K., (1997), Simulation of earthquake ground motion in Memphis, Tennessee, *Proceedings of the Eleventh World Conference on Earthquake Engineering*, June 23-28, 1997, Acapulco, Mexico, Elsevier Science, Paper 1302.

IS 456: 2000, *Plain and Reinforced Concrete Code of Practice (Fourth Revision)* Bureau of Indian Standards: New Delhi.

IS 800: 1984 (Fourth reprint / 1988) *Code of Practice for General Construction in Steel (Second Revision)* Bureau of Indian Standards: New Delhi.

IS 1893: 1984 *Criteria for Earthquake Resistant Design of Structures*, Bureau of Indian Standards: New Delhi.

IS 4326: 1976 *Code of practice for earthquake resistant design and construction of buildings (first revision)* Bureau of Indian Standards: New Delhi.

IS 13920: 1993, *Ductile Detailing of Reinforced Concrete Structures Subjected to Seismic Forces* - Code of Practice, Bureau of Indian Standards: New Delhi.

IS 13935: 1993, *Repair and Seismic Strengthening of Buildings – Guidelines*, Bureau of Indian Standards: New Delhi.

Kaplan, W., and Lewis, D.J., (1971), *Calculus and Linear Algebra,* NY: Wiley.

Nichols, J.M., (1999) Assessment and repair of certain masonry buildings after the Newcastle Earthquake, 13, 1, 11-12.

Press *et al.*,(1994), *Numerical Recipes in Fortran* (Cambridge: Cambridge UP).

Richter, C.F., (1958), *Elementary Seismology,* San Francisco: Freeman. viii+767.

Rosenblueth, E., (1960), The earthquake of 28 July 1957 in Mexico City, *Proceedings of the 2nd International Conference on Earthquake Engineering,* 1, 359-79.

Shiono, K., (1995) Interpretation of published data of the 1976 Tangshan, China Earthquake for the determination of a fatality rate function, *Japan Society of Civil Engineers Structural Engineering / Earthquake Engineering,* **11,** 4, 155s-163s.

USGS, (1977), *Studies related to the Charleston, South Carolina Earthquake of 1886 – A Preliminary Report*, Geological Survey Professional paper 1028, USGPO: Washington.

Chapter 7: Building Damage

by

Daniel P. Abrams[1]
Hanson Engineers Professor of Civil and Environmental Engineering
University of Illinois at Urbana-Champaign

1. Abstract

An overview of damage observations for building structures resulting from the 2001 Bhuj Earthquake in the state of Gujarat is presented. Damage ranged from slight cracking of masonry buildings to complete collapse of multistory concrete frame buildings over distances exceeding 300 kilometers from the epicenter. Reasons for damage patterns are surmised from observations and interviews with locals and are the opinion of the author. Damage observations are correlated with distances from the epicenter to provide a general understanding of possible attenuation relations, and to suggest what damage scenarios are possible for other geographical regions, in particular the Central United States.

2. Introduction

The Bhuj or Republic Day Earthquake that struck the state of Gujarat at 8:47am on January 26, 2001 was one of the major earthquakes to occur in the world in the last few decades. The moment magnitude of 7.9 indicated the energy release to be as high as the previous Alah Bund Earthquake of 1819 suggesting a shorter reoccurrence interval than previously thought for typical intraplate earthquakes in stable continental regions. The long attenuation distances of the earthquake resulted in damage to the built environment as far as 300 kilometers from the epicenter.

Though tragic, the spread of damage provided an interesting portrayal of the gradation of damage possible for varying intensities of ground motion. Damage-distance relations for building structures in particular are of interest not only for the local Gujarati population, but also for earthquake engineers and researchers worldwide who attempt to predict performance of their structures located a given distance from a scenario earthquake of a given magnitude.

Direct inferences between observed damage and distance from the epicenter of an earthquake cannot be drawn because individual structures vary in capacity and are subjected to variable seismic demand forces. Directionality and site effects influence ground accelerations at a particular building site making comparisons of damage with distance difficult. Moreover, individual building structures are designed with different structural configurations, with materials of different strengths and with a different quality of construction. However, apparent damage-distance relations, as presented herein, help to organize the presentation of post-earthquake observations and suggest what levels of damage may be likely at distances from other earthquakes in regions of similar seismicities as that found in Gujarat.

---

[1] DPA, 1245 Newmark Civil Engineering Laboratory, 205 N. Mathews, Urbana, Illinois, 61801 USA, email: d-abrams@uiuc.edu

During a tour of Gujarat two weeks following the earthquake, the investigative team of the Mid-America Earthquake Center visited cities, towns and villages at distances from the epicenter ranging from a few kilometers to over 250 kilometers. Names of observation sites are given in Figure 7-1 with their approximate distances from the epicenter. Damage is reported herein for the cities of Ahmedabad, Ghandidham, Bhuj and Morbi, as well as towns of Bhachar, Anjar and Halvad, and villages of Lodai, Dudhai and MotiMalwan.

Extensive damage in the form of total building collapse was observed even at the largest distances from the epicenter, and conversely, little damage was observed in a small village just a few kilometers to the south of Bhuj. Because nearly all of the buildings in the state were constructed of reinforced concrete and/or masonry of some sort, a wealth of information is available on the seismic performance of such structures as well as the significance of local site effects, and construction quality.

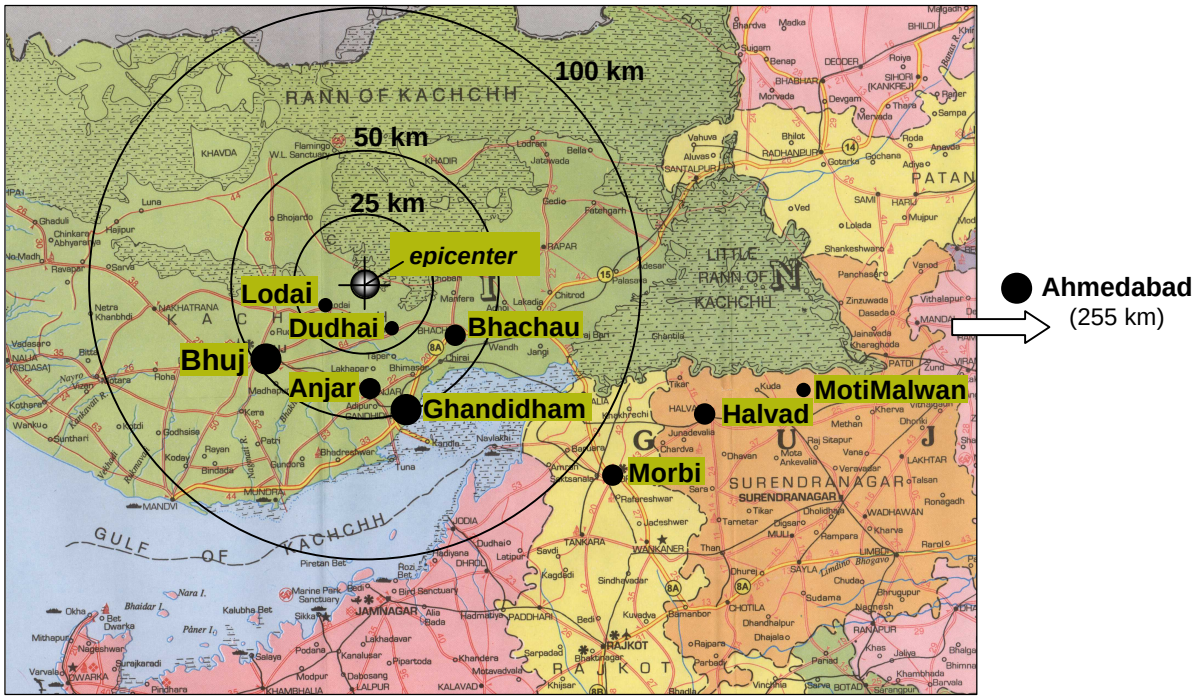

Figure 7-1: Distances from epicenter within northwest Gujarat

3. Features of the Bhuj Earthquake

The epicenter of the Republic Day Earthquake was located approximately 50 km northeast of the city of Bhuj in the northwest Indian state of Gujarat. The epicenter was near the southern boundary of the Rann of Kachchh between the Kutch Mainland fault and the Katrot-Bhuj fault. The earthquake was the second strong motion to hit this area in the past 182 years. Often regarded as the "forgotten" earthquake, the Allah Bund earthquake of 1819 occurred north of the town of Bhuj. This northwestern region of Gujarat is located in the highest seismic zone of the country (Zone 5) per the Indian Standard Criteria for Earthquake Resistant Design of Structures (IS 1893-1984).

The devastation caused by this earthquake was extensive. Unofficial estimates of the death toll exceeded 100,000 people. Villages within 20 kilometers of the epicenter were completely

destroyed as nearly every stone in rubble masonry walls separated from the mud mortars. Complete collapse of dozens of reinforced concrete frame buildings as tall as ten or more stories was phenomenal in the towns of Bhuj, Gandidham, Anjar and Bachau. Liquefaction features were of a similar caliber as those reported in the history books from the 1811-12 New Madrid earthquakes of the Central United States. Water gushed from the soil for several hours following the earthquake, and in some cases with sprout diameters as large as four meters. Fresh water ponds formed following the earthquake in the arid desert climate that had not seen rain for six months. Examples of lateral spreading from liquefaction were prevalent within a 100-km radius of the epicenter.

Relatively short, continental faults like that found in northwest Gujarat and the New Madrid seismic zone can produce great earthquakes, and do so within hundreds of years rather than thousands. Aftershock measurements done by the Mid-America Earthquake Center in Gujarat helped to define the nature of the fault mechanisms with a goal to improve estimates on reoccurrence times and epicentral locations. A second parallel between India and the Central U.S. is the spread of earthquake motions across wide exposure areas. Because of the long attenuation distances possible in this region of India, the Bhuj earthquake was felt farther than 1000 miles away in the eastern and southern parts of the country. One is reminded of the New Madrid earthquake ringing church bells in Boston, a similar distance from the epicenter as Bhuj is from Calcutta.

Correlations between Gujarat and the Central U.S. go farther than seismicity. The preparedness of the local people in the villages and towns close to the epicenter, as well as in the city of Ahmedabad approximately 250 kilometers away, was nearly as poor as that of the people in Mid-America. Little if any seismic rehabilitation was done prior to the Bhuj earthquake though this area of India is in their highest seismic zone. A low number of insured properties suggested again the limited awareness of the public towards earthquake hazards.

The economic loss attributable to direct damage for the Bhuj earthquake has been estimated at $5 billion, which is an order of magnitude less than that estimated for a repeat of the 1812 New Madrid earthquake. This is because the earthquake hit a relatively sparsely populated and remote area lacking the industrial facilities and transportation networks common to the Central United States. However, only about 2% of this loss, or $100 million was attributable to damage to insured property. Only 10% to 12% of the population had earthquake insurance.

Figure 7-2: Collapse of historic wall in Ahmedabad

4. Building Damage in Ahmedabad

The city of Ahmedabad is the largest in the state of Gujarat with over six million people in the greater area, and the second largest in Western India. The second largest textile industry in the country is located within this thriving city named after Sultan Ahmed Shah who founded the city in 1411 A.D. The historical center of the city faired well during the earthquake though there was some significant damage to ancient brick masonry walls (Figure 7-2) surrounding the city center.

The only measured record of ground accelerations in the

state of Gujarat was at the site of a new Passport Building in Ahmedabad. Measured accelerations at this location were not large with a peak measured horizontal ground acceleration of about 0.1g. Yet 24 multi-story buildings collapsed and 45 more were damaged so badly that they were demolished. Ironically, these were newer residential buildings constructed in the last decade.

Ahmedadbad has experienced rapid growth over the last decade, and as a result, a large percentage of the city's 20,000 buildings were constructed in the last ten years. A number of new contractors have emerged in recent times to meet this demand with variable experience in construction.

Figure 7-3: Typical residential construction with soft story at ground level

Nearly all of the 24 collapsed buildings were multistory residential buildings ranging in height from four to ten stories. A common feature among many of these structures was an open base story that was used for parking. The soft story at the ground level was dominant in Ahmedabad because of a municipal regulation limiting the occupancy area of a building relative to the lot size. Plan dimensions of buildings were governed by a floor-space index, defined by the ratio of the sum of the total useable floor area divided by the lot area. For normal lot sizes, this index was controlled to be less than one and did not include the area of the ground floor if left open for parking. For larger lot sizes, the index was limited to a value of two. As a result, residential buildings were typically constructed with reinforced concrete frames that were infilled with masonry (usually burned clay bricks) above the ground story (Figure 7-3). A common damage pattern for these building types was the collapse of the soft ground story. As noted in Figure 7-4, a typical four plus one (i.e. four stories plus ground story) configuration in the background retained its integrity while the adjacent building, identical in architecture, collapsed. This was a common observation.

Figure 7-4: Collapse of soft-story building in Ahmedabad

Despite the poor selection of building configuration, a good number of soft-story structures remained stable. Collapsed buildings were usually observed as isolated cases of an individual building surrounded by other similarly designed buildings that did not collapse. This suggests that the configuration was not the only factor to cause collapse. Variances in construction quality, properties of construction materials or local site effects must also have played a role. In some cases, building collapses were a result of adding a water tank or swimming pool at the roof level without providing the necessary strengthening of the structure to resist the increased inertial forces.

A few collapsed buildings in Ahmedabad lost lateral-force capacity at more than just the base story. Complete collapse of all five stories of a school building (Figure 7-5) occurred. Forty-five students taking exams on the morning of Republic Day were killed as a result of this collapse. Reasons for collapse at every story are perhaps different than those for the single soft-story collapses. It is difficult to discern the exact cause of a failure simply by observing the stack of slabs. Obviously, the demand forces or displacements of the seismic excitation exceeded the lateral strength or deformation capacity of the unbraced columns. Again, if masonry filler walls or panels were placed within the plane of the lateral-force resisting frames, then collapse of the entire story would have been less likely to occur.

Figure 7-5: Collapse of five-story school building in Ahmedabad

A less dramatic, but relevant, form of damage than the complete building collapses was cracking of unreinforced clay-unit masonry buildings. As noted earlier, infill-frame systems were by far the most predominant form of construction in Ahmedabad. Masonry bearing wall construction was however used for older one or two-story residential construction. These buildings did not collapse and therefore no lives were lost as a result of their behavior. However, damage in the form of cracking did present large economic losses for owners of these buildings. In many cases, occupants continued to live in damaged buildings while they were being repaired. Cracks above window and door openings (Figure 7-6), in stairwells, along ceiling-wall interfaces and in shear walls were common. Cracks often extended through the entire width of a multiwythe wall. Because construction of these buildings was quite similar to construction in the Central and Eastern United States, case study buildings in Ahmedabad provide an interesting example of what extents of damage may be likely in Mid America. St. Louis is approximately 270 km from the epicenter of a future New Madrid earthquake whereas Ahmedabad is about 255 km from the epicenter of the Bhuj earthquake.

Figure 7-6: Damage to URM house in Ahmedabad

Figure 7-7: Rehabilitation of soft-story building in Ahmedabad

Visiting building sites in Ahmedabad two weeks following the earthquake afforded the opportunity to observe how local building owners and contractors were repairing and rehabilitating buildings. Several examples were seen where an undamaged building adjacent to a collapsed building was being rehabilitated as a result of fear or paranoia on the part of building owners. Commonly, unreinforced brick masonry walls were added to an open soft-story (Figure 7-7) to brace concrete columns. Though these additional masonry elements may appear to be an added lateral strength, they may

not possess the deformation capacity to adequately work with the flexible frame components. These masonry infills

are likely to crack in the next earthquake and not brace the columns as intended. Other times, steel angles were placed around a concrete column to form a truss mechanism, but without the benefit of a structural analysis to properly size members or design welds connecting each member. Still other examples included the placement of concrete jackets, or the addition of a mortar coating around an existing column. Reinforcement within these jackets or coatings was not necessarily anchored sufficiently at the top of the column, so again intended enhancements in lateral strength are likely not be realized in a future seismic event. The variety of ad-hoc methods devised by individual contractors demonstrated the need for education of the local construction industry regarding sound structural engineering practices. Such education must occur prior to the earthquake as a preparedness action so that repair measures may be implemented without hesitation soon after a disaster. This is a lesson that can be learned by contractors in other regions of the world as well as India.

5. Distribution of Building Damage across Region

As noted in the table below, the city of Ahmedabad was 255 km from the epicenter. Damage was limited to approximately 2% of the buildings in this urban area and would have been much worse had the earthquake struck closer. Building collapses similar to those found in Ahmedabad were found in higher percentages in communities closer to the epicenter. For example, the soft-story failures were predominant across the entire affected region, particularly in and around Bhuj, Anjar, Ghandidham and Bachau. In addition, damage to other building types, including collapse of stone masonry dwellings, was coomon within a close proximity of the epicenter.

Table 7-1: Distance of communities from epicenter and degree of damage

Community	Type	Distance from Epicenter (km)	Degree of Damage	Mercali Intensity
Dudhai	village	14	complete destruction	XII
Lodai	village	16	complete destruction	XII
Bachau	town	32	severe damage	X
Anjar	town	34	destruction of city center	XI
Ghandidham	city	38	collapse of buildings	IX
Bhuj	city	42	severe damage	IX
Morbi	town	100	destruction of city center	VII
Halvad	town	119	destruction of city center	VIII
MotiMalwan	village	150	destruction of city center	XI
Ahmedabad	city	255	2% of buildings collapsed	VI

As a rough guide to the extent of damage with distance, ten communities are listed in Table 7-1 in order of their distance from the epicenter. The degree of damage and the apparent Modified Mercali Intensity scale (Richter, 1958) as given in the table are based on subjective opinion of the author and are given to help organize the discussion of building damage. MMI was assessed on

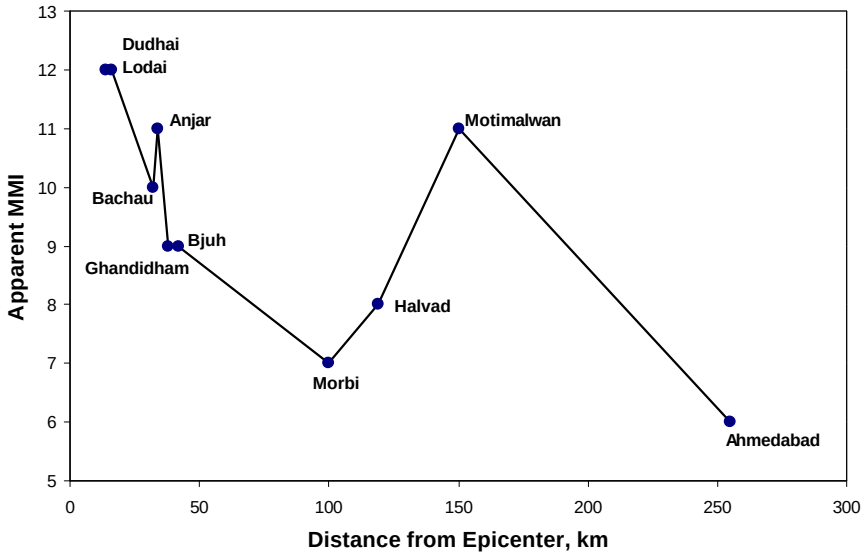

Figure 7-8: Apparent MMI vs. distance relation

the degree of average observed damage across a community rather than a single building. Thus, the apparent MMI values in the table are higher for small villages with uniform destruction than for cities where collapse of individual buildings was observed. The data given in Table 7-1 is shown in Figure 7-8.

Villages of Dudhai and Lodhai close to the epicenter (14 km and 16 km) both suffered total destruction. As noted in Figure 7-9, one and two-story dwellings constructed of uncut stone masonry were shaken to rubble. Virtually no building was spared across the entire community. Peak ground accelerations required to cause this level of damage are estimated in excess of 1.0g. Similar degrees of destruction were also observed in the town center of Anjar (34 km from the epicenter) where building collapses also included reinforced concrete frame buildings (Figure 7-10).

Figure 7-9: Devastation of village of Lodai

As would be expected, damage intensity in general reduced with distance from the epicenter. However, two points on the curve of Figure 7-8 show anomalies to this relation. The small village of MotiMalwan, 150 km from the epicenter, had severe destruction of buildings within its older city center (Figure 7-11). Damage to this village was much more extensive than that observed in towns and villages within a third of the distance from the epicenter. Also, residential buildings within the older city center of Halvad were uniformly destroyed (Figure 7-12) at 119 km whereas damage in the neighboring town of Morbi was limited to

Figure 7-10: Destruction of Anjar town center

Figure 7-11: Stone masonry building damage in Motimalwan

Figure 7-12: Stone masonry building damage in Halvad

Figure 7-13: Building collapse in Ghandidham

Figure 7-14: Soft-story collapse in Bhuj

cracking of masonry with collapse limited to a few buildings. As noted in Figure 7-1, both MotiMalwan and Halvad are close to the edge of the Little Rann of Kachchh (5 km and 14 km

respectively) suggesting that the more severe damage at these two locations was attributable to amplification effects at the edge of this basin.

Perhaps the most striking examples of destruction to engineered construction were found in Bhuj, Ghandidham and Bachau where collapse of dozens of multi-story reinforced concrete frame buildings had occurred. Several building collapses in Ghandidham of three to ten-story concrete buildings such as that shown in Figure 7-13 were attributable again to soft first stories though a variety of other structural design problems were observed including columns punching through slabs, poor detailing of reinforcing steel and questionable construction quality. Similar types of collapses and building failures occurred in the regions of new development surrounding Bhuj (Figure 7-14). One building in Bhuj (Figure 7-15) completely overturned as a result of fracture of column reinforcing steel from foundations.

Figure 7-15: Overturned five-story building in Bhuj

Figure 7-16: Masonry damage in Bhuj

Brick masonry construction was not prevalent in the area because clay deposits were not available locally. However, stone masonry construction was common. Rubble stone construction was typical for one or two-story dwellings in villages and small towns. Found in larger towns and cities, cut stone was often used at the corners of a building to confine rubble stone placed within a wall between the corners. This type of construction proved to be more resilient to collapse than the rubble construction found in the villages, though considerable damage was observed due to falling of rubble stones from walls. Damage to one and two-story masonry buildings was prevalent throughout the area, such as the damage shown in Figure 7-16 in Bhuj. Whereas the death toll as a result of the damage to cut-stone masonry was less than that of rubble stone masonry and much less than that for reinforced concrete construction, the performance of these buildings was unacceptable in terms of the total economic loss. There were many examples where the damage was so extensive that buildings had to be demolished and rebuilt.

6. Concluding Remarks

The mass destruction of buildings and other forms of construction in Gujarat provides the background for a compelling argument that earthquakes still have the potential to cause serious disasters to life and property. The large death toll of over 100,000 people indicates that life-safety goals for building design and construction are not yet fulfilled. Concrete buildings with massive slabs and overly weak lateral-force resisting elements once again were shown to be a major threat to human life. As well, weak unreinforced masonry construction was shown to be vulnerable to strong ground shaking. Without aggressive rehabilitation programs in other earthquake-prone areas of the world where these construction forms exist, similar damage statistics are likely to be repeated.

Indian seismic codes and detailing practices for buildings are technically sound and similar in theory to those used in the United States. However, without code enforcement and third-party review, future earthquakes will continue to result in significant losses despite advancements in engineering design and construction technology.

The populace generally believes that infrequent earthquakes will take some time to strike and that there is plenty of time to take action to mitigate their effects. The Republic Day Earthquake

proved this myth to be untrue. The primary lesson of the reoccurrence of this "forgotten earthquake" is that our time to research, prepare and mitigate future seismic hazards is limited, and the pace of future efforts must be accelerated.

7. Acknowledgments

The research reported on in this paper was funded by the Mid-America Earthquake Center. The MAE Center is supported primarily by the Earthquake Engineering Research Centers Program of the National Science Foundation under Award Number EEC-9701785. A MAE Center reconnaissance team examined earthquake damage and recorded aftershocks for an eight-day period commencing two weeks following the earthquake. Gratitude is expressed to Mr. Ramesh Raikar of Strutwel Desingers and Consultants in Mumbai for his gracious hosting of the MAE Center team. Appreciation is extended to the Institute of Science and Technology for Advanced Studies and Research in Vallabh Vidyanagar for their valuable assistance in deploying the Center's seismic instrumentation, in particular Mr. Kirit Budhbhatti of this institute. The generous efforts of Mr. Apurva Parikh and his father, Nayan Parikh of Multi-Media Consulting Engineers in Ahmedabad are also acknowledged for his help with the investigation. Professor Sudhir Sapre of the Center for Environmental Planning and Technology is thanked for his help identifying damaged buildings in Ahmedabad.

8. References

Indian Standard 1893-1984: Criteria for Earthquake Resistant Design of Structures, Fourth Edition, Indian Standards Institution, New Delhi, June 1986.

Richter, Charles F., *Elementary Seismology*, W.H. Freeman and Company, San Francisco, 1958.

Chapter 8: Performance of Engineered Buildings

by

S.K. Ghosh[1]
S.K. Ghosh and Associates, Inc.

This chapter discusses the performance of engineered construction, the post-earthquake strengthening of reinforced concrete buildings, as well as Indian standards and codes of practice regulating earthquake-resistant construction. Seismological and geotechnical aspects of the earthquake are not discussed here. The map of the affected area in Figure 7-1 of Chapter 7 is also not reproduced here, but needs to be referred to.

1. Performance of Engineered Construction

Performance of engineered construction was investigated by the MAE team in Ahmedabad, Morbi, Gandhidham, Bhuj, Anjar and Bhachau located approximately 250, 150, 50, 48, 40, and 35 km away from the epicenter, respectively.

2. Ahmedabad (Approximately 250 km from epicenter)

The only strong motion instrument in the entire area affected by the Bhuj earthquake was in the basement of a multistory building in Ahmedabad. The recorded peak ground acceleration was 0.1g (Figure 8-1). Ground motion of this intensity should not cause significant structural damage to properly engineered construction. Yet more than 70 multistory residential buildings collapsed in Ahmedabad. The reasons for such disproportionate damage were fairly apparent.

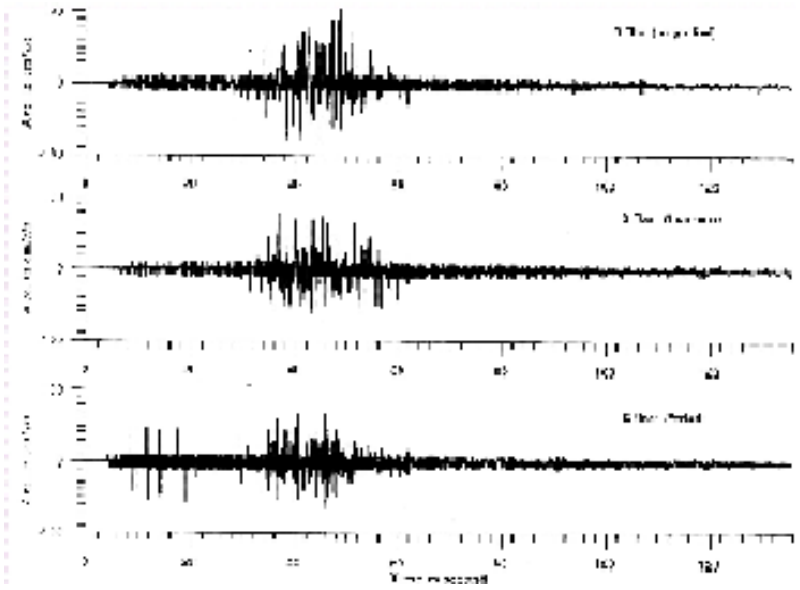

Figure 8-1: Accelerogram recorded at basement of a building in downtown Ahmedabad

[1] SKG, 3344 Commercial Avenue, Northbrook, IL 60062 USA,
email: skghosh@aol.com

3. Building Period versus Ground Motion Period

Short-period components of ground motion typically die out faster than the long-period components of ground motion as earthquake shocks travel away from the source of an earthquake. Typically, at long distances away from the epicenter, the ground motion has predominantly long-period components.

From the copy available to the MAE Center team of the sole ground motion record, it was not possible to discern the predominant period. However, it would be safe to speculate that the predominant periods were 0.5 sec. and longer. This in itself would explain the lack of damage to shorter buildings in Ahmedabad. The buildings that collapsed were in the ground plus four to ground plus ten-story height range. Buildings in this height range, particularly considering the type of construction, most likely had elastic fundamental periods in the range of the predominant periods of the ground motion. The consequent near-resonant response must have been, at least in part, responsible for much of the damage sustained.

4. Soft Soil

Goel has made an important observation with respect to the soils on which the collapsed Ahmedabad buildings were founded. According to him, "Although a cursory analysis of location of building collapses would indicate no particular pattern, a careful analysis reveals that most of the buildings that collapsed lie along the old path of Sabarmati River….Note that the path of most of the buildings that collapsed in areas west of the Sabarmati River are closely aligned with the old path of the river…just west of the present river path. The south, southeast of the city, especially the Mani Nagar area, where additional collapses were observed, falls between two lakes, indicating the presence of either poor soil conditions or possibly construction on non-engineered fills. While the evidence presented…is strong, it would be useful to further verify these conclusions with field testing."

5. Type of Construction

Multi-story residential buildings (and most other multi-story buildings) in Ahmedabad, the rest of India, and indeed in much of the rest of the world, are constructed of reinforced concrete frames, with the openings in those frames infilled with unreinforced clay brick masonry.

There is a problem inherent in the use of unreinforced masonry infills. Initially, while they are intact, they impart significant stiffness to a building which, as a consequence, attracts strong earthquake forces. The resulting deformations are often more than sufficient to cause cracking or even explosive failure of the infilled masonry. When that happens, the period of the building lengthens significantly all of a sudden. Although this usually is beneficial in terms of attracting less earthquake forces, depending on the nature of the earthquake ground motion, the opposite may be the case. In the 1985 Mexico earthquake, with the predominant 2-second period of the ground motion in downtown Mexico City, a building attracted stronger earthquake forces with the loss of the infill. Also, very importantly, the altered earthquake forces must be resisted essentially by the bare frame. If the frame lacks that capability, severe damage or collapse may result.

6. Stiffness Discontinuity or Soft Story

In virtually all Indian cities, the multi-story residential buildings of the type described above, have open ground stories for parking of automobiles, because the small lots on which such buildings are typically built do not allow for open parking (Figure 8-2). This means an almost total absence of infills at the ground level, thus creating a very distinct stiffness discontinuity or a soft story. Virtually all the earthquake-induced deformations in such a building occur in the columns of the soft story, with the rest of the building basically going along for a ride. If these columns are not designed to accommodate the large deformations, they may fail, leading to catastrophic failure of the entire building, as was the case with many buildings in Ahmedabad and elsewhere.

Figure 8-2: Typical soft-story residential building

7. Discontinuity of Vertical Load Path

The local municipal corporation in Ahmedabad imposes a Floor Surface Index (FSI), which restricts the ground floor area of a building to be no more than a certain percentage of the lot area. It is, however, permitted to cover more area at upper floor levels than at the ground floor level. The same is the situation in many other Indian cities as well. Thus, most buildings have overhanging covered floor areas at upper floors, the overhangs frequently ranging up to 5 feet or more. The columns on the periphery of the upper floors do not continue down to the ground level. The columns at the ground floor level also may or may not align with the columns at the upper levels. Significant vertical discontinuities are therefore caused in the lateral-force-resisting system.

8. Non-Ductile Detailing

Goel has reported: "The columns for low-rise residential buildings, up to ground plus four stories (G + 4), rest on shallow isolated footings located about 5 ft (1.52 m) below the ground level. For taller buildings, say up to ground plus ten stories (G + 10), the column foundations are still open footings located at a depth of 8 to 10 ft (2.44 to 3.05 m); sometimes the foundation may also have tie beams. The column sizes for low-rise buildings (G + 4) are about 9 x 18 in. (230 X 460 mm) with ties consisting of mild steel smooth No. 2 (6 mm dia.) bars at a spacing of about 8 to 9 in. (200 to 230 mm). The beams tend to be much deeper to accommodate large spans and overhangs, giving rise to strong beam-weak column construction. The column sizes for taller buildings tend to be a little bigger, usually 12 inch by 24 inch with No. 3 (10 mm dia.) deformed steel ties at a spacing of 8 to 9 in. (200 to 230 mm). The beam size in taller buildings may be similar to the column size. These ties always end up with 90-degree hooks.

Such nonductile detailing of reinforced concrete construction is common around the world, including pre-1973 reinforced concrete construction in California, although details vary from place to place and depending upon the age of a building. In addition to all of the above, column reinforcement is typically spliced right above the floor levels; splice length in columns as well as beams is often insufficient; continuity of beam reinforcement over and into the supports is often also insufficient.

The large deformations that take place in soft story columns also impose extreme shear demands on them. The meager lateral reinforcement described above not only provides poor confinement

the shear strength available is also quite low. As a result, many ground floor columns failed in a brittle shear mode, or in a combined shear plus compression mode, bringing down the supported building (Figure 8-3). Many times in columns that had not failed, diagonal shear cracking was evident.

Figure 8-3: Non-ductile detailing of column

9. Torsion

The typical soft-story residential building described above is torsionally quite flexible at the ground floor level. If appreciable eccentricities between the center of mass and the center of rigidity are introduced because of asymmetric placement of walls or other reasons, significant torsional motions may result. These may subject columns on one side of a building to excessive deformations. If not adequately designed to accomodate such deformations, the columns may fail, contributing to building collapse. According to Goel, "deformations due to torsion may have contributed to failure of at least one building" in Ahmedabad.

10. Detailing of Shearwall core and connection to remainder of Structure

The typical soft-story residential building described above relies upon the shearwall core(s) around stairwell(s) and/or elevator shafts to resist most of the lateral load at the ground floor level. Up the height of the building, the shearwalls do unload increasing percentages of story shears onto the frames, providing the floor diaphragms connecting them are rigid enough in-plane to impose equal displacements on the shearwalls and the frames. Several deficiencies were observed.

The ratio of cross-sectional area of shearwalls to plan area of building was often quite low. The shearwalls are typically "about 4 to 6 inches thick with very light reinforcement consisting of two layers of mesh formed with No. 3 or 4 bars at vertical and horizontal spacings of about 18 inches. Such detailing was often insufficient to resist the lateral loads at the ground floor level; severe shear cracking of shearwalls at the ground level was often observed. The shear cracking often did not extend above the ground floor level, reflecting reduced shear demand on the walls.
The shearwall core was often connected to the rest of the building only through the floor slabs, with no beams framing into the shearwalls. The anchorage of slab reinforcing into the elevator core was often insufficient. As a result, the shearwalls sometimes just pulled out from portions of the building, leaving them devoid of much lateral resistance.

11. Material Quality

There were indications that deficient material quality might also have contributed to structural damage, or even collapse. Goel, in his recent paper, showed the bottom of a column in a partially collapsed building. "The concrete has simply disintegrated within the reinforcement cage, when touched, the concrete felt sandy with little cement. Also note that the 90-degree hooks have opened up, which leads to little or no confinement of the concrete. Many of the times, the concrete cover to reinforcement was noted to be less than half-inch, most of the cover was provided by the plaster used to smooth the column surface. It is worth noting that most of the water supply in the outer part of the city is through ground water which is salty in taste. Usually the same water is used in preparing the concrete for construction. Therefore, the presence of salts may have also affected the concrete quality."

12. Morbi (Approximately 150 km from Epicenter)

Morbi has a number of ceramic tile factories on its outskirts. Vertical cracking was observed in a tall masonry chimney in one of those factories (Figure 8-4). Another chimney had apparently lost several feet at the top.

Figure 8-4: Cracked masonry chimney outside Morbi

One notable structure in the town of Morbi is Mani Mandir, a huge, two-story stone masonry building of four continuous wings along the four faces, with a large courtyard in the middle. In the inner courtyard is a stone masonry temple. Except for some parapet damage, both the outer structure and the inner temple appeared to be in good shape (Figures 8-5, 8-6).

Figure 8-5: Mani Mandir – outer structure, Morbi

Figure 8-6: Mani Mandir – inner temple, Morbi

There was significant damage to major masonry buildings in the center of the town of Morbi. These buildings included the old palace of the former ruling family (Figure 8-7). The damage appeared to be due to loss of parapets, but also to the roof pulling out of masonry walls, indicating insufficient anchorage.

Figure 8-7: Old palace of the former ruling family, Morbi

13. Gandhidham (Approximately 50 km from Epicenter)

Gandhidham has a large number of multistory commercial as well as residential buildings of infilled reinforced concrete frame construction that suffered severe damage or collapse.

Figure 8-8 shows two adjoining commercial buildings in the business district of the city. The ground stories of both buildings have collapsed. Interestingly, the ground-level columns of the corner building punched through the slab at the first suspended level (Figure 8-9). This particular phenomenon has rarely been observed in past earthquakes.

There was another interesting case of the shear core of a building having totally separated from the building itself (Figure 8-10). The right wing of the building had collapsed, while the left wing was still standing up in a damaged state. The shear core itself was more or less intact.

Figure 8-8: A pair of adjoining commercial buildings with soft-story failure, Gandhidham

Figure 8-9: Pushing of ground-level column through slab

Figure 8-10: Core separated from rest of building

14. Bhuj (Just under 50 km from Epicenter)

The old, walled city of Bhuj, with a population of 160,000, was the city closest to the epicenter. Engineered buildings in the older parts of town, including the business district, were of masonry or infilled reinforced concrete frame construction. Newer engineered buildings were mostly on the outskirts of the city and were predominantly of infilled reinforced concrete frame construction. The infill in modern buildings can be unreinforced concrete block masonry, as well as clay masonry.

There was extensive damage to all types of engineered construction. The business district was virtually deserted two and a half weeks after the earthquake and few buildings stood unscathed. In the heart of the city are palaces that once belonged to the former ruling family. The "new" palace, a massive three-stories tall well-engineered, well-constructed, cut-stone masonry building had performed admirably well. About the worst damage was some parapet loss in one area of the building (Figure 8-11). The old palace of the same height, which stood on the same grounds, of rubble stone masonry construction, by contrast, had sustained extensive damage (Figure 8-12). Repairs to the old palace will be too expensive to be practicable.

Figure 8-11: New palace of the former ruling family, Morbi

Figure 8-12: Old palace of the former ruling family, Morbi

Figure 8-13: Recently built apartment complex in Bhuj with soft-story

Figure 8-14: Overturned building, Bhuj

A relatively new upscale apartment complex on the outskirts of town had extensive damage, including collapse of ground-level soft stories over much of the complex (Figure 8-13).

A rare case of a building having overturned was also found at Bhuj (Figure 8-14). The reason could not be definitively established, although there was speculation that the cause might have been differential settlement of the foundations.

15. Anjar (Approximately 40 km from Epicenter)

The town of Anjar was almost totally destroyed (Figure 8-15). It was not possible to distinguish between engineered and non-engineered buildings. Here and there, a few multistory buildings stood after a fashion, with their soft bottom stories invariably gone.

Figure 8-15: Complete collapse of buildings, Anjar

16. Bhachau (Approximately 35 km from Epicenter)

The town of Bhachau was a scene of almost total destruction. There were unmistakable signs of significant ground displacements. Figure 8-16 shows a fountain of concrete that is broken into pieces. The failure of such a structure of no significant height would typically be the result of ground displacements, rather than earthquake forces. The base of the utility pole in the foreground of Figure 8-17 also showed significant recession of the ground.

The building of Figure 8-17 and two nearly identical neighboring buildings facing the same street were each two stories tall at the front (the side facing the street) and three stories tall at the back, because of a sloping site; each building suffered a soft-story failure in the basement or the lowest level. The street-level story of the neighboring building had sunk by nearly a story height. The building neighboring that one had suffered almost total collapse. It can be said with assurance that all multistory buildings in town with soft stories had suffered soft story failures.

Figure 8-16: Cracked reinforced concrete fountain, Bhuj

Figure 8-17: Utility pole and building with soft-story failure below street level, Bachau

17. Post-Earthquake Strengthening of Reinforced Concrete Buildings

The multi-story residential buildings sustaining significant earthquake damage or suffering collapse in Ahmedabad were mostly in upscale neighborhoods of the city. Owners of repairable buildings and even of buildings that did not undergo any significant damage were anxious to get repair or strengthening done, which they obviously could afford. A surprising amount of repair and strengthening work was well underway only two and a half weeks after the earthquake. Unfortunately, the overwhelming majority of such work appeared to make little engineering sense. There appeared to be hardly any engineering involvement; the owners appeared to be dealing directly with builders and contractors. The following were observed:

1) In perhaps the simplest of repairs, damaged infilled unreinforced masonry walls were being replaced with the same unreinforced (mostly) clay brick masonry (Figure 8-18). Properly done, this, of course, would neither enhance nor lower the seismic resistance of the buildings concerned.
2) Unreinforced masonry walls were being added at the ground level, where they did not exist before, either between existing columns, or sometimes with an existing column only at one end of a wall (Figure 8-19). In the absence of careful consideration to the layout of these walls, particularly with reference to the layout of walls in the upper levels, this particular strengthening strategy appears to be questionable.
3) Existing reinforced concrete columns had been or were being jacketed by reinforced concrete, with additional reinforcing bars in the jacket. These bars in the jacket, however, did not continue down to the column footing. At the upper end, the reinforcing bars were not made continuous with the reinforcement in the members framing in (Figures 8-20a, b). These jackets will simply "peel way"- at the beginning of the next earthquake, not adding to the seismic resistance of the building presumably strengthened by them.
4) Clay brick masonry columns with light steel framing around, with the masonry and the steel encased in concrete, were being added (Figure 8-21). The author is not aware if such columns have been tested and their behavior under simulated seismic loading studied. In any case, the light steel framing which was the only reinforcement, did not continue down to the footing, or made continuous with reinforcement in the framing members at the top.
5) The same light steel framing was being installed around existing reinforced concrete columns with the plaster often not removed from the concrete (Figure 8-22), with the existing column and the steel framing encased in new concrete. The remarks made under Item 4 above also apply to these columns.
6) Sometimes a clay brick masonry column or a steel I-column had been installed against an existing concrete column, the two lightly tied together (Figure 8-23), with the whole thing to be apparently encased in concrete. The added column might continue down to the footing at the lower end. There definitely was no continuity at the top. These again appeared to be untested measures of questionable benefit.
7) Corner columns had been added to buildings at the ground level where no such column existed before (Figure 8-24). While this would appear to be a sensible thing to do, in the absence of continuity at the top and the bottom, these columns are likely to be ineffective as well.

Ironically, at least in one case, more attention appeared to have been paid to the continuity of steel columns acting as temporary supports, than to the continuity of permanent columns. The plate welded to the top of the I-columns in Figure 8-25 had a reinforcing bar hook welded on top,

which in turn had been welded to the bottom reinforcement in the reinforced concrete member above.

Figure 8-18: Damaged infilled unreinforced masonry walls being replaced

Figure 8-19: Unreinforced masonry walls being added at ground level building

Figures 8-20a & b: Reinforced bars in jacket not made continuous with reinforcement in members framing in

Figure 8-21: Added clay brick masonry columns with light steel framing around

Figure 8-22: Light steel framing installed around existing reinforced concrete column

Figure 8-23: Clay brick masonry column installed against an existing column

Figure 8-24: Corner column added to building at ground level

Figure 8-25: Continuity at top end of steel column acting as temporary support

18. Indian Codes and Standards

India has, for quite some time now, had sophisticated codes and standards. The three documents relevant to this discussion are:

1. IS 1893:1984 – Indian Standard Criteria for Earthquake Resistant Design of Structures (Fourth Revision).
2. IS 4326:1993 – Indian Standard Earthquake Resistant Design and Construction of Buildings – Code of Practice, and
3. IS 13920:1993 - Indian Standard Ductile Detailing of Reinforced Concrete Structures subjected to Seismic forces - Code of Practice

IS 1893 states: “It is not intended in this standard to lay down regulations so that no structure shall suffer any damage during earthquake of all magnitudes. It has been endeavored to ensure that, as far as possible, structures are able to respond without structural damage to shocks of moderate intensities, and without total collapse to shocks of heavy intensities.”

IS 1893 contains a seismic zoning map. The object of this map is to classify the area of the country into a number of zones in which one may reasonably expect earthquake shock of more or less the same intensity in the future. The modified Mercalli Intensity associated with the various zones is V or less, VI, VII, VIII, and IX and above for Zones I, II, III, IV, and V, respectively.

It may be noted that Bhuj is in Seismic Zone V, while both Ahmedabad and Mumbai (Bombay) are in Zone III.

IS 4326 is intended to cover the specified features of design and construction for earthquake resistance of buildings of conventional types. In case of other buildings, detailed analysis of earthquake forces is required. Recommendations regarding restrictions on openings, provision of steel in various horizontal bands and vertical steel in corners and junctions in walls and at jambs of openings are based on extensive analytical work. Many of the provisions have also been verified experimentally on models by shake table tests.

IS 4326: 1976 'Code of practice for earthquake resistant design and construction of buildings,' while covering certain special features for the design and construction of earthquake resistant buildings, included some details for achieving ductility in reinforced concrete buildings. With a view to keeping abreast of the rapid developments and extensive research in the field of earthquake resistant design of reinforced concrete structures, the decision was made to cover provisions for the earthquake resistant design and detailing of reinforced concrete structures separately.

IS 13920 incorporates a number of important provisions not covered in IS 4326:

a) As a result of the experience gained from the performance in earthquakes of reinforced concrete structures that were designed and detailed as per IS 4326: 1976, many identified deficiencies were corrected in IS 13920.
b) Provisions on detailing of beams and columns were revised with an aim of providing them with adequate toughness and ductility so as to make them capable of undergoing extensive inelastic deformations and dissipating seismic energy in a stable manner.
c) Specifications on seismic design and detailing of reinforced concrete shear walls were included.

The other significant items incorporated in IS 13920 are as follows:

a) Material specifications are indicated for lateral- force-resisting elements of frames.
b) Geometric constraints are imposed on cross-section of flexural members. Provisions on minimum and maximum reinforcement have been revised. The requirements for detailing of longitudinal reinforcement in beams at joint faces, and splices, and anchorage requirements are made more explicit. Provisions are also included for calculation of design shear force and for detailing of transverse reinforcement in beams.
c) For members subjected to axial load and flexure, dimensional constraints have been imposed on the cross section. Provisions are included for detailing of lap splices and for the calculation of design shear force. A comprehensive set of requirements is included on the provision of special confining reinforcement in those regions of a column that are expected to undergo cyclic inelastic deformations during a severe earthquake.
d) Provisions have been included for estimating the shear strength and

flexural strength of shear wall sections. Provisions are also given for detailing of reinforcement in the wall web, boundary elements, coupling beams, around openings, at construction joints, and for the development, splicing and anchorage of reinforcement.

While the common methods of design and construction have been covered in IS 13920, special systems of design and construction of any plain or reinforced concrete structure not covered by this code may be permitted on production of satisfactory evidence, regarding their adequacy for seismic performance by analysis or tests or both.

It is interesting to note that the provisions of IS 13920 apply to reinforced concrete structures that satisfy one of the following conditions:

a) The structure is located in seismic zone IV or V;
b) The structure is located in seismic zone III and has an importance factor of greater than 1.0;
c) The structure is located in seismic zone III and is an industrial structure; and
d) The structure is located in seismic zone III and is more than 5 stories high.

Thus, the residential buildings in Ahmedabad with ground + 4 stories are exempt from the requirements of IS 13920.

The above codes, as noted earlier, are quite sophisticated. IS 13920:1993 is, in fact, greatly influenced by ACI 318-89. However, code enforcement practically does not exist in India. Central and State governments would at times require code compliance for buildings owned by them. For other buildings, code requirements are seldom, if ever, enforced. Local jurisdictions typically do not have a mechanism in place to enforce code requirements. This not only explains much of the damage observed to engineered buildings, but also indicates that the promise of a bright future is not on the horizon.

19. Possible Areas of Code Improvement

The legal building codes of most legal jurisdictions (cities, counties, states) within the United States are based on one of three so-called model codes. The *Uniform Building Code* (UBC), typically adopted in the western half of the country, roughly speaking; *the BOCA National Building Code* (BOCA/NBC), usually adopted in the northeastern quarter of the country; and the *Standard Building Code* (SBC), mostly adopted in the southeastern quarter of the country. These three were expected to be replaced by one unified model code for the entire country: the *International Building Code*(IBC), the first edition of which was published in April 2000. The IBC is slowly being adopted in various jurisdictions around the country. A competing model building code, NFPA 5000, being developed by the National Fire Protection Association based in Quincy, Massachusetts, is expected to be published in 2002. A new edition of the UBC, the BOCA/NBC as well as the SBC used to be published every three years. The IBC is expected to maintain the same schedule. The seismic design provisions of the UBC have traditionally been based on the *Recommended Lateral Force Requirements* (Blue Book) published by the Structural Engineers Association of California (SEAOC). The seismic design provisions of the latest editions of the BOCA/NBC and the SBC are based on the 1991 NEHRP Provisions. Both allow seismic design by the ASCE 7 Standard *Minimum Design Loads for Buildings and Other Structures*, 1995 edition, which has its seismic design provisions based on the 1994 NEHRP Provisions. The seismic design provisions of the 2000 IBC are based on the 1997 NEHRP

Provisions. The seismic design provisions of NFPA 5000 are expected to be based on ASCE 7-02, which in turn will draw its seismic design provisions from the 2000 NEHRP Provisions.

The treatment of soils in seismic design changed drastically in the 1994 edition of the NEHRP Provisions. A four-tier soil classification was replaced by a six-tier classification. Instead of one soil factor, there were now two site coefficients: an acceleration-related or short-period coefficient and a velocity-dependent or long-period coefficient. While the traditional soil factor was only a function of the soil type at the site, each of the two new site coefficients, in addition to being a function of the same, was additionally a function of the seismicity at the site. For the same soil type or site class (as it is called now), the site coefficients are typically higher in regions of low seismicity and lower in regions of high seismicity. Finally, while the maximum value of the traditional soil factor was 2, the maximum values of the new short-period and long-period site coefficients are 2.5 and 3.5 respectively. The new scheme is adopted into the 1997 UBC, the 1995 and 1998 editions of the ASCE 7 standard and the 2000 IBC. The author believes that this new scheme is worth looking into whenever an update of IS 1893 is undertaken.

The 1988 edition of the *Uniform Building Code* introduced a table of vertical structural irregularities and a separate table of plan structural irregularities. If a building became classified as structurally irregular by the criteria in one of the tables, depending on the type of irregularity, restrictions applied to the building. It might be limited in height on regions of significant seismicity, or dynamic analysis might be required as the basis of design, and so forth. These provisions were adopted into the 1991 NEHRP Provisions, are thus part of the *BOCA/National Building Code* and the *Standard Building Code*, and with minor modifications are also to be found in the 1997 NEHRP Provisions and the 2000 IBC. These provisions would also be worthwhile considering for an update of IS 1893.

United States building codes have not allowed the use of unreinforced masonry in regions of moderate and high seismicity since the early to mid-seventies. Such a ban would be impractical for India. However, one idea that may be worthwhile exploring is in fact practiced in Mexico. They brace the frame bays to be infilled with unreinforced masonry, as shown in Figure 8-26. This has the benefit of lowering the deformations that would be imposed on the unreinforced masonry. More importantly, loss of unreinforced masonry is likely to be over smaller areas at a time and is thus likely to be more gradual and smaller in overall impact. For instance, such bracing would automatically become required if it is mandated that no more than 1 m^2 (11 sft) of masonry can be left unreinforced.

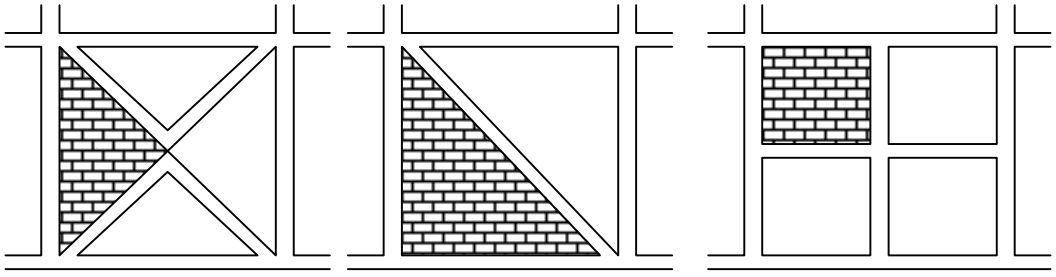

Figure 8-26: Bracing of frame bays infilled with unreinforced masonry

20. Acknowledgments

The author is indebted to Mr. R. N. Raikar, Manging Director, Structwel Designers & Consultants Pvt. Ltd., Mumbai, who acted as de facto host to the MAE Center team. He is also grateful to Mr. Kirit Budhbhatti, who facilitated arrangements and logistics for the MAE Center team. Mr. Kirit Budhbhatti's untiring efforts were crucial to the success of the seismology-related undertakings of the MAE Center team.

The author is grateful to his associate, Dr. Madhu Khuntia, for his invaluable help with the preparation and review of the manuscript. Another associate, Dr. Kihak Lee, was of much help with the processing of the many figures.

Some of the material in this chapter has been published in a paper by the author in the March-April 2001 issue of the *PCI Journal*, published by the Precast/Prestressed Concrete Institute, Chicago, IL.

21. References

American Society of Civil Engineers, *ASCE Standard Minimum Design Loads for Buildings and Other Structures*, ASCE 7-88, ASCE 7-93, ASCE 7-95, ASCE 7-98 (also ANSI A58-55, ANSI A58.1-72, ANSI A58.1-82), New York, N.Y., 1990, 1993, 1995, 2000.

Building Officials and Code Administrators International, *The BOCA National Building Code*, Country Club Hills, IL, 1993, 1996, 1999.

Building Seismic Safety Council, *NEHRP (National Earthquake Hazards Reduction Program) Recommended Provisions for the Development of Seismic Regulations for New Buildings (and Other Structures)*, Washington, D.C., 1991, 1994, 1997.

Goel, R.K., "Performance of Buildings During the January 26, 2001 Bhuj Earthquake," to be published in *Earthquake Spectra*, Earthquake Engineering Research Institute, Oakland, CA.

International Code Council, *International Building Code*, Falls Church, VA, 2000.

International Conference of Building Officials, *Uniform Building Code*, Whittier, CA, 1988, 1991, 1994, 1997.

Seismology Committee, Structural Engineers Association of California, *Recommended Lateral Force Requirements and Commentary*, San Francisco (later Sacramento), CA, 1974, 1988, 1996, 1999.

Southern Building Code Congress International, *Standard Building Code*, Birmingham, AL, 1994, 1997, 2000.

Chapter 9: Performance of Lifelines and Industrial Facilities

by

Mark Aschheim[1]
Assistant Professor of Civil and Environmental Engineering
University of Illinois at Urbana-Champaign

1. Overview

The state of Gujurat is one of the most industrialized of the country. The region is served by several major ports on the Gulf of Kachchh and by highways, railroads and airports. Pipelines and powerlines also cross the region. The most urbanized part of the state is the Ahmedabad-Vadodara (Baroda) industrial belt, east of the most-heavily shaken epicentral region. Although performance of these facilities often was very good, damage did occur. Locations of significant damage, described in the following, are indicated on the map of Figure 9-1.

2. Transportation Structures and Networks

The epicentral region is served by national and state highways, railroads, and three airports. Disruption of the transportation system occurred primarily because of damage to bridges and culverts. No major highway bridges collapsed; use of one major river bridge was impeded due to damage, and two minor reinforced concrete slab culverts collapsed. Only one railroad bridge was reported to be damaged. The Ahmedabad airport remained operational and the Bhuj airport was restored to service the same day of the earthquake.

Highways

The state of Gujarat contains approximately 69,000 km of surfaced roads (excluding city streets), with National Highways comprising 1877 km and State Highways comprising 19518 km. Extensive damage to roadways was not observed during the reconnaissance. Damage to highway pavements was reported only near Rapar, as a result of lateral spreading.

Bridges

The most disruptive damage to the highway system was the loss of bearing support at the Surajbari Creek Bridge, located on the heavily-traveled National Highway 8A. Two reinforced concrete slab culverts collapsed, on a minor road northeast of Bhuj, due to the failure of unreinforced masonry abutment backwalls. Other bridges sustained minor damage at expansion joints, bearings, masonry piers, and reinforced concrete deck railings. Minor bridge damage occurred as far as 250 km east of the epicenter in Ahmedabad and 70 km north of the epicenter, toward the Pakistani border. This damage is described below.

3. Bridge Damage in the Epicentral Region

Surajbari Creek Bridge

The Surajbari Creek Bridge (Figure 9-2) is a two-lane bridge that provides passage over the Little Rann of Kachchh on National Highway 8A, joining the Rajkot and Kachchh Districts.

[1] MA, 2118 Newmark Civil Engineering Laboratory, 205 N. Mathews, Urbana, IL 61801 USA
email: aschheim@uiuc.edu

Figure 9-1: Locations of damaged lifelines and industrial facilities

Constructed in 1968, the reinforced concrete balanced cantilever bridge has 35 spans totaling 1204 meters in length. The superstructure is a two-cell box girder, having main spans of 32.92 m in length, with cantilevers of 8.38 m and suspended spans of 10.06 m in length. The superstructure was supported on steel rocker and roller bearings. The bearings are supported on reinforced concrete cellular piers that are 4.5 meters in height. The abutments are reinforced concrete. Caissons provide support to the piers and abutments. The caissons have an outside diameter of 9.80 m and extend 17.37 m below the piers to competent soils.

The bridge was closed to traffic following the earthquake due to lateral movement of the superstructure. It was reported that all bearings supporting the superstructure spans were damaged. Significant movement took place at the expansion joints at the abutments (Figure 9-3); movement at the south abutment left the superstructure approximately 3 inches lower than the abutment, with the expansion joint open approximately 8 inches. Liquefaction was widespread in the area, with numerous sand blows evident in the vicintiy; workers reported water spouts as high as 1.5 m. The bearings were replaced with temporary wood and masonry block supports (e.g. Figure 9-4), allowing a single lane of traffic to be restored two days after the earthquake. Reduced capacity continued until March 2, when traffic was diverted to a new bridge that was under construction at the time of the earthquake, just east of the existing bridge.

New Surajbari Creek Bridge

Figure 9-5 shows the new Surajbari bridge under construction at the time of the earthquake. Reinforced concrete blocks provided to restrain transverse movement of the deck reportedly were damaged in the earthquake, and expansion joints were damaged by pounding in the longitudinal direction. Workers reported that the fills at the southern approach to the bridge settled 3 m during the earthquake. Ground cracks of several inches width extending approximately parallel to the roadway were visible at several locations just south of the bridge (Figure 9-6), with liquefaction evident at the lower portions that were not filled (Figure 9-7).

Figure 9-2: View to northeast of Surajbari Creek Bridge

Figure 9-3: Movement of superstructure and loss of bearing support at the south abutment

Figure 9-4: Temporary wood and masonry bearing blocks at southern abutment

Figure 9-5: The new Surajbari bridge, under construction

Figure 9-6: View of the southern approach to the new Surajbari bridge. Settlement of 3 m was reported. Ground cracks on the order of 3 inches in width were aligned parallel to roadway

Figure 9-7: Ponded water and salt deposits remaining from liquefaction visible in the foreground; the southern approach to the new Surajbari bridge is in the background

Khari River Bridge

The Khari River Bridge is located on State Highway 45 approximately 12 km north of Bhuj near the town of Rudramata (Figure 9-8). The two-lane bridge was constructed in 1966 and spans a

total of 168 m. The superstructure and piers are reinforced concrete, and the abutments are made of coursed stone masonry. Each slab-girder span is 16.8 m in length and is supported on mild steel plate bearings. The piers consist of reinforced concrete trestles; each trestle is founded on a single circular caisson 8 m in diameter and 10.1 m deep below the cap.

Damage to the bridge consisted of minor spalling of concrete near the base of pier 5 (Figure 9-9), some diagonal cracking and spalling of concrete in the girder webs, near the bearings (Figures 9-10 and 9-11), and damage at the expansion joints, particularly at the north abutment (Figure 9-11). Extensive ground cracking in the area appeared to be the result of lateral spreading (Figures 9-12 and 9-13). Rocks and brush were placed on either side of the bridge approach to restrict traffic to one lane at the center of the bridge.

Figure 9-8: View of Khari River Bridge to the northwest. Note extensive ground cracking visible in the foreground

Figure 9-9: Spalling of concrete at the base of the columns of the trestle at Pier 5

Figure 9-10: Diagonal crack in the girder web emanating from the bearing on the left, at Pier 8

Figure 9-11: Broken railing at the north abutment and spalling of the girder web concrete at the bearing of Pier 1

Figure 9-12: View to southeast from bridge deck, showing ground cracking indicative of lateral spreading

Figure 9-13: View to southwest from bridge deck, showing extensive ground cracking

Culvert Damage

Only a small fraction of the many culvert crossings in the region suffered damage significant enough to affect traffic flow. Two reinforced concrete slab culverts collpased, on a minor road approximately 25 km northeast of Bhuj (Figure 9-14). The abutments were made of coursed stone masonry. In these cases, the stone backwalls collapsed, causing collapse of the supported slabs. At other locations throughout the epicentral region, the stone abutment sidewalls collapsed, jeopardizing support for the adjacent roadway. At these locations traffic was restricted to a single lane away from the area of the collapsed sidewall. Drought conditions allowed traffic flow to continue on hastily made temporary routes around the minor culverts that were taken out of service.

4. Bridge Damage in Outlying Areas

India Bridge

Access to the northern portion of the Rann of Kachchh was restricted by the military. Members of the MAE Center team observed a 10-span reinforced concrete slab-girder bridge that crosses a small arm of the Great Rann just north of the town of Khavda on State Highway 45. The deck moves some 10-15 cm; pounding at expansion joints caused concrete to spall and damage at the abutments. No girders lost bearing support, however.

Falku Bridge

The Falku Bridge is a two-lane 10-span reinforced concrete bridge spanning a total of 200 m. The reinforced concrete slab-girder superstructure is supported on coursed stone masonry piers (Figure 9-15). Longitudinal pounding at the expansion joints caused damage to the expansion joints and the reinforced concrete railing (Figure 9-16). Cracks also developed in the masonry piers and spread footings (Figure 9-17). The bridge remained open to traffic. Similar railing damage was observed at other bridges that also remained open to traffic.

Figure 9-14: Collapsed reinforced concrete slab culverts

Figure 9-15: Overview of the Falku Bridge

Figure 9-16: pounding of expansion joints caused damage to concrete deck railing

Figure 9-17: cracking of masonry piers and damage to masonry foundations

Nehru Bridge

The city of Ahmedabad is built on the banks of the Sabarmati River. Seven major bridges cross this river. While most of these bridges were not damaged in this earthquake, the presence of any damage is significant given that the epicenter was approximately 250 km from the city.

Figure 9-18: Overview of Nehru Bridge

Figure 9-19: Repaired expansion joint of Nehru Bridge

The Nehru Bridge is an 11-span reinforced concrete bridge spanning 442 meters over the Sabarmati River, built in 1959. The superstructure is a hollow-cell box girder, consisting of balanced cantilever and suspended spans (Figure 9-18). The concrete gravity piers are supported on two groups of 8 caissons. Damage to the bridge consists of minor pounding of expansion joints; a repaired joint is shown in Figure 9-19.

5. Railroads and Rail Bridges

The state has nearly 5300 route kms of railways in broad, meter, and narrow gauges. The rail system withstood the earthquake with relatively little damage. Trains to Ghandidam resumed service on January 29, but temporary repairs and speed restrictions caused delays. Service to Bhuj had been suspended prior to the earthquake for gauge conversion, and resumed on February 3, four days later than originally scheduled.

Lateral spreading and subsidence along the approach to the Navlahki Port caused the main access road and railroad track to drop below sea level (Figure 9-20). The superstructure of a major steel plate girder bridge just east of the Surajbari Creek bridges displaced, affecting the track alignment. A number of old masonry arch railroad bridges also sustained damage, but none collapsed. The railroad station building at Ratnal, approximately 25 km southeast of Bhuj, suffered a partial collapse (Figures 9-21 and 9-22).

Figure 9-20: Damaged road and track at Navlahki Port

Figure 9-21: Railroad station at Ratnal; partial collapse hidden from view

Figure 9-22: Partial collapse of railroad station building

6. Port and Harbor Facilities

Major port facilities are located along the Gulf of Kachchh, with the largest port in India being located at Kandla. Kandla handles 40 million metric tons of cargo per year, or about 17% of the nation's cargo. Forty smaller ports in the state of Gujarat handle a total of 25 million tons per year, with 10 of these being all-weather ports. Substantial damage occurred to the Kandla and Navlahki ports. The Mundra port, constructed one year prior to the earthquake with private assistance, was reported to have no significant damage.

Kandla Port (Figure 9-23) suffered damage to five older wharfs and to its warehouses and operations buildings. None of the gantry cranes derailed. The port was closed for one week following the earthquake. Operations resumed on February 3 at about 30-40% of capacity. The port was operating at about 40-50% of capacity on February 14. Repair costs are expected to amount to $30 million.

Damage to the five older wharfs is reported to consist of flexural and shear cracking at the tops of the reinforced concrete piles, possibly related to ground failure at the site. The newer wharfs, supported on larger diameter piles, were undamaged. Five warehouses had structural damage. Figure 9-24 shows shear failures that developed in a large number of short reinforced concrete columns that were provided to accommodate ventilation grilles in a warehouse. Where column lengths were larger, column damage was less severe (Figure 9-25). A water tank supported on the reinforced concrete framing of a warehouse structure was damaged (Figure 9-26). The shear failure in the beam and damage to the column appear to have been induced by the presence of the eccentric stairs. Damage to the corrugated asbestos roofing of another warehouse occurred at the connection to the roof truss (Figure 9-27). A two-story office building at the port collapsed (Figure 9-28). The pile-supported control tower was leaning significantly (Figure 9-29), as was an office structure at the gate (Figure 9-30). Liquefaction in this area has been reported, and the ground surface was disrupted.

Figure 9-23: Undamaged tower cranes at Kandla Port

Figure 9-24: Shear failures of short reinforced concrete columns, Kandla Port

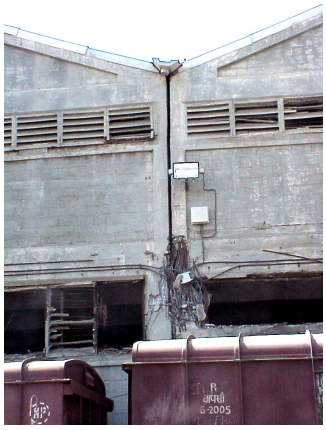

Figure 9-25: The influence of column clear length on severity of shear failure

Figure 9-26: Damage to a water tower at Kandla Port

Figure 9-27: Damage to corrugated asbestos roofing at roof truss, Kandla Port

Figure 9-28: Weak-story collapse of an office building, Kandla Port

Figure 9-29: Leaning control tower, Kandla Port

Figure 9-30: Leaning entry gate building, Kandla Port

Figure 9-31: Collapsed stone wall on road to Kandla Port, indicating acceleration to the northeast was strong enough to collapse one wall to the southwest

A masonry wall on the main road to Kandla Port failed to the southwest, suggesting that ground accelerations were strongest toward the northeast (Figure 9-31).

Significant damage also occurred at the Navlahki port. A road and rail line serving the port were built on fill that was placed approximately 100 years ago. Lateral spreading to the south and subsidence caused over a kilometer of the main access road and railroad track to drop, with portions inundated during high tide (Figure 9-20). Soil failure caused a wharf to tilt several inches toward the north (Figure 9-32) and caused a sea wall to move several meters to the south (Figure 9-33). Warehouses at the port also collapsed (Figures 9-34 and 9-35).

Figure 9-32: Failed wharf, Navlahki Port

Figure 9-33: Failed seawall, Navlahki Port

Figure 9-34: Collapsed warehouse, Navlahki Port

Figure 9-35: Collapsed warehouse, Navlahki Port

7. Industrial Facilities

Major industries in the epicentral region produce salt, fertilizer, ceramics, and petrochemicals. The Kachchh district reportedly produces 70% of the world's salt supply. Many multistory and large-span single-story buildings in the epicentral area were damaged or partially collapsed (Figures 9-36 to 9-38).

Western India Sea Brines Salt Plant

A six-story salt processing building collapsed (Figure 9-39) just west of Bhachau, killing 9 people. The plant was in operation 24 hours per day. Damage to adjacent warehouse building (Figure 9-40) consisted of cracking of unreinforced masonry infill (Figure 9-42), cracking of masonry supports for steel roof trusses (Figure 9-41), and damage to asbestos corrugated roofing and separation of the roofing from the perimeter walls (Figure 9-42). Sand blows indicated liquefaction had occurred at the site, and water continued to seep out nearly 3 weeks after the earthquake, on February 15.

Figure 9-36: Damage to a warehouse near Kandla Port

Figure 9-37: Damage to warehouses near Bhachau

Figure 9-38: Damaged industrial buildings in the vicinity of Bhachau

Figure 9-39: Collapsed 6-story salt processing plant

Figure 9-40: Damaged warehouses at the salt plant

Figure 9-41: Damage to masonry pedestals supporting the steel trusses and masonry walls

Figure 9-42: Separation and damage to the joint between corrugated asbestos roofing and the masonry walls

The ceramics industry in Morbi manufactures roofing tiles and washbasins. The chimneys of numerous small plants dot the landscape; most remained standing. Damage to the chimney at one plant is shown in Figure 9-43; cracking of the masonry occurred in those locations where circumferential steel bands were not present. The unreinforced masonry walls of the kiln suffered partial collapse (Figure9-44), disrupting production.

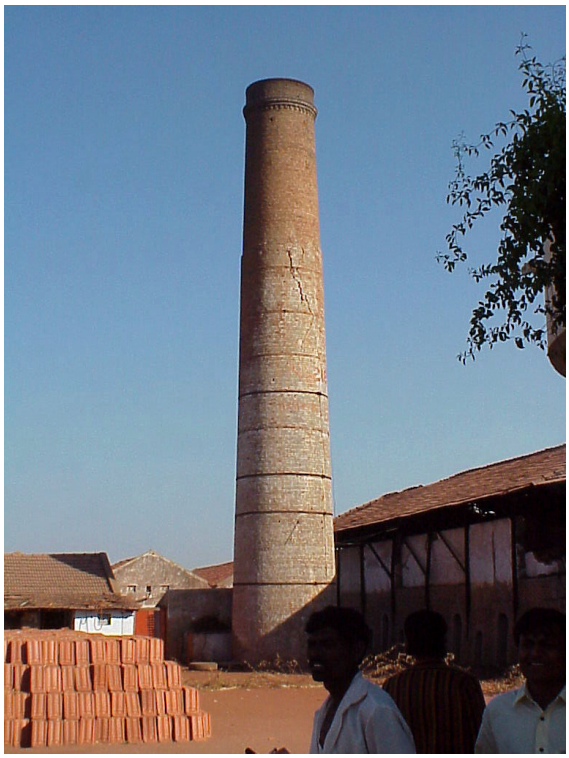

Figure 9-43: Masonry chimney cracked where circumferential steel bands were not present, Morbi

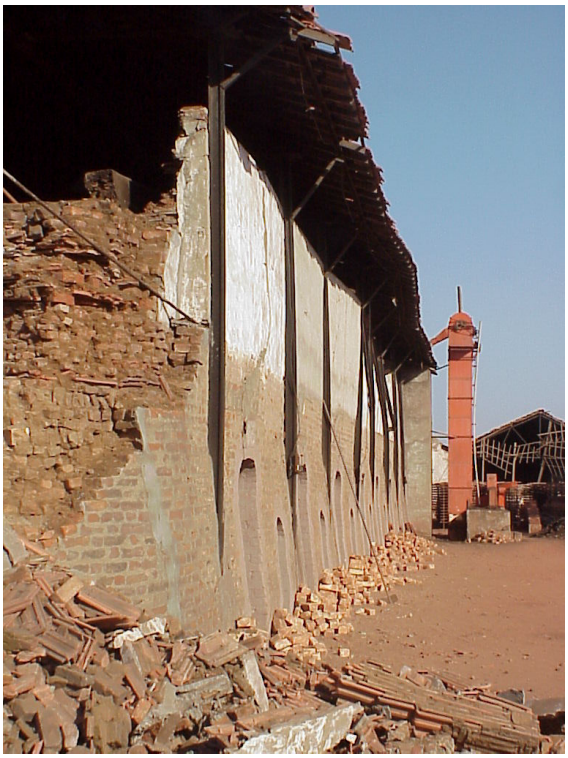

Figure 9-44: Collapsed unreinforced masonry wall at ceramic roofing tile kiln, Morbi

8. Utility Lifelines

Electrical Power

Over a dozen substation buildings were reported to have collapsed and about 45 were damaged, immediately causing power outages in the epicentral region. No power plants are located in the immediate epicentral area. Only minor damage was reported at a coal-fired plant at Panandhro, approximately 180 km from the epicenter. Transmission towers and high-voltage transmission lines appeared to be undamaged, but local distribution was affected by falling power poles and collapsing buildings (Figure 9-45). Interaction between a transmission tower and its supporting soils appeared to induce liquefaction, just south the Surajbari Creek Bridge and adjacent to other areas that had liquefied (Figure 9-46).

Figure 9-45: Electrical power distribution system was vulnerable to damage from building collapses

Figure 9-46: Transmission tower induced liquefaction adjacent to an area that had liquefied. The southern approach to the new Surajbari Creek Bridge is in the background

Water

Extensive damage was reported to the water pumping and pipeline transmission system. Five elevated water tanks constructed of reinforced concrete were reported to have collapsed in the Malia-Morbi region, of several hundred such tanks in the epicentral region. Two elevated water tanks in the village of Lodai were not heavily damaged, despite their location close to the epicenter (Figure 9-47). Some well casings were reported to be bent or had collapsed, or had sand intruding through the perforated walls. Changes in the dissolved solids content of groundwater affected potable water quality. Standing water in Anjar risked public health and safety (Figure 9-48).

Communications

Telephone communications were disrupted by the failure of reinforced concrete infill walls in central offices and switching facilities. A fiber optic cable was reported to have been severed. Where disrupted, telephone service was available within several days to a week after the earthquake. Cellular service was reported to be available once electrical power had been restored.

Figure 9-47: One of the two reinforced concrete water tanks in Lodai, near the epicenter

Figure 9-48: Standing water in Anjar posed a risk to public health and safety

9. Conclusions

Lifelines and industrial facilities performed reasonably well in the M_w 7.7 Republic Day Earthquake, considering both the magnitude of the earthquake and the performance of non-engineered construction. Specific observations are as follows:

1. Although there were no collapses of significant bridges, movement at expansion joints and damage to bridge bearings was sufficient to affect alignment, causing reductions in traffic capacity.

2. Unreinforced masonry abutment walls were prone to collapse. The collapse of backwalls caused the collapse of roadway spans, while the collapse of sidewalls required that traffic be routed away from the failed walls, reducing capacity.

3. Liquefaction, lateral spreading, and settlement appeared to play a significant role in damage to wharfs, seawalls, railways, roadways, buildings and industrial facilities.

4. The collapse of structural and nonstructural components of buildings used to house equipment, people, or goods was critical to the continued operation of the ports, industrial facilities, and telephone system, as well as the transmission and distribution of electric power.

It appears that those structures and facilities that performed reasonably well were designed explicitly for seismic actions (e.g. bridges, elevated water tanks, and some port facilities). This suggests that institutional measures to ensure that good seismic design practice is achieved, such as requiring the use of seismic codes, third party review, and special inspection, were successful when applied. Components that did not appear to have been designed for seismic actions, such as unreinforced masonry buildings and substations, bridge abutments, and retaining structures, often created vulnerabilities in the systems and facilities in which they were used. To improve the performance of lifelines and industrial facilities in the future, the design of all critical components should consider seismic actions and the potential for ground failure.

10. References

Ballantyne, Donald, “Earthquake in Gujurat, India, Jan. 26, 2001—EERI Preliminary Report from the Field-February 10, 2001,” Learning from Earthquakes, Earthquake Engineering Research Institute, available from http://eeri.org/Reconn/bhuj_Fieldreport1.htm.

Bridges in Gujurat, Roads and Buildings Department, Government of Gujurat, October 1989.

EERI, “Preliminary Observations on the Origin and Effects of the January 26, 2001 Bhuj (Gujurat, India) Earthquake, EERI Special Earthquake Report, April, 2001.

Eidinger, John M., ed., “Gujurat (Kutch) India Earthquake of January 26, 2001 Lifeline Performance,” Technical Council on Lifeline Earthquake Engineering, Monograph No. 19, April, 2001 (draft).

Socio-Economic Review—Gujurat State 1999-2000, Budget Publication No. 30, Directorate for Economics and Statistics, Government of Gujurat, Ghandinagar, Februrary, 2000, available from http://www.gujaratindia.com/ser-1.html.

Chapter 10: Seismic Vulnerability Predictions for Reinforced Concrete Structures

by

T.Rossetto[1]
Graduate Research Assistant
Imperial College of Science Technology and Medicine

1. Abstract

Extensive structural damage to both rural and modern reinforced concrete constructions resulted as a consequence of the Bhuj Earthquake on the 26th January 2001. This paper describes a vulnerability study that was carried out for the major towns in the Gujarat region with the aim of assessing whether the observed severity and distribution of damage could have been predicted prior to the earthquake. A procedure for the seismic assessment of populations of reinforced concrete structures is presented, which adopts empirical vulnerability curves derived from an extensive database of worldwide observational post-earthquake statistics of building damage. Through a comparison of the vulnerability predictions with available data on RC building damage in Ahmedabad, conclusions are made as to the effect of site conditions, earthquake duration, local design and construction practice on the seismic vulnerability of the structures.

2. Preamble

At 03:16:41 UTC on the 26th January 2001 a strong earthquake shook the ground in North West India. The Bhuj earthquake was of magnitude Ms7.9[2], with epicenter at 23.33N 70.32E in the vicinity of Bhachau. Extensive structural damage was seen to occur in towns and villages within a radius of 110 km from the epicenter[3]. Total collapse was observed in 461,593[4] rural houses of rubble masonry construction, with weak mortar or mud mortar bonds, in the Gujarat area. Many block-masonry and reinforced concrete structures were also severely affected by the ground shaking, with the collapse of several newly built multi-story reinforced concrete frame buildings being observed in the city of Ahmedabad, 230 km from the epicenter. This paper aims to assess whether or not such a severity and spread of damage could have been predicted if a vulnerability study had been carried out prior to the event. The assessment is carried out for reinforced concrete constructions in different locations, through the use of vulnerability curves. These curves describe the variation in the probability of exceedence of a series of damage limit-states with increasing ground motion severity. A comparison is then made between the predicted and observed damage distribution in RC buildings in Ahmedabad.

3. The Vulnerability Curves

The vulnerability curves used to carry out the damage distribution prediction were developed by the author as part of a study financed by the SAFERR research-training program[5]. The vulnerability curves were originally generated with a view to their application in the assessment of European constructions, but include data regarding 99 observations of post-earthquake damage distributions in populations of reinforced concrete buildings, made for 19 earthquakes worldwide.

---

[1] TR, London SW7 2BU UK.
email: tizi.rossetto@ic.ac.uk
[2] US Geological Survey.
[3] Field observations made by the Mid-America Earthquake Center reconnaissance team.
[4] Data as of 02/27/01 obtained from www.gujaratindia.com.
[5] Tossetto T., “Vulnerability Curves for Seismic Assessment of Reinforced Concrete Buildings”, PhD Thesis.

DAMAGE INDEX	DAMAGE STATE	DUCTILE FRAMES	NON-DUCTILE FRAMES	INFILLED FRAMES
0	NONE	No Damage	No Damage	No Damage
10	SLIGHT	Fine cracks in plaster partitions/infills	Fine cracks in plaster partitions/infills	Fine cracks in plaster partitions/infills
20	LIGHT	Onset of structural damage Hairline cracking in beams and columns near joints (<1mm)	Start of structural damage Hairline cracking in beams and columns near joints (<1mm)	Cracking at wall-frame interfaces Diagonal wall cracks Limited crushing at b/c connections
30				
40				
50	MODERATE	Cracking in most beams & columns Some yielding in a limited number Larger flexural cracks & start of spalling	Cracking in most beams & columns Some yielding in a limited number Shear cracking & spalling is limited	Increased brick crushing & onset of structural damage Some diagonal shear cracking in members
60				
70				
80	EXTENSIVE	Ultimate capacity reached in some elements-large flexural cracking, spalling & re-bar buckling Short column failure	Loss of bond at lap-splices, bar pull-out, broken ties Re-bar buckling or shear failure in elements	Extensive cracking of infills, falling bricks, out-of plane bulging Partial failure of many infills, heavier damage in frame, some members may fail in shear
90				
100	PARTIAL COLLAPSE	Collapse of a few columns, a building wing or single upper floor	Shear failure in many columns or impending soft-story failure	Partial collapse from shear failure of beams &/or columns Near total infill failure
	COLLAPSE	Complete or impending building collapse	Complete or impending building collapse	Complete or impending building collapse

Table 10-1: Typical building damage associated with the Homogenized RC Damage Scale

DAMAGE INDEX	HRC-SCALE	HAZUS 99	VISION 2000	FEMA 273	EMS-98	MSK	AIJ	ATC-13	ATC-20	EPPO (Greece)
0	NO DAMAGE	NO DAMAGE LIMIT STATE								
10	SLIGHT	Slight Damage	Fully Operational	Immediate Occupancy	Grade 1	D1	Slight	Slight	"Green" Tag	"Green" Tag
20	LIGHT				Grade 2	D2	Minor	Light		
30										
40				Damage Control						
50	MODERATE	Moderate Damage	Operational		Grade 3	D3	Moderate	Moderate	"Yellow" Tag	"Yellow" Tag
60				Life Safe						
70			Life Safe					Heavy		
80	EXTENSIVE	Extensive Damage		Limited Safety	Grade 4	D4	Severe			
90			Near Collapse	Collapse Prevention				Major	"Red" Tag	"Red" Tag
100	PARTIAL COLLAPSE		Partial Collapse				Collapse			
	COLLAPSE	COLLAPSE LIMIT STATE								

Table 10-2: The approximate correlation between the HRC Scale and other damage scales.

The vulnerability curves use the Homogenized Reinforced Concrete (HRC) damage scale to assess structural performance. This damage scale consists of seven limit states ranging from "no damage" to "collapse", each described in terms of the typical damage to be expected in four main reinforced concrete structural systems (Table 10-1). The damage scale is approximately correlated to other existing damage scales through comparison of the relative damage state descriptions (Table 10-2). Each damage state is further associated with an index value (DI_{HRC}) which is related experimentally to the structural response parameter of maximum inter-story drift ratio ($ISD_{max\%}$). Four equations are proposed relating $ISD_{max\%}$ and DI_{HRC} for different structural systems:

$$DI_{HRC} = 34.89 Ln(ISD_{max,\%}) + 39.39 \quad , R^2 = 0.991 \quad \textit{for non-ductile MRF}$$

$$DI_{HRC} = 22.49 Ln(ISD_{max,\%}) + 66.88 \quad , R^2 = 0.822 \quad \textit{for infilled frames}$$

$$DI_{HRC} = 39.31 Ln(ISD_{max,\%}) + 52.98 \quad , R^2 = 0.985 \quad \textit{for shear-wall}$$

$$DI_{HRC} = 27.89 Ln(ISD_{max,\%}) + 56.36 \quad , R^2 = 0.760 \quad \textit{for general structures}$$

The relationships are derived from a total of 105 experimental observations obtained from dynamic tests published in technical reports and have been further verified against the results of pseudo-dynamic tests on large-scale structures carried out as part of the European Union funded PREC8 and ICONS research networks. The relationships are used to define the HRC damage-state limits in terms of $ISD_{max\%}$ (Table 10-3). These values are then used to derive the limit state exceedence probabilities from the collected damage distributions.

ISD (%)	All Structures	MRF	Infilled Frames	Shear-Walls
No Damage	< 0.13	< 0.32	< 0.05	< 0.26
Slight	< 0.19	< 0.43	< 0.08	< 0.34
Light	< 0.56	< 1.02	< 0.30	< 0.72
Moderate	< 1.63	< 2.41	< 1.15	< 1.54
Extensive	< 3.34	< 4.27	< 2.80	< 2.56
Partial Collapse	< 4.78	< 5.68	< 4.36	< 3.31
Collapse	> 4.78	> 5.68	> 4.36	> 3.31

Table 10-3: $ISD_{max\%}$ limits defining the HRC damage limit states

The resulting vulnerability curves are shown in Figure 10-1, for the case where peak horizontal ground acceleration (pga) is used to represent the ground motion severity. The 90% confidence bounds are also shown in this figure and are determined from t-distributions fit to the scatter of the observed exceedence probabilities over pga intervals of 0.1g.

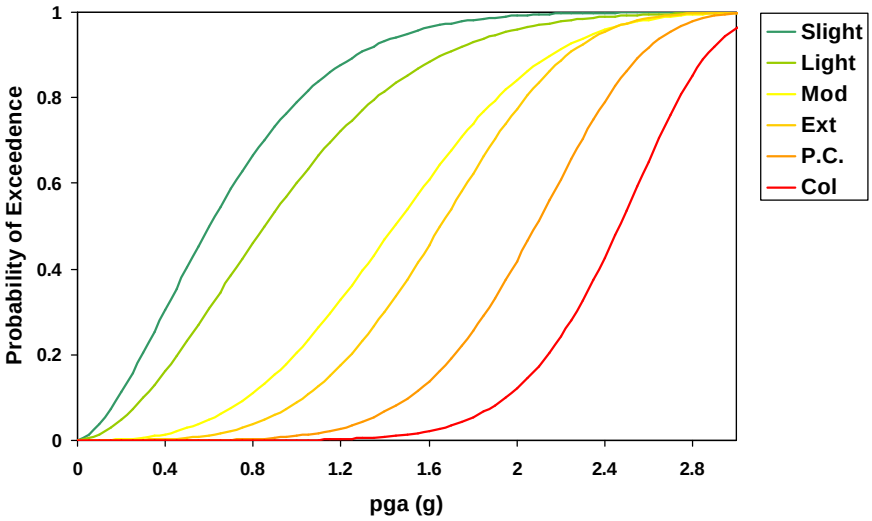

	Vulnerability Curve Parameters			
Relationship		**Mean**	**Lower$_{90\%}$**	**Upper$_{90\%}$**
Damage State	b	a	a	a
Slight	1.6	1.5654	0.1210	3.8140
Light	1.8	0.9216	0.1430	2.5630
Moderate	3.0	0.2300	0.0590	0.9140
Extensive	4.0	0.0929	0.0010	0.2320
Partial Collapse	5.8	0.0097	5e-5	0.0270
Collapse	8.0	0.0005	5e-6	0.0065

Figure 10-1: Empirical vulnerability curves for reinforced concrete structures, Rossetto T. PhD Thesis

4. Ground Motion Estimation

No ground motion recording instruments were located in the epicentral region at the time of the earthquake. From macro-seismic data, the Bhuj earthquake was assigned magnitudes Ms7.9 and Mw7.7[6], with an estimated epicenter at 23.33N 70.32E and focal depth of 23.6 km. No surface rupture was observed for the fault, however, from aftershock observations, the Center for Earthquake Research and Information, (CERI, Memphis), predicted the fault to be of ENE-WSW trend, with a Southward dip of 45-50º and with a fault surface rupture projection of 23.70N±0.10, 70.00-70.60E. The location of the nearest ground motion recording instrument was at Ahmedabad approximately 230 km from the epicenter. A pga value of 0.11g was determined from this accelerogram, but the record was otherwise unusable due to instrument mis-calibration. In the absence of instrumentation, attenuation relationships are looked at here to describe the ground motion distribution associated with the event.

The fault activity within the Kachchh region can neither be associated with the Himalayan seismic belt nor with the Makran subduction zone, but is rather an intra-plate phenomenon. Little is known about such tectonic environments and no attenuation relationships have in the past been developed specifically for this location. Hence four attenuation relationships, derived for different locations and tectonic environments, are investigated to describe the

[6] US Geological Survey, California.

attenuation of peak ground acceleration in the Gujarat region of India. The characteristics of these relationships are summarised in Table 10-4.

Relationship	Event	M	Distance	Area
Ambrasseys et al. (1996)[7]	Shallow	Ms	d_{fault}	Europe & Middle East
Joyner & Boore (1988)[8]	Shallow	Mw	d_{fault}	USA
Sharma (1998)[9]	Subduction	Mw	d_{fault}	Himalayas, India
Youngs & Chiou (1997)[10]	Subduction	-	d_{hypo}	Worldwide

Table 10-4: Comparison of the considered attenuation relationships

The ability of the relationships to describe the ground motion for both far and near field conditions is assessed through a comparison with pga values recorded at Ahmedabad and deduced from field-measurements of a statue movement in Bhuj, respectively. The mentioned statue, shown in Figure 10-2, underwent a permanent displacement of 5cm in the E32°S direction, (thus indicating that the predominant direction of ground motion at Bhuj was N58°W). A lower-bound pga of 0.8g was determined through consideration of the forces required to overcome friction. The permanent displacement of the statue results from the cumulative effect of all peaks exceeding this acceleration value in the record. An upper bound estimate of 1.05g is obtained from the empirical relationship of Ambrasseys and Srbulov (1994)[11], which relates pga to permanent displacement through the analysis of a sliding block subjected to 937 strong motion records from 76 shallow events.

Figure 10-2: Measurement of the permanent displacement of the statue of Sardar Ballabhai Patel in Bhuj

A comparison of the pga attenuation with source distance predicted by the four relationships is given in Figure 10-3. In all cases soft soil conditions were assumed, with the epicentral location and preliminary fault solution determined by USGS and CERI respectively, being used for the ground motion calculation.

[7] Ambrasseys, N.N., Simpson, K.A., Bommer, J.J., (1996)," Prediction of horizontal response spectra in Europe", *EqEng & StrDyn*, Vol. 25, pp 371-400.
[8] Boore, D.M., Joyner, W.B., Fumal, T.E., (1997), "Equations for estimating horizontal response spectra and peak acceleration from Western North American earthquakes: A summary of recent work", *Seismological Research Letters*, Vol. 68, No. 1, pp 128-152.
[9] Sharma M.I., (1998), "Attenuation relationship for estimation of PGHA using data from strong motion arrays in India", *Bull. Of Seis. Soc. Of Am., Vol. 88, No. 4, pp 1063-1069.*
[10] Youngs, R.R., Chiou, S.-J., (1997), "Strong ground motion attenuation relationships for subduction zone earthquakes", *Seismological Research Letters*, Vol. 68, No. 1, pp 58-73.
[11] Ambraaeys, N., Srbulox., (1994), "Attenuation of earthquake induced displacements", *EqEng & StrDyn*, Vol. 23, pp 467-487.

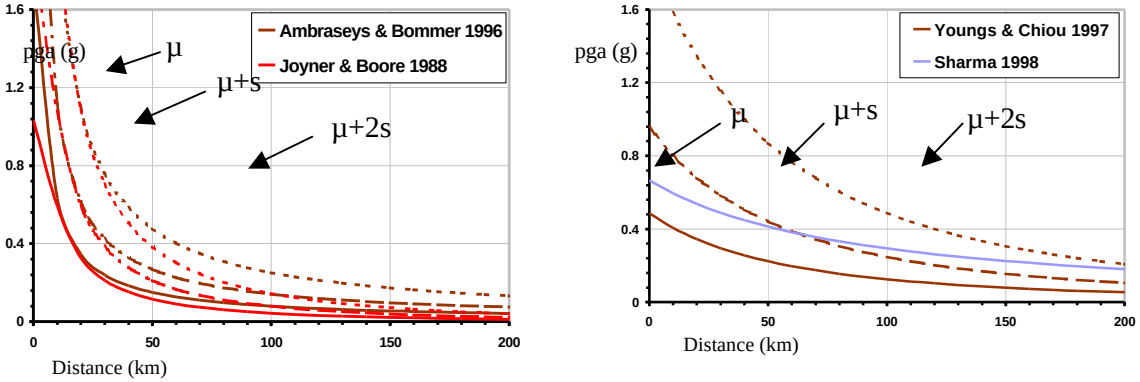

Figure 10-3: Comparison of the considered attenuation relationships

Error (%)	Ahmedabad (0.11g)			Bhuj (0.8g)		
Relationship	**μ**	**(μ+s)**	**(μ+2s)**	**μ**	**(μ+s)**	**(μ+2s)**
Ambrasseys et al. (1996)	-63	-34	+17	-76	-57	-23
Joyner & Boore (1988)	-90	-82	-66	-80	-63	-33
Sharma (1998)	+43	-	-	-56	-	-
Youngs & Chiou (1997)	-53	-9	+79	-67	-35	+28

Table 10-5: Comparison of error in pga prediction (%) given by the attenuation relationships

Table 10-5 summarizes the error in pga prediction for the Ahmedabad and Bhuj sites for the mean (μ), (μ + s) and (μ+2s) relationships. From these comparisons it can be concluded that the Youngs and Chiou (1997) attenuation relationship gives the optimum representation of the near and far-field motions with the (μ + 1.3s) curve giving the best fit to the validation data, (error of +11% Ahmedabad and –20% for Bhuj).

5. Vulnerability Prediction

Using the attenuation relationship of Youngs and Chiou (1997) for (μ + 1.3s) it is possible to estimate the ground motion severity for all the major towns in Gujarat, and hence predict the expected damage distribution at each. In the case of Ahmedabad and Bhuj however, the measured pga value of 0.11g and representative pga value of 0.9g respectively, are used for this purpose. In all cases, bare RC frames are assumed as the predominant structural type and the results of the vulnerability estimation are illustrated in Figures 10-4 and 10-5.

A post-earthquake survey was carried out by the Indian Government to identify damaged buildings in Ahmedabad. The results of the survey showed that out of approximately 50,000 RC buildings in Ahmedabad, 152 collapsed or are to be demolished, 27 were heavily damaged and 90 were moderately damaged by the earthquake. The spatial distribution of these buildings is shown in Figure 10-6 and the predicted mean and upperbound damage distributions for Ahmedabad are compared to the observed statistics in Figure 10-7.

It is evident from Figure 10-7 that the damage observed as a consequence of the earthquake is much higher than that predicted, even in the case that the upper-bound vulnerability curves are used. Consequently, the discrepancy in prediction may not be due to the general inability of the vulnerability curves to predict damage, but could be caused by a number of factors that

distinguish both the earthquake ground motion and the local building stock from that typical in Europe.

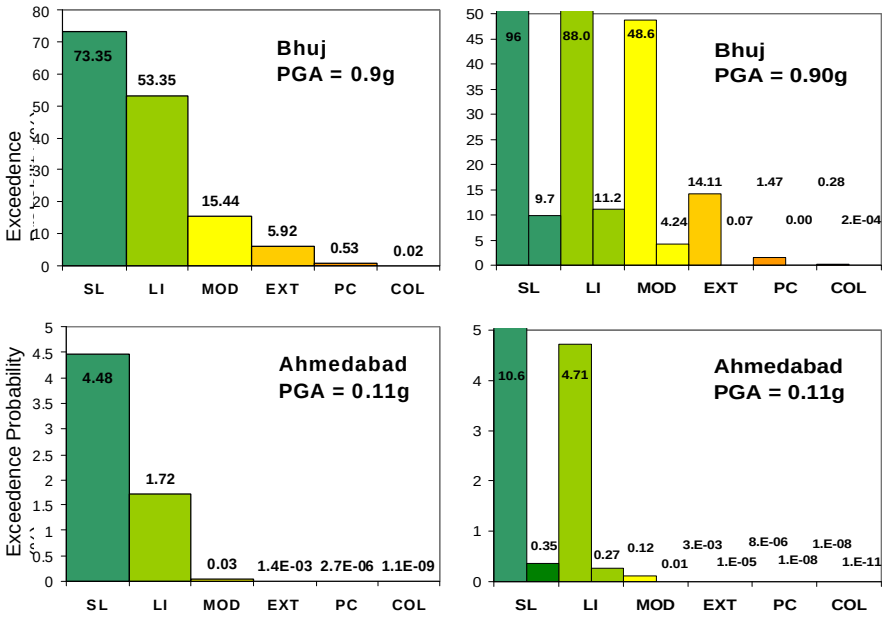

(a) Mean vulnerability prediction

(b) 90% Confidence bounds for predicted vulnerability

Figure 10-4: The RC building vulnerability predicted using the HRC-Scale and empirical curves

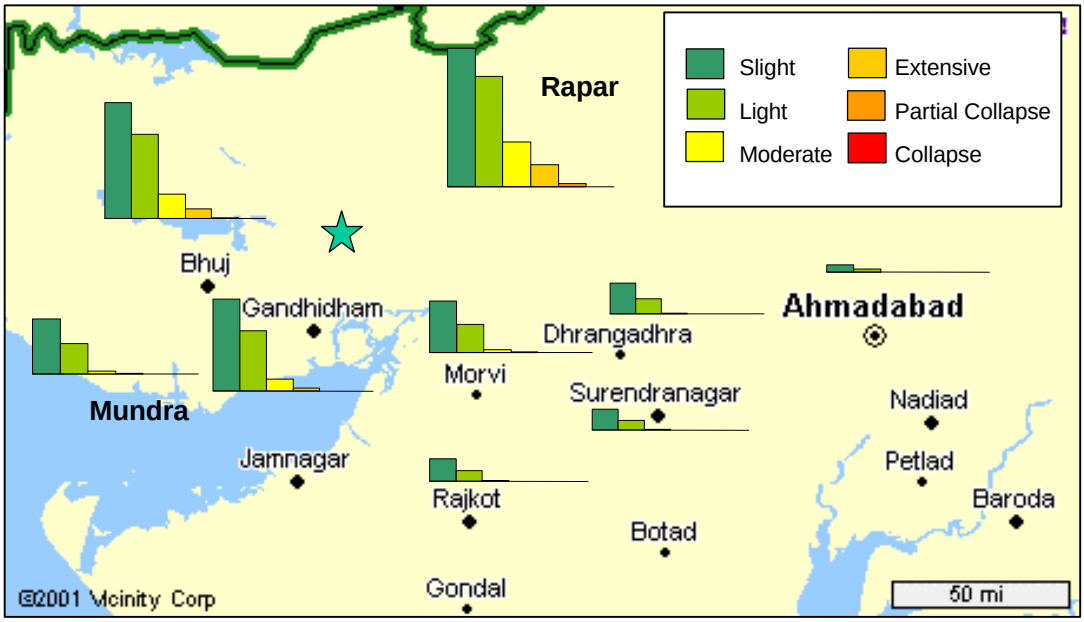

Figure 10-5: Prediction of RC building vulnerability distribution in Guharat for the Bhuj Earthquake 2001

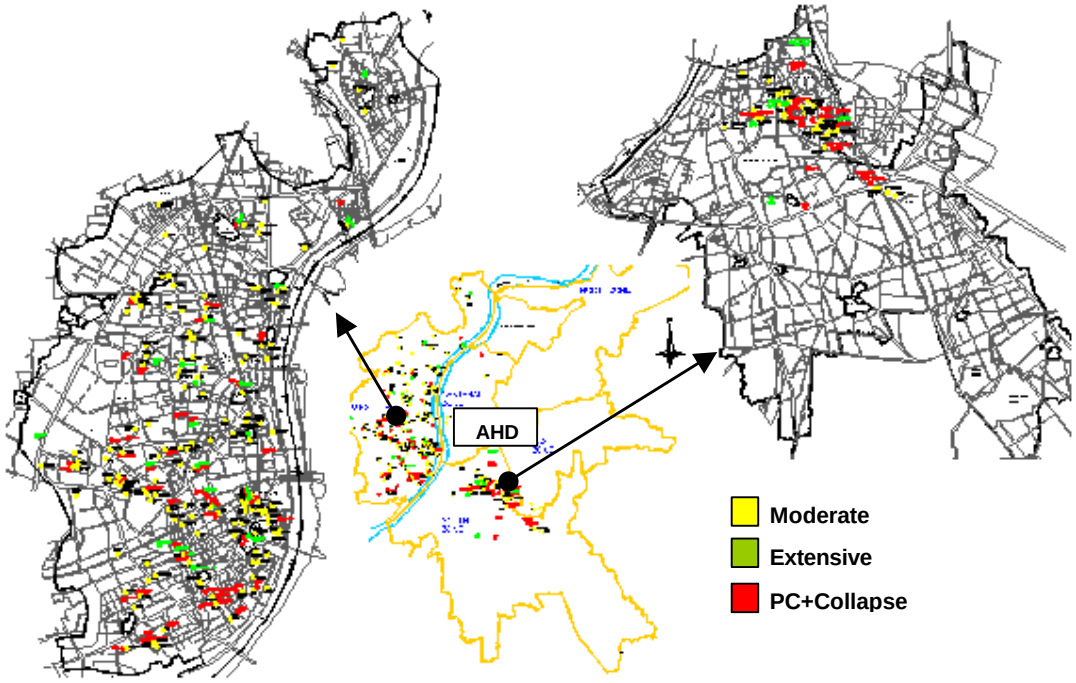

Figure 10-6: Observed RC building damage in Ahmedabad after the Bhuj Earthquake 2001, maps courtesy of Mr A.Parikh, Multi Media Consulting Engineers, Ahmedabad, India

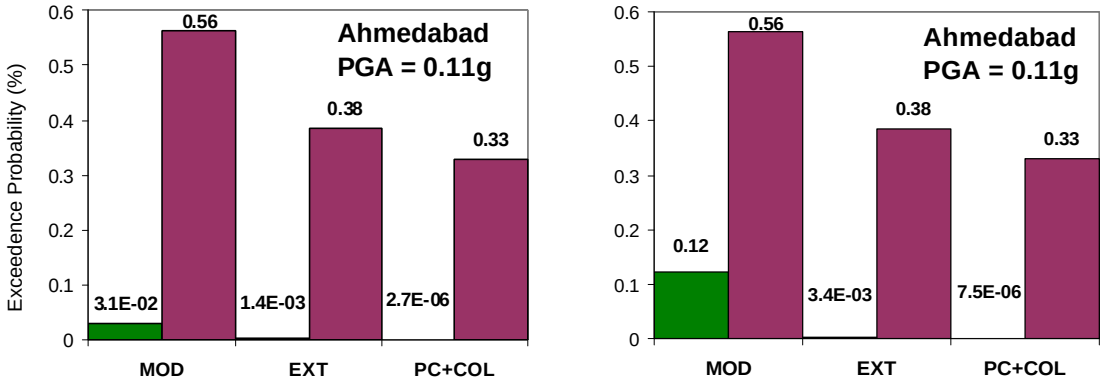

(a) Comparison with mean prediction

(b) Comparison with upper 90% confidence bound prediction

Figure 10-7: Comparison of the observed and predicted damage distributions for Ahmedabad

Site effects and the extended duration of the ground motion are thought to have contributed significantly to the observed damage. From Figure 10-6 it is evident that the damage is highly localized, being restricted to the West and South Zones of the city. It is known that in the past Ahmedabad had many lakes which were infilled for construction purposes. The location of these is not known; however, field observations revealed evidence of prior settlement in certain damaged building locations. Hence it is possible that local amplification

of the ground motion may have taken place due to the presence of soft soil or poorly consolidated fills beneath the buildings.

The Gujarat earthquake was of long duration, the main shock reported to have lasted 85 seconds at Bhuj. The degree of stiffness degradation and cumulative damage caused by an earthquake of this duration is not accounted for by the vulnerability curves used herein. This is due to their being derived mainly from data concerning European earthquakes, which are typically of smaller magnitude and shorter duration. This factor is seen to contribute significantly to the underprediction in vulnerability obtained from the curves.

A field mission to the epicentral region gave the opportunity for first-hand observation of the typical construction practice and structural failure modes in Ahmedabad. Most of the collapsed buildings were multi-story reinforced concrete moment resisting frames built in the last 5 years. . Though Ahmedabad is categorized as a high seismic risk area by the Indian Code, these buildings were not designed for earthquake loading. In the vast majority of cases, building failure occurred as a result of soft ground story collapse. This was caused by the presence of stiffness discontinuities in elevation between the ground story (typically void of either infill or shear walls), and the floors above. Due to inadequate reinforcement and connection between stairwells or elevator cores and the rest of the frame structure, these elements were not seen to contribute to the lateral resistance of the building. The use of individual column footings (usually untied) as foundations is also thought to have been an additional source of structural instability.

A further major cause of building collapse was mass eccentricity due to the construction of unplanned extensions and the placement of large water tanks on building roofs. In the latter case, the tanks were often supported on columns which failed during the earthquake event and consequently induced additional damage through impact onto the roof. The detailing deficiencies typical of gravity design, (e.g. short lap-splices, positioned at column ends with non-staggered termination, lack of adequate confinement reinforcement, 90° hooks and lack of reinforcement in joints), were observed in the damaged buildings and are thought to have further limited the deformation capacity of members and hence precipitated failure. The problem of reduced deformation capacity was further agravated by poor material quality. Corroded reinforcement steel was observed in many locations as well as the presence of weak concrete within joint areas (born through addition of water to increase workability).
The typical building configuration, construction practice and materials are therefore thought to be the main cause of the high vulnerability observed in the buildings of Ahmedabad compared to that predicted by the fragility curves for European structures. The predominance of a soft-story mode of failure is furthermore expected to be one of the main causes of descrepancy between the observed and predicted vulnerabilities. This is due to the fact that the vulnerability curves are based on observations made of heterogeneous structural configurations and failure modes, and hence are not able to account for the predominance of a single collapse mechanism.

Figure 10-8: Soft-story failure of the Ashardeep Buildings, Ahmedabad

Figure 10-9: Example of tank-induced damage in Ahmedabad

6. Summary

Vulnerability predictions for reinforced concrete buildings affected by the Bhuj Earthquake 2001, were carried out for the major cities of Gujarat using fragility curves generated for European constructions. Comparison of the predictions with the observed distribution of damage to RC buildings in the location of Ahmedabad showed large discrepancies. The underprediction in building vulnerability is attributed to a number of factors. The typical configuration and construction practice in the buildings in Ahmedabad were seen to cause premature structural collapse via soft-story mechanism formation at the ground story. Post-construction extensions and roof-top watertanks further contributed to the structure instability. It is concluded that these factors, together with the increased damage potential of the ground motion due to possible site amplification and earthquake duration effects, bring the structures to exhibit a higher vulnerability than would be expected in a population of typical European buildings for the same ground motion parameter values.

7. Acknowledgments

This paper is the result of participation in the Indian earthquake field mission organized by the Mid-America Earthquake Center. The author's participation was financed by the Earthquake Field Training Unit of Imperial College of Science, Technology and Medicine, London.

Chapter 11: Socio-Economic Aspects

by

Sue E. Dotson[1]
Administrative Manager of the Mid-America Earthquake Center
University of Illinois at Urbana-Champaign

1. Abstract

An overview of public perception and reaction to the January 26, 2001, Bhuj Earthquake in the state of Gujarat is presented, incorporating societal, economic and insurance issues. Although located in an area where devastating earthquakes have occurred in the past, the site of the 2001 Bhuj Earthquake found a population unaware of its seismic vulnerability, a government with limited disaster recovery planning in place, and an insurance industry that offered earthquake coverage only as a supplement to other policies, with a special premium rate. As a result, a shocked and grief-stricken population was faced with frustrating bureaucratic delays in rescue operations and devastating personal financial losses while the nation faced losses of tens of thousands dead, hundreds of thousands injured and an economic loss of an estimated $2.2 billion in revenue.

2. Introduction

When a major earthquake shattered the Indian state of Gujarat on January 26, 2001, seismologists were not surprised. Since 1956, India has experienced five such intraplate earthquakes, the worst of which killed as many as 9000. The Bhuj earthquake, named after the desert city located 20 km away from the epicenter, sits in an area which has historically experienced devastating earthquakes. An earthquake of similar size struck the area in 1819 killing about 2000 people. As recently as 1956, a 6M event was centered nearby at Anjar.[2]

Like the New Madrid Seismic Zone in the U.S., this area of the Indian subcontintent is one of low-frequency high-consequence earthquakes. As a result, residents of Gujarat were unaware and unconcerned with the seismic hazard. This was not true of the government. In the mid-1990s, the Union Urban Development Ministry's Building Materials and Technology Promotion Council conducted extensive surveys of natural disaster risks in every part of India. The resulting two-volume *Vulnerability Atlas of India* was published in 1998 and recommends appropriate safe building practices for every region of India. Also in place is the National Building Code of 1983 that offers guidelines in terms of safe seismic design. But four out of five Indian homes are designed by the home owners themselves and there is no licensing system for engineers. Safety laws are in place but rarely enforced.

The nation of India regularly faces a wide array of natural disasters, including earthquakes and cyclones. Disaster plans designed by the national government's Crisis Management Group are in place, but they provide primarily for the movement of medical and military personnel into affected areas. Search and rescue technology is limited and disaster drills are not practiced. India has no evacuation or disaster mitigation plans in place. Effectively transporting relief supplies is a major obstacle.

---

[1] SED, 1243 Newmark Civil Engineering Laboratory, 205 N. Mathews, Urbana, IL 61801 USA
email: sdotson@uiuc.edu
[2] *Science*, February 2, 2001.

Until 2000, only one insurance company, General Insurance Corporation (GIC), a state-owned monopoly, offered earthquake coverage as part of its standard policy. Following a series of earthquakes in the early 1990s, however, GIC followed private insurance practice and discontinued this coverage as part of a standard package; it was offered only with payment of an additional premium.[3]

While the state of Gujarat refines 55% of India's petroleum products and produces 45% of its pharmaceuticals, the Gujarat earthquake struck an area where most of its inhabitants live primarily from handicraft production, refining salt, fishing and agriculture.[4] Some livestock remains that survived both last year's devastating drought and the recent earthquake. For those who earn their livings primarily through handicrafts, the immediate future is bleak. The Self-Employed Women's Association (SEWA) estimates it will take two to five years for these artisans to reestablish their livelihoods.[5] The estimated economic loss to the nation (excluding building replacement costs) is $2.2 billion; India's annual gross domestic product is about $500 billion.[6]

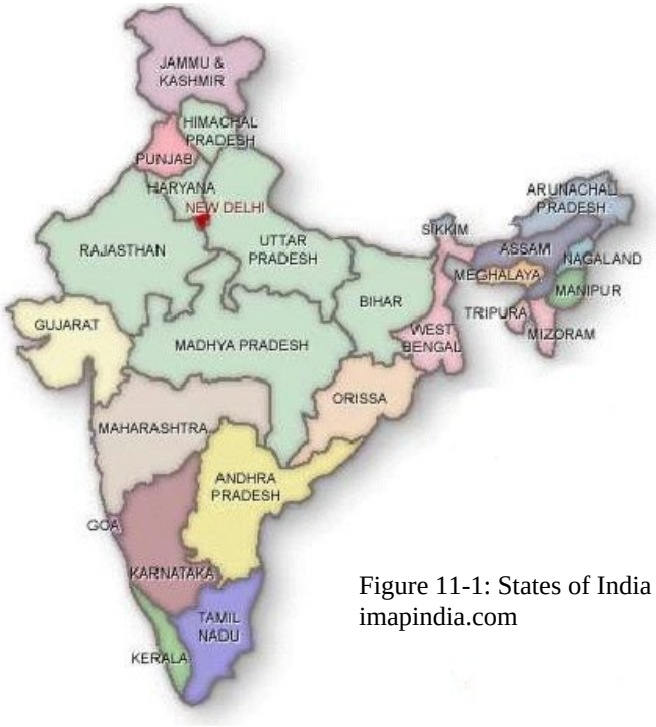

Figure 11-1: States of India
imapindia.com

3. Public Reaction

In the hours immediately following the Gujarat earthquake, the Indian government was unable to respond quickly and effectively to the emergency. Occurring amid national celebrations of Republic Day, the earthquake shed light on the deficiencies of Indian disaster relief efforts. More than five-and-a-half hours elapsed after the earthquake before officials in Delhi held a meeting to discuss the crisis. A governmental rescue effort took almost twenty-four hours to organize. Thirty-six hours after the disaster, cranes and earthmoving equipment still were not in place to help in rescue efforts, despite the knowledge that the first forty-eight hours after a disaster are critical in saving lives, and despite the fact that Gujarat is the second most industrialized state in India.

[3] *India Today*, February 12, 2001.
[4] *International Herald Tribune*, February 7, 2001.
[5] Www.OxfamAmerica.org.
[6] *International Herald Tribune*, February 7, 2001.

Because the earthquake occurred on a day of national celebration, the majority of people were in their homes; most of the collapsed buildings were apartment buildings and private homes. The shock and grief of survivors quickly gave way to desperate efforts to rescue victims. Household tools, sledgehammers and bare hands were used to try to rescue survivors.

Providing medical care to survivors proved a daunting task. With many hospitals in ruins, medical treatment was often carried out in tents or even in open-air operating "rooms," surgeries performed using local rather than general anesthesia. Army field hospitals were set up as volunteers struggled to deliver emergency medical supplies.

Against the backdrop of this desperate rescue effort were the practicalities of survival. Hundreds of thousands were left homeless at a time when evening temperatures dropped to near freezing. Aftershocks produced panic among survivors and those whose homes were still standing were often too frightened to return to them. Slow distribution of relief supplies only added to feelings of panic and despair; distribution of tents, food, and water to survivors came more quickly from private relief agencies than from the Indian government.

The psychological toll on survivors has been harsh. Some lost their entire families. As rescue efforts gave way to recovery of victims, family members often performed last rites for family members themselves, crafting funeral pyres from dry wood and available debris. Many victims will never be recovered. In a follow-up study in Latur after the deadly 1993 earthquake there, it was estimated that 40% of the population had considered suicide and 60% suffered from Post-Traumatic Stress Disorder; similar statistics are expected in Gujarat. The Nehru Foundation for Development (NFD) is coordinating the task of providing counseling and rehabilitation for the affected residents of Gujarat. A booklet titled *Coping with Earthquakes: A Citizens' Handbook* has been compiled by NFD to help answer questions about health, home repair, sanitation, and psychological trauma. NFD is also coordinating information dissemination about governmental programs available for victims.[7]

Children have been particularly traumatized by the earthquake and aftershocks. A widespread effort to disseminate information about recognizing and dealing with shock in children is underway. Psychologists have warned that if treatment for these children is overlooked, the effect of the earthquake may have a lifelong impact on the children. Fear, insecurity and grief now may lead to anxiety, panic and depression in adulthood.[8] The Gujarat Council for Educational Research and Training has organized special programs aimed at dealing with psychological stress in children. These programs will be focused on primary schools in earthquake-affected areas.

Figure 11-2: Young earthquake survivor. Oxfam America

As shock gave way to anger, two primary targets emerged: the government and builders.

4. Government Recovery and Relief Efforts

While scientists in Delhi located the epicenter within minutes after the earthquake struck, the information was not transmitted to the central government until about six hours later due to a

[7] *India Today*, February 12, 2001.
[8] *Ahmedabad Times*, February 9, 2001.

failure of telecommunications links. Despite claims of regular testing, cell phones that had been distributed to each district revenue collector in Gujarat did not function and could not be used to transmit information at the time of the earthquake.

While both the army and the civilian Rapid Action Force (RAF) were on the scene relatively quickly, they had neither the training nor the equipment to deal with the situation. The government was very inefficient in directing recovery and relief supplies to needed areas. In Gandhidham, for example, heavy machinery took days to arrive despite the fact that nearby Kandla Port, though damaged, was partially operational. After struggling for three days to bring heavy equipment into Ahmedabad, the railways, which had suffered damage but were running, were finally asked for assistance. Volunteers talk of supplies lying on roadsides and of emergency equipment sitting idle because there was no one to operate it. There were no road maps to provide to volunteers attempting to deliver relief supplies or to teams of doctors trying to reach interior villages.

Governmental relief efforts did become more organized over the days following the earthquake. The Gujarat State Electricity Board assigned 1500 workers to round-the-clock duty to bring electricity back to Bhuj which had lost its entire power grid. This effort was accomplished in just three days. Tents, food, water and medicine began to arrive in the affected areas within four days. The 22,500 army troops deployed to the area are credited with working nonstop to provide relief.[9]

Figure 11-3: Survivors amid rubble. Red Cross

Still, most of the credit for rescue, recovery and relief is being given to the population of the affected areas, to local organizations and to private groups, both domestic and international. Condemnation of the government's inefficiency and lack of response to one of India's worst natural disasters has shaken public confidence in the government. After citing examples of heroic relief efforts underway by private citizens, one of India's leading news magazines, *India Today*, stated "Now if only the slothful Government could march in tune with the dynamism of its own society."[10]

5. The Building Industry

The collapse or near-collapse of 171 buildings in Ahmedabad that led to more than 700 deaths is being popularly blamed on the government's willingness to turn a blind eye toward unscrupulous builders as well as the builders themselves. Official complaints from residents about poor construction techniques are coming to light and may bring about mandatory building guidelines.[11]

Figure 11-4: Survivors search for victims. Oxfam America

In one instance in Ahmedabad, a ten-story apartment

[9] *India Today*, February 12, 2001.
[10] *Ibid*.
[11] *Ibid*.

building collapsed. Although the Bureau of Indian Standards code specifies that a building of any size should have a separate frame to support major utilities, the building's stairs, elevators, and water tank were all supported by four central columns that were also supporting the building itself. Evidence shows that steel rods used in the beams and columns were undersized and the foundation was not planned to take into account the unplanned addition of a penthouse level and swimming pool on top of the structure. Thirty-three people died in the collapse.[12]

In another case, a new apartment building, already occupied but uninspected by the local building authority, gave way under the weight of illegal construction and insufficient support for the building's utilities, loaded on an already cracked beam-column frame. Twelve died in that collapse.[13]

A further survey showed that only ten of Ahmedabad's 1,000 high rise buildings had permission for occupancy, or what is called building use (BU).[14] While there is currently a freeze on all construction activity in Ahmedabad, Vadodara, Surat, Rajkot, Bhavnagar and Jamnagar, speculation abounds that the state government will revoke all construction freezes to appease the powerful building lobby. The state of Gujarat had only recently revised rules permitting construction of buildings as tall as thirteen stories in Ahmedabad, Badodara and Surat and allowing eleven-story construction in Rajkot, Bhavnagar and Jamnagar; the previous limit had been ten stories. Charges have now been lodged against one builder, one architect, and one structural engineer in connection with deaths resulting from a collapsed apartment building.[15]

Figure 11-5: Destroyed buildings in Rapar. GEES

Good design, good construction, and good materials can create buildings able to withstand strong seismic force and still remain stable. If guidelines for earthquake-resistant construction, available since 1970, are followed, widespread devastation is avoidable. The Gujarat Housing Board's 30,000 low-income apartments not only withstood the earthquake but suffered relatively little damage.[16] However, in a country where 80% of the homes are designed by home owners and

[12] *The Times of India*, February 9, 2001.
[13] *Ibid*.
[14] *The Times of India*, February 13, 2001.
[15] *The Sunday Times of India*, February 11, 2001.
[16] *The Times of India*, February 13, 2001.

engineers are not licensed, it is difficult to foresee a time where most dwellings can be considered to have been built safely.[17]

The issue of safety is affecting the housing market. Fearful of returning to apartment buildings now considered unsafe, former residents are demanding accommodations on lower floors. The demand for apartments in low-rise buildings has skyrocketed, along with prices. Rents for small apartments on the lower level of a building have risen 30%-40% since the earthquake and demand for single story homes is more than twice the available supply. In areas not directly affected by the earthquake, such as Mumbai, apartments available on upper floors of high-rise buildings are sitting empty and resale of apartments in older buildings has fallen dramatically.[18]

The manufacturing sector has also been affected. Many diamond workers in Surat have refused to return to the job fearing entrapment in their small workspaces with narrow, limited exits, which are kept locked for security reasons.[19] While factories throughout Gujarat are intact, the earthquake has caused widespread panic and exodus among immigrants who worked the assembly lines. It may take months before full production will be able to resume. Those laborers who do remain have raised their wage demands threefold.[20]

In view of the widespread devastation that struck throughout Gujarat, the government in Delhi has announced that it plans to make building safety guidelines mandatory. Lying on four fault lines, Delhi is considered particularly vulnerable to catastrophe; experts believe at least 50% of Delhi's buildings are not earthquake-resistant. Other earthquake-prone metropolitan areas like Mumbai are also a cause of concern.[21] In Kataria, a small town in North Gujarat, India Railways plans to replace its damaged railroad station with an earthquake-resistant construction, the first in India. Railroad managers are also contemplating rebuilding residential quarters for railway workers using these same techniques.[22] Proposals were being considered by the government to rebuild 80,000 housing units throughout the affected areas for those people living below poverty level using earthquake-resistant design.[23]

6. Insurance Industry

The financial cost of the Gujarat earthquake will be borne primarily by the government and by the victims themselves. Following the devastating 1993 earthquake in Maharashtra which left 10,000 dead and 25,000 homes destroyed in Latur, the governmental Tariff Advisory Committee (TAC) excluded earthquake coverage from the standard policy offered by the stated-owned General Insurance Corporation. Taking effect in 2000, the tariff revision offered exclusions for several risks, including earthquakes, floods and riots, at discounts of up to 30% on the overall premium. The owners of most large buildings chose to insure at the lowest rates possible excluding many hazards, while individual households seldom have any policy at all.[24]

One TAC member estimates that only "about 5 per cent"[25] of the households under the standard policy have opted for earthquake coverage. The insurance industry's biggest liability from the

[17] *India Today*, February 12, 2001.
[18] *Ibid*.
[19] *The Times of India*, February 9, 2001.
[20] *Ibid.*, February 13, 2001.
[21] *India Today*, February 12, 2001.
[22] *The Times of India*, February 9, 2001.
[23] *The Sunday Times of India*, February 11, 2001.
[24] *India Today*, February 12, 2001.
[25] *Ibid*.

Gujarat earthquake will result not from property losses but from pay outs of life insurance policies. It now appears that less than 2% of insurance company's liability from the earthquake will result from property losses; the remainder will result from loss of human lives.[26] This imbalance emphasizes just how grossly underinsured property is.

As private insurers analyze risks, the cost for earthquake coverage will undoubtedly rise. The Insurance Regulatory and Development Authority has begun work on a new map of the country to better assess earthquake risks, with a proposal to bring the entire state of Gujarat into the highest risk category.[27]

Figure 11-6: Collapsed House in Bhuj. Red Cross

Public awareness of the need for all types of insurance has been heightened following the Gujarat earthquake. In Ahmedabad applications for life insurance policies have increased by 12%. A sharp increase in applications for optional earthquake coverage is also reported there. But the actual increase in the number of policies being issued as a result of such applications is less than 20%. Stringent processing requirements and the mandatory acquisition of a structural engineer's certificate for all post-earthquake property policies has slowed new coverage to a trickle.[28]

The effect is being felt outside the immediate earthquake site as well. Acceding to public demand, builders in at least one city, Vadodara, have started including natural disaster insurance on behalf of residents on all its constructions. The Jayraj Group, an insurance company that has branched into the construction business, is now obtaining a ten-year policy on its constructions; of the total premium amount, residents will pay for two years and the company will pay for the remainder.[29]

7. Economic Impact

In terms of immediate overall impact to the Indian economy, earthquake losses are less than might be expected. The major industrial sectors in Gujarat were strong enough to survive the earthquake. India's largest refinery at Jamnagar and a 450-megawatt nuclear power station survived almost unscathed, although all the privately owned salt refineries were damaged and nonfunctional following the earthquake. Excluding replacement costs for property, it is estimated that economic loss will reach $2.2 billion. That figure could top $5.5 billion, however, if factories are unable to reach pre-earthquake production levels within a few weeks.[30]

[26] *Ibid*.
[27] *The Sunday Times of India*, February 11, 2001.
[28] *Ibid.*, Feb. 11, 2001.
[29] *The Gujarat Age*, February 12, 2001.
[30] *International Herald Tribune*, February 7, 2001.

Kutch, the worst-affected district, is one of the least industrialized in the nation. Surat, too, has reported very little damage to industrial infrastructure. In Ahmedabad damage has been largely confined to residential buildings. The damage to the port of Kandla, Gujarat's largest, which accounts for 17% of maritime cargo in the entire country, will undoubtedly have long-term economic repercussions.[31]

Table 11-1: Gujarat's Economic Impact on the Domestic Economy

Petroleum Refining	55%
Pharmaceutical Production	45%
Cotton Production	31%
Textile Manufacture	24%
Industrial Investment	20%
Shipping	17%
Industrial Output	13%
Industrial Facilities	10%
Total Exports	33%
Gross Domestic Product	11%

Worker absenteeism is adversely affecting economic recovery. Personal tragedies as well as fear of recurrence of another earthquake have caused suspension of production and shutting of businesses that might otherwise be operational. Production of diesel pumps in Rajkot came to a complete halt when line employees stopped coming to work. Some hotels have shut because managers, waiters and cleaning staff no longer show up to care for guests.[32] Retail sales in Gujarat have plummeted. Inventories lost in the earthquake have yet to be replaced but, moreover, a shift of purchasing power among consumers, especially the middle class, has occurred, as spending is now concentrated on building and repair of property rather than on consumer goods.

If businesses can weather the short-term effects, however, an upturn is predicted within a few months. Reconstruction of buildings should spark a revival of consumer spending as these labor-intensive activities provide employment and pump money back into the Gujarati economy. Demand for consumer goods, both as replacement items and new acquisitions, is anticipated. It is speculated that fear of living in high-rise buildings will trigger widespread growth in new suburban areas.[33]

Figure 11-7: Port of Kandla lies idle. Geoinfo.usc

[31] *India Today*, February 12, 2001.
[32] *Ibid.*, February 12, 2001.
[33] *Ibid.*

The Gujarati banking industry has formulated a relief package that would provide loans at below-market rates and waive penalties on payback of existing loans for two years in earthquake-affected areas. A committee set up to deal with the emergency is offering these loans to small businesses, the self-employed and start-up ventures in an effort to restore and rehabilitate business throughout Gujarat. Loans at below-market rates may also be offered for repair or construction of houses and small shops.[34]

Until the earthquake, Ahmedabad had a growing reputation of providing excellent opportunities and good living conditions for India's professional sector. Companies had begun to relocate there or had opened branch offices specifically to take advantage of Ahmedabad's growth and reputation. Compared to other urban areas like Delhi or Mumbai, Ahmedabad offers minimal commuting time, a wide array of entertainment and cultural activities and a safe living environment, particularly appealing to female professionals. Now companies are worried that thousands of non-Gujarati professionals will seek opportunities elsewhere, especially since most had not yet bought property and have no compelling reason to remain. Many corporations are trying to reassure their professional workers by offering to house them in low-rise or single family dwellings. Given the shortage of such accommodations, however, and the dramatic increase in price in those that are available, it is unclear if this effort will prove successful.[35]

8. Conclusions

The catastrophic earthquake of January 26, 2001, in the state of Gujarat has focused sharp attention on the seismic vulnerability of India. While recommendations are in place to guide interested builders and home owners in creating structures that may withstand strong seismic force, adherence is voluntary; building codes are often ignored. Faced with widespread devastation, tragic loss of life and large economic loss, the central government in Delhi is considering making building guidelines mandatory throughout the country while working to revise its slow and inadequate disaster response procedures.

The population's increased interest in acquiring coverage to insure against natural disaster losses and losses of life has risen since the earthquake. An expected revision to India's seismic risk map that will place the entire state of Gujarat in the highest risk category will undoubtedly bring about an increase in the cost of earthquake coverage. Whether this rise in premiums will deter prospective policy holders remains to be seen.

The state of Gujarat's active and growing economy faces recovery and restructuring following the earthquake. Because the industrial infrastructure there survived with relatively little damage, it is not anticipated that much shift will occur in production capabilities other than in the short-term. Workers who fled the area in fear following the earthquake are expected to return, lured by the growing economy. There is some speculation that relocation among non-Gujarati professionals may hamper economic recovery in the state.

The natural resilience and community spirit of the Gujaratis themselves will form the basis for recovery efforts there. Known for a sense of enterprise and self-sufficiency, the Gujaratis are viewed as an inspiration. Their tragedies may inspire a national reawakening to important issues such as building guidelines and disaster recovery.

[34] *The Times of India*, Feb. 10, 2001.
[35] *The Sunday Times of India*, February 11, 2001.

9. References

Ahmedabad Times, February 9, 10, 2001.

The Asian Age, February 10, 12, 2001.

The Economic Times, February 12, 2001.

Geotechnical Earthquake Information Server (GEES). http://geoinfo.usc.edu/gees/India.

The Gujarat Age, February 10, 12, 2001.

Gujaratplus. http://gujaratplus.com./.

India Today, February 12, 2001, Special Gujarat Issue.

International Herald Tribune, February 7, 2001.

Oxfam America. www.oxfamamerica.org.

Science, February 2, 2001.

The Sunday Times of India, February 11, 2001.

The Times of India, February 9, 10, 13, 2001.

World Health Organization. www.whosea.org/gujarat/gujarat4.htm.

Compare Infobase Pvt. Ltd. www.economywatch.com/.

Chapter 12: Correlations with Mid-America

by

Arch C. Johnston[1]
Director, Center for Earthquake Research and Information
The University of Memphis

1. Geology and Seismology

The main rationale for deploying the MAE Center Disaster Investigation Team to India in the wake of the Bhuj earthquake was the striking parallel between the Kutch region of western India and the Reelfoot rift of Mid-America (Figure 12-1). To extend the comparison, both regions have experienced very large earthquakes in prehistoric and historic times. The 26 January 2001 Bhuj earthquake afforded the unprecedented opportunity to examine with modern techniques and instruments, a similar earthquake to the great 7 February 1812 earthquake in the New Madrid seismic zone.

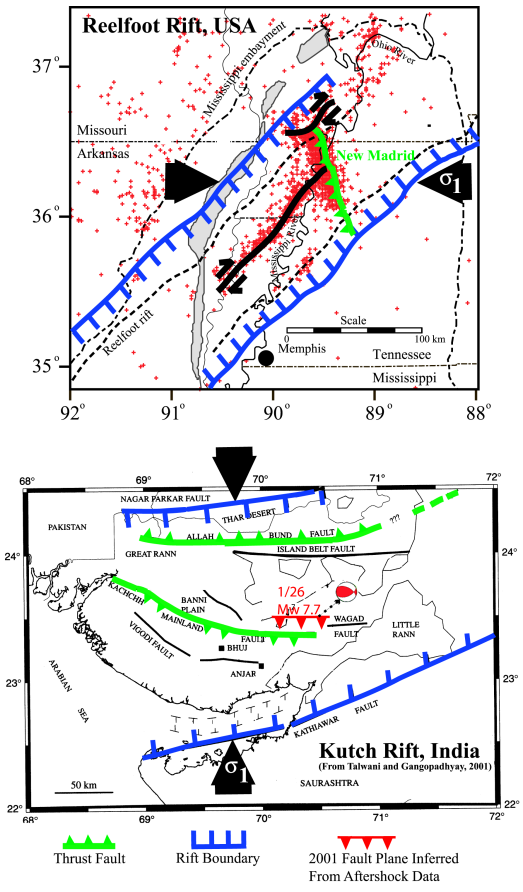

Figure 12-1: The Reelfoot rift of Mid-America (top) and the Kutch rift of western India (bottom), both at the same scale. Outer rift flanks are shown in blue; prominent thrust faults in green. Both rifts experienced their most recent episode of major extension in the Mesozoic era but both currently are under compression (black arrows). For Reelfoot the compression is oblique to the rift so strike-slip (black) as well as thrust (green) faulting results. But as in the Kutch rift the major thrust faults form normal to the prevailing horizontal compressive stress

The classification of the Kutch region as a "stable continental region" or SCR is not without controversy because Kutch lies much closer to an active plate boundary zone than does the Reelfoot rift (see Table 12-1). However, Gordon (1998) did not include the Kutch peninsula in

[1] ACJ, CERI, Box 526590, Memphis, TN 38152, USA
email: Johnston@ceri.memphis.edu

his update of "diffuse" plate boundaries, and L. Kanter in Johnston *et al*. (1994) mapped Kutch as part of the Indian SCR because it was separated from the Chaman transform plate boundary with Asia by at least 200 km of thick, relatively undisturbed sediments of the Indus alluvial basin. The Indus sediments are deposited on the Proterozoic crust of the North India craton. Hence, the Kutch rift is well characterized as a failed (ie, did not open to new oceanic crust) intracontinental rift imbedded in the Indian SCR. It is currently being reactivated or compressed under the north-south compressional stresses generated by the India plate's collision with Asia along the Himalayan front. The Reelfoot rift of Mid-America is a similar failed continental rift imbedded in

Table 12-1. Comparison of the New Madrid and Bhuj Earthquakes

Attribute	**New Madrid, USA 7 February 1812**	**Bhuj, India 26 January 2001**
Host geologic structure	Failed intracontinental rift: **Reelfoot rift**	Failed intracontinental rift: **Kutch rift** or graben
• Age of rifting	Precambrian (with major re-activation in the Mesozoic)	Mesozoic (Jurassic)
• Rift orientation to regional tectonic stress regime	Oblique, angle ~30° - 40°	Perpendicular, angle ~90°
• Regional crustal class	Stable Continental Region	Stable Continental Region
• Crustal thickness	~40 km	~40 km
• Regional crustal age	Proterozoic (0.9 – 1.6 b.y.)	Proterozoic (0.9 – 1.6 b.y.)
• Distance from plate boundary or ATR	1,200–1,500 km to Rocky Mts. or Caribbean P.B.	300 – 400 km to Chaman transform (Asia-Pakistan)
Source Fault: type	**Reelfoot fault**: thrust	**Unnamed**: blind thrust
• Orientation to regional stress	~ Perpendicular (see Fig. 1)	~ Perpendicular (see Fig. 1)
• Length	70 – 90 km	35 – 55 km[†]
• Dip/down-dip width	30° – 40°/45 km[#]	40° - 50°/30 – 45 km[†]
• Surface rupture	Probably (3-7 m, sharp fold)	Probably not
• Prior large earthquakes	Yes, at least two	Unknown
• Prior large earthquakes in the rift fault system	Yes, ~1400 AD, 900 AD, and 500 AD	Yes, in 1819 (Allah Bundh) and ~1100 AD
Mainshock: Seismic Moment	$10x10^{27}$ dyn-cm (M_w 8.0)[#]	$4x10^{27}$ dyn-cm (M_w 7.7)
• Body-wave magnitude	m_b = 7.4 (estimated)	m_b = 6.9
• Liquefaction field	Large and severe	Large and severe (see chpt. 3)
• Maximum intensity (MMI)	XI –XII	XI – XII
• Intensity felt limit	> 2000 km	> 2000 km
• Aftershock sequence	Robust, at least 4 M_w = 6.5	Weak, M_w = 5.8 largest

[†] from aftershock hypocenter locations [#] modeled or estimated in Johnston (1996)

the North American SCR and currently undergoing transpressional reactivation, although at a probable slower deformation rate than Kutch is experiencing.

The occurrence of the 2001 Bhuj earthquake provides two additional reasons to regard Kutch earthquakes as comparable to New Madrid SCR earthquakes rather than representing diffuse plate boundary seismic activity. One reason is the type of fault motion that occurred during the Bhuj mainshock. The other concerns the source scaling relation between the mainshock size (seismic moment or M_w) and the dimensions of its source fault and the duration of slip on the fault.

If the Bhuj mainshock was part of the diffuse plate boundary of the Chaman transform zone in Pakistan, it should serve to accommodate the northward movement of India relative to Asia. The mainshock, however occurred on an east-west oriented thrust fault that dips to the south (see Chapter 2). The mainshock rupture was nearly pure thrust so that its slip vector is nearly north-south. This results in the northern block (the footwall) moving southward and under the southern, hangingwall block. Hence the footwall's displacement is exactly opposite the velocity vector of India's motion relative to Asia. Rather than accommodating India-Asia plate motion, the Bhuj mainshock appears to have contributed to the north-south compressional shortening of the Indian craton, much as Bilham and England (2001) recently showed for the great 1897 Assam earthquake of northeastern India. The Reelfoot rift is also being compressed but because it is oblique to the east-west compression, the New Madrid faults exhibit a mixture of right-lateral strike-slip as well as thrust faulting (Figure 12-1).

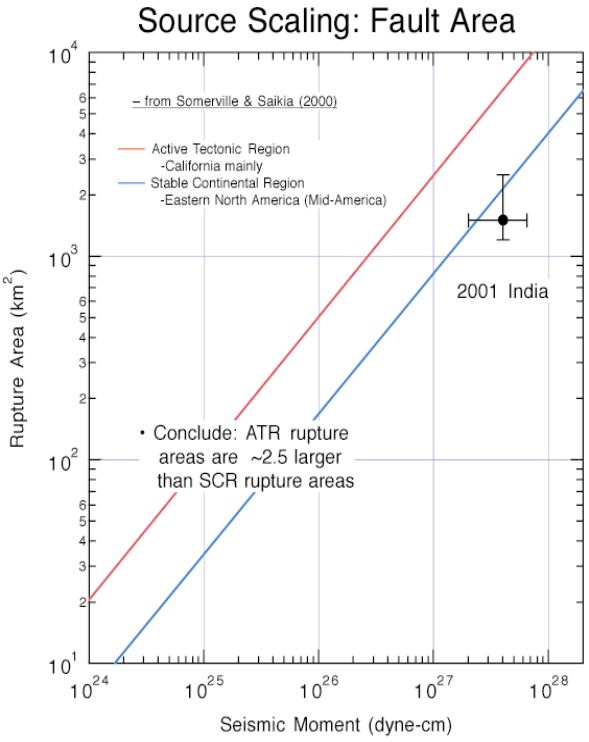

Figure 12-2: Fault size versus earthquake size (seismic moment) for active tectonic regions like California (red) and stable continental regions like Mid-America (blue). The slope of the blue source-scaling line was specified only by assuming self-similarity between small and large SCR earthquakes. However, the fault area from precise Bhuj aftershock locations, validates the self-similarity assumption. This removes a large source of uncertainty in seismic hazard assessments in SCRs

The scaling relationship between the Bhuj mainshock seismic moment or energy release and its source fault may be the most important lesson of all for its seismic hazard implications for Mid-America. The precise hypocentral locations obtained by the MAE Center's seismic instrument deployment (Chapter 3) define the mainshock's fault dimensions as roughly 40-50 km length and 30-45 km down-dip width. This is shown in Figure 12-2 as a fault area of 1500 km^2 with an uncertainty range of 1200 – 2500 km^2. Even with this large uncertainty it is clear that the Bhuj mainshock fault is much smaller than expected for an upper magnitude 7 earthquake in active tectonic regions. Why this difference occurs between active and

stable continental crustal regions is one of the outstanding questions in seismology, one that a rigorous study of the Bhuj earthquake and the Kutch tectonic setting will surely help to answer.

The implications of a distinct source scaling for SCR earthquakes for Mid-America's seismic hazard are great. Simply put, Figure 12-2 shows that in stable continental regions like Mid-America we can expect to have larger earthquakes on smaller faults than is true in active regions. Because the thicker crust of SCRs permits a greater down-dip width, Mid-American SCR faults can be much shorter than those in the western U.S. to generate the same size earthquake. Moreover, since the seismic energy is released over a smaller area, duration of slip is less but magnitude of slip is greater, leading to high-to-very-high rates of moment or energy release relative to large earthquakes in active regions. This is just another way of expressing power or rate of energy release/work done during an earthquake rupture. The relative power level relates directly to the amplitude of generated ground motions: the more powerful the earthquake the greater amplitude ground motions it produces. The hope is that the research to be carried out on the data from the Bhuj mainshock and aftershocks will lead to much more realistic models of seismic sources in Mid-America and other SCR regions subject to low-probability-but-high-consequences events exemplified by the Bhuj earthquake.

2. References

Bilham, R. and P. England (2001). Plateau 'Pop-Up' in the Great 1897 Assam Earthquake, Nature, **410**, 806-809.

Gordon, R.G. (1998). The Plate Tectonic Approximation: Plate Nonrigidity, Diffuse Plate Boundaries, and Global Plate Reconstructions, Annual Reviews of Earth and Planetary Sciences, **26**, 615-642.

Johnston, A.C. (1996). Seismic Moment Assessment of Earthquakes in Stable Continental Regions—III. New Madrid 1811-1812, Charleston 1886 and Lisbon 1755. Geophysical Journal International, **126**, 314-344.

Johnston, A.C., K.J. Coppersmith, L.R. Kanter, and C.A. Cornell (1994). The Earthquakes of Stable Continental Regions: Assessment of Large Earthquake Potential, EPRI Report TR-102261, J. Schneider, editor, Electric Power Research Institute, Palo Alto, California.

Somerville, P. and C. Saikia (2000). Ground Motion Attenuation Relations for the Central and Eastern United States. Project Report, U.S. Geological Survey, Award 99HQGR0098, 10 pp.